Craig Hauser, BSc

Experimental Investigation and Optimization of a Dryer Prototype for Pharmaceutical Applications

MASTER'S THESIS

to achieve the university degree of

Diplom-Ingenieur

Master's degree programme: Chemical and Process Engineering

submitted to

Graz University of Technology

Supervisor

Univ.-Prof. Dipl.-Ing. Dr.techn. Johannes Khinast

Institute of Process and Particle Engineering

Dipl.-Ing. Manuel Kreimer

Graz, november 2017

research center pharmaceutical engineering

TU Graz
Graz University of Technology

University of Technology Graz
Institute of Process and Particle Engineering

Experimental Investigation and Optimization of a Dryer Prototype for Pharmaceutical Applications

Master Thesis

Craig Denny Hauser, BSc.
born on 14.11.1989

December 2016 - November 2017

Supervisors:

Univ.-Prof. Dipl.-Ing. Dr.techn. Khinast Johannes

Dipl.-Ing. Dr. Aigner Isabella

Dipl.-Ing. Kreimer Manuel

AFFIDAVIT

I declare that I have authored this thesis independently, that I have not used other than the declared sources/resources, and that I have explicitly indicated all material which has been quoted either literally or by content from the sources used. The text document uploaded to TUGRAZonline is identical to the present master's thesis.

02.11.2017

Date

Signature

Acknowledgements

I wish to express my gratitude to Prof. Johannes Khinast, head of the Institute of Process and Particle Engineering of the TU Graz and CEO of the Research Center Pharmaceutical Engineering (RCPE), for giving me the opportunity to realize this paid master thesis in an exciting field of industrial relevance.

I would like to thank my supervisor DI. Kreimer Manuel for his excellent guidance and persistent help as well as for proofreading my thesis. Without his valuable participation and input this master thesis would not have been possible.

Furthermore I would like to thank Dr. Aigner Isabella and DI. Zettl Manuel for their help and assistance during my time at the RCPE.

I would also like to thank the entire lab team, especially Piller Michael, for his thorough instructions on the measurement devices, the technicians, the IT-department and all the people who helped me with my work.

I would now like to thank my friends, which constantly supported me.

Finally, I must express my very profound gratitude to my parents and to my girlfriend for providing me with unfailing support and continuous encouragement throughout my years of study and through the process of researching and writing this thesis. This accomplishment would not have been possible without them. Thank you.

Abstract

In the pharmaceutical industry, many of the products such as tablets, capsules or dragees are in solid dosage form and require at least one drying process during their production. The selection of a proper drying technology depends on the properties of the material to be dried, such as their form, thermal sensitivity, drying kinetics, cohesiveness and others.

In this work, a continuously operating, indirect heated, contact paddle dryer prototype was tested and optimized for drying wet pharmaceutical powders, while not changing the particle size distribution.
Drying experiments were conducted with Ibuprofen ($x_{50} = 25\mu m$) as test substance. The feed material was prepared by addition of water up to a content of 30 wt.%. Homogenous blending of Ibuprofen with water was achieved with a high shear mixer. The drying performance was evaluated by variations in feed flow, water content of feed material, drying air flow rate and shaft speed. Based on the findings of the test runs the dryer was continuously modified to improve the drying process. The influence of the drying process on the powder properties was evaluated by particle size and flowability measurements. Samples were analyzed for raw, wet and dried Ibuprofen to investigate the impact of mixing and drying on powder properties. In addition, light microscopy images were recorded to detect particle agglomeration and/or attrition.

The particle size distribution of the Ibuprofen powder increased slightly after mixing with water due to agglomeration. Up to 99.6% of the moisture in the powder was removed by drying. Successful drying was achieved for feed flows up to 2.5 kg/h and a shaft speed of ~60 rpm. Higher feed flows resulted in blockage of the outlet. Higher shaft speed created a dusty environment in the dryer with increased evaporation rates, but led to a higher probability of blocking. A lower air flow rate resulted in a slightly higher water content of the dried product and a higher water load of the air. The flowability of the powder increased with increasing water content, resulting in fewer material accumulations in the dryer and therefore a lower hold-up. Steady state operation was reached only for a few test runs.
The Paddle configuration and the outlet design has to be enhanced for drying of different materials. Further improvements of the dryer are necessary to enable continuous drying of powder-like materials. In general, the drying technology is suitable to dry wet Ibuprofen powders without changing the particle size distribution.

Zusammenfassung

Viele Produkte in der pharmazeutischen Industrie wie Tabletten, Kapseln oder Dragees, liegen in fester Darreichungsform vor und benötigen während ihrer Produktion zumindest einen Trocknungsschritt. Die richtige Trocknungstechnologie hängt von vielen verschiedenen Materialeigenschaftes des Trocknungsgutes ab, wie z.B. die Form, Temperaturempfindlichkeit, Trocknungsgeschwindigkeit, Kohesivität des Materials, u.v.m.

In dieser Masterarbeit wurde ein Prototyp eines kontinuierlich betriebenen, indirekt beheizten Kontakt-Trockners für die Trocknung von pharmazeutischen Pulvern, ohne Änderung der Partikelgröße des Trocknungsgutes, getestet und optimiert.
Trocknungsversuche mit Ibuprofen ($x_{50} = 25\mu m$) als Testsubstanz wurden durchgeführt. Das Aufgabematerial wurde durch Zugabe von Wasser bis zu einem Wassergehalt von 30 Gew.% hergestellt. Homogenes Mischen von Wasser und Ibuprofen wurden durch einen Mischer mit hoher Scherwirkung erzielt. Die Fördermenge und der Wassergehalt des feuchten Materials, der Luftdurchsatz und die Umlaufgeschwindigkeit der Welle wurden auf ihre Auswirkungen auf den Trocknungsprozess untersucht. Basierend auf den Erkenntnissen der Trocknungsexperimente wurde der Trockner fortlaufend modifiziert und adaptiert. Der Einfluss des Trocknungsprozesses auf die Pulvereigenschaften wurde durch Partikelgrößen- und Fließfähigkeitsmessungen untersucht. Proben von unverarbeitetem, feuchtem und getrocknetem Ibuprofenpulver wurden analysiert um den Einfluss des Mischens und Trocknens auf die Pulvereigenschaften zu untersuchen. Zusätzlich wurde das Pulver unter einem Lichtmikroskop untersucht um Agglomeration und/oder Abrieb der Partikel festzustellen.

Durch Agglomeration der Partikel stieg die Partikelgrößenverteilung des Ibuprofenpulvers nach Mischen mit Wasser leicht an. Bis zu 99.6% der im Feedmaterial enthaltenen Feuchtigkeit wurden entzogen. Eine erfolgreiche Trocknung wurde mit Fördermengen von bis zu 2.5 kg/h und einer Umlaufgeschwindigkeit der Welle von ~60 rpm erzielt. Höhere Fördermengen verursachten Verstopfungen des Trocknerauslasses. Höhere Umlaufgeschwindigkeiten der Welle erzeugten viel Staub. Dies erhöhte leicht die verdampfte Menge an Wasser, führte aber zu einer höheren Verstopfungswahrscheinlichkeit des Trocknerauslasses. Geringe Luftdurchsätze erhöhten leicht den Wassergehalt des Produktes und der Luft. Das Fließverhalten des Ibuprofenpulvers wurde vor allem bei einem hohen Wassergehalt deutlich verbessert. Dies äußerte sich durch geringere Materialanhäufungen im Trockner und dadurch einem geringerem Hold-up. Ein stationärer Zustand wurde nur in wenigen Versuchen erreicht.
Die Paddelanordnung und die Gestaltung und Anordnung des Trocknerauslasses muss verbessert werden um verschiedene Trocknungsgüter zu trocknen. Weitere Verbesserungen des Trockners sind notwenig um ein kontinuierliches Trocknen von Pulver zu ermöglichen. Die getestete Trocknungstechnologie ist geeignet um feuchtes Ibuprofenpulver zu trocknen ohne die Partikelgrößenverteilung zu verändern.

Contents

List of Figures

List of Tables

List of Symbols

a	$-$	Slope
A_{out}	m^2	Area of the air outlet
AR	$\mu m/\mu m$	Aspect ratio
BFE	mJ	Basic flowability energy
C	vol %	Compressibility
$\acute{C}$	vol %	Compressibility without water
CI	$-$	Carr Index
E	mJ	Energy
F_{max}	μm	Maximal Feret diameter
F_{min}	μm	Minimal Feret diameter
f	$-$	Compression conversion constant
ffc	$-$	Flow function
G	kg/s	Mass flow of drying air
FRI	$-$	Flow rate index
H	$-$	Hausner Ratio
$Hold\text{-}up$	kg	Hold-up of the dryer
L	kg/s	Mass flow of product to be dried
m	kg, g	Mass
$m_{cond,i}$	kg	Mass of collected condensate between stop i and i-1
$m_{dried,out,i}$	kg	Mass of dried Ibuprofen that left the dryer between stop i and i-1
m_{dry}	kg	Dry mass
m_{evap}	kg, g	Total mass of evaporated water
$m_{evap,i}$	kg, g	Mass of evaporated water between stop i and i-1
m_{H_2O}	kg	Mass of water

$m_{\mathrm{H_2O}\,in\,air,i}$	kg	Mass of water in air that left the dryer between stop i and i-1
$m_{\mathrm{H_2O}\,lost\,air,i}$	kg	Mass of water that left the dryer with the lost air between stop i and i-1
m_{Ibu}	kg	Mass of dry Ibuprofen
$m_{in,i}$	kg	Mass that entered the dryer between between stop i and i-1
$m_{out,i}$	kg	Mass that left the dryer between between stop i and i-1
m_{split}	g	Mass of the Ibuprofen sample after the level procedure with a 50mm split vessel.
m_{total}	kg	Total mass
$m_{wet,in,i}$	kg	Fed mass of wet Ibuprofen between stop i and i-1
$\dot{m}_{air,in,i}$	kg/h	Average mass flow of drying air at the inlet of the dryer between stop i and i-1
$\dot{m}_{air,out}$	kg/h	Averaged measured mass flow of drying air at the outlet of the dryer of the whole test run
$\dot{m}_{air,out,i}$	kg/h	Average measured mass flow of drying air at the outlet of the dryer between stop i and i-1
$\dot{m}_{cond}$	g/h	Average measured condensate mass flow
$\dot{m}_{dried,out}$	kg/h	Average mass flow of dried product at the outlet of the dryer
$\dot{m}_{evap,meas}$	g/h	Average measured mass flow of evaporated water
$\dot{m}_{evap,th}$	g/h	Theoretical calculated mass flow of evaporated water
$\dot{m}_{\mathrm{H_2O}\,in\,air}$	g/h	Average measured mass flow of water in the air
$\dot{m}_{\mathrm{H_2O}\,lost\,air}$	g/h	Average measured mass flow of water in the lost air
$\dot{m}_{humid\,air,out}$	kg/h	Average measured mass flow of the humid exhaust air at the outlet of the dryer
$\dot{m}_{wet,in}$	kg/h	Average mass flow of the wet feed material
M	mol/g	Molar weight
M_{air}	mol/g	Molar weight of air
$M_{\mathrm{H_2O}}$	mol/g	Molar weight of water

n	mol	Amount of substance
P	Pa, bar	Pressure
P_{air}	Pa, bar	Partial pressure of Air
$P_{\mathrm{H_2O}}$	Pa, bar	Water vapor pressure
$P^s_{\mathrm{H_2O}}$	Pa, bar	Water vapor pressure at saturation
P_{lab}	Pa, bar	Ambient pressure in the laboratory
P_{norm}	Pa, bar	Normal pressure
P_{total}	Pa, bar	Total pressure
PM_{real}	μm	Perimeter of the real particle
PM_s	μm	Perimeter of the surface equivalent circle
$q_{r,i}$	$1/\mu$m	Density distribution of class i
$q_{3,i}$	$1/\mu$m	Volume density distribution of class i
$Q_{r,i}$	%	Cumulative distribution of class i
$Q_{3,i}$	%	Volume or mass distribution of class i
R	J/mol K	Gas constant
S	–	Sphericity
$Span$	–	Span of a particle size distribution
SE	mJ/g	Specific energy
SI	–	Stability index
t	min, h	Time
t_i	min, h	Time between two stops of the dryer
t_total	min, h	Total experiment time
T	°C, K	Temperature
$T_{air,out}$	°C, K	Average temperature of the humid exhaust air at the outlet of the dryer
T_{norm}	°C, K	Normal temperature
$v_{air,out,i}$	m/s	Average velocity of the humid exhaust air between stop i and i-1
V	m^3	Volume
V_0	ml	Total volume before compression

$V_{0,b}$	ml	Total volume of Ibuprofen before compression
$V_{0,w}$	ml	Total volume of water before compression
$V_{c,b}$	ml	Total volume of Ibuprofen after compression
$V_{c,w}$	ml	Total volume of water after compression
V_{end}	ml	Total volume after compression
$V_{\mathrm{H_2O}}$	ml	Volume of water vapor
V_{split}	ml	Volume of the Ibuprofen sample after the level procedure with a 50mm split vessel
$\dot{V}_{split}$	$\mathrm{Nm^3/h}$	Air flow
VMD	μm	Volume mean diameter
w	$\mathrm{kg_{H_2O}/kg_{total}}$	Water content based on total mass
$w_{dried,i}$	$\mathrm{kg_{H_2O}/kg_{total}}$	Water content of the dried product at stop i
w_{wet}	$\mathrm{kg_{H_2O}/kg_{total}}$	Water content of the wet feed material
$\acute{w}$	$\mathrm{kg_{H_2O}/kg_{dry}}$	Water content based on dry mass
x	μm	Particle size
x_{10}	μm	Volume or mass median diameter
x_{50}	μm	Volume or mass median diameter
x_{90}	μm	Volume or mass median diameter
$\bar{x}_i^*$	μm	Geometric mean diameter of class i
X_1	$\mathrm{g_{H2O}/kg_{dry}}$	Water load of feed material
X_2	$\mathrm{g_{H2O}/kg_{dry}}$	Water load of dried product
Y	$\mathrm{g_{H2O}/kg_{air}}$	Water load of air
$Y_{after\ filter}$	$\mathrm{g_{H2O}/kg_{air}}$	Averaged measured water load of the humid air after the filter
$Y_{air,out,i}$	$\mathrm{g_{H2O}/kg_{air}}$	Averaged measured water load of the humid air at the outlet of the dryer
Y_1	$\mathrm{g_{H2O}/kg_{air}}$	Water load of drying air at the inlet
Y_2	$\mathrm{g_{H2O}/kg_{air}}$	Water load of drying air at the outlet
Φ_i	$^\circ$	Internal angle of friction
Φ_c	$^\circ$	Angle of the effective yield locus

φ	%	Relative humidity
φ_i	%	Average relative humidity of the air between stop i and i-1
ρ	kg/m^3	Density
ρ_{air}	kg/m^3	Density of air
$\rho_{air,norm}$	kg/m^3	Density of air under normal conditions
ρ_b	kg/m^3	Bulk density of Ibuprofen
$\rho_{humid\,air}$	kg/m^3	Density of humid air
ρ_t	kg/m^3	Tapped density
ρ_{vapor}	kg/m^3	Density of water vapor
ρ_w	kg/m^3	Density of water
σ	kPa	Normal stress
σ_1	kPa	Principal normal stress
σ_c	kPa	Unconfined yield strength
σ_E	kPa	Normal stress at the end point of the yield locus
σ_M	kPa	Center of Mohr´s circle
σ_R	kPa	Radius of Mohr´s circle
$\sigma_{xx,st}$	kPa	Normal stress at the pre-shear point at steady state
τ	kPa	Shear stress
τ_0	kPa	Cohesion
τ_E	kPa	Shear stress at the end point of the yield locus
$\tau_{xy,st}$	kPa	Shear stress at the pre-shear point at steady state

1. Introduction

In this work, a continuously operating, indirect heated contact paddle dryer prototype from Hosokawa was tested and optimized for drying of wet pharmaceutical powders, while not changing the particle size distribution. As test substance, Ibuprofen with a mean particle size of 25 µm and a water content of up to 30 wt.% was used. The raw Ibuprofen was blended with water in a high shear mixer to form a wet powder for the drying experiments. At first, different paddle configurations and installations were tested to find the optimal setup for drying wet Ibuprofen with respect to mixing, the material transport and the residence time of the powder in the dryer. Afterwards the feed flow, water content, air flow rate and shaft speed were varied to investigate their influence on the drying performance. The drying capacity of the dryer and the residual water content of the dried product were determined. Experimental investigations of the particle size and flow behavior before and after drying were made. The drying technology should be designed that the particle size is not changed by drying (due to agglomeration or attrition of the particles). Also the influence of drying and the water content of the wet Ibuprofen powder on the flow behavior was tested with a powder rheometer.

1.1. Drying

The process of drying is one of the most energy intensive processes and plays an important role in various sectors, such as the food and the pharmaceutical industry and affects many economies worldwide [1]. The drying of solid materials, in the form of powders and granules, is a critical process in the manufacture of many types of chemical products [2].
Drying applications consume a large amount of the worlds produced energy and therefore require special attention to make them more efficient and environmentally friendly while they should also be cost-effective. All these dimensions need to be taken into account when a drying system is designed, analysed or assessed. Understanding drying processes requires the application of analysis methods from thermodynamics, heat, mass and momentum transfer, psychometrics, porous media, materials science and also chemical kinetics altogether. Drying of a wet material can take milliseconds or couple of months, depending on the drying conditions and material [1].

Approximately 75% of all chemical manufacturing processes involve particulate solids at some stage. In the pharmaceutical industry, transport, storage, and handling of particulate solids are especially important because nearly 80% of the products are in solid dosage form [3]. The drying process can influence different manufacturing steps such as tableting and encapsulation and can influence critical quality attributes of the final product [2]. The manufacture of a drug that will be distributed in non-liquid form such as tablets, capsules and dragees is carried out in three stages:

- Synthesis of intermediate products
- Final synthesis of the drug
- Manufacture of dosage forms

After each stage the products are dried. The selection of a proper drying technology for these products depends on the properties of the material such as their form, thermal sensitivity, drying kinetics, cohesiveness and others [4]. The reasons for drying are almost as diverse as the dried materials [5]. Foods are dried to inhibit microbial development and quality decay and to preserve them for storage and shipment without the need for refrigeration [5]. Drying may also be carried out to improve the handling characteristics of powders and to stabilize moisture-sensitive materials, such as pharmaceuticals [2].

Drying is a complex process involving transient heat and mass transfer to remove a solvent (in general water or moisture) from a solid or liquid. [2, 4, 5]. Therefore, drying is a thermal separation process and typically occurs by evaporation or sublimation of the solvent [1].
Drying is per definition a thermally driven process. The energy is transferred as heat from the surrounding environment or drying agent to the wet solid as a result of convection, conduction, radiation or a combination of these effects [4]. The heat evaporates the liquid in the wet solid, and the vapor is transferred into the surrounding gas [2]. Two main processes occur simultaneously during drying [4]:

- Heat transfer from the surrounding environment towards the moist material to evaporate the moisture at the material surface
- Transfer of the moisture inside the material to the surface

The fundamental mechanism of moisture transfer within a wet solid material can be separated into four modes of transfer [1]:

- Capillary flow of moisture in small interstices
- Moisture diffusion due to concentration gradients
- Vapor diffusion due to partial pressure gradients
- Diffusion in liquid layers adsorbed at solid interfaces

The heat evaporates the liquid in the product, and the vapor is transferred into the surrounding gas.

In figure 1.1 the moisture content (W) over time (t) of a typical drying process of a moist material is shown. During drying of a moist solid with heated air, the air supplies the necessary heat to evaporate the moisture and also acts as a drying agent and absorbs the evaporated water of the moist material. The first part of the process (A - B) in figure 1.1 shows the warming up of the solid, during which the solid surface conditions come into equilibrium with the drying air. General, this period consumes only a negligible amount of energy compared to the energy consumption of the overall drying cycle. The period A – B is governed mostly by transient heat transfer processes which can be diffusively or convectively controlled.

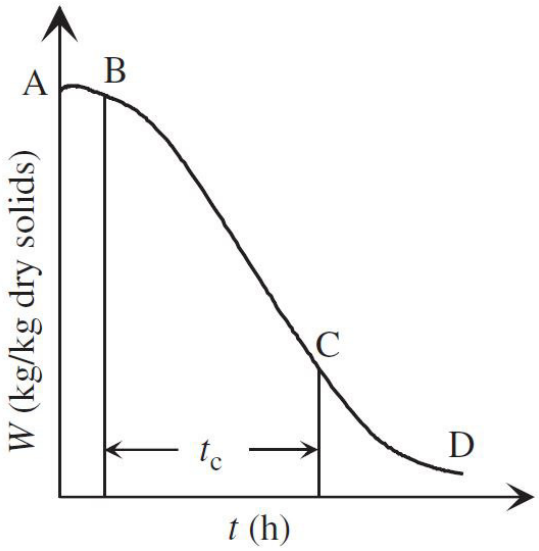

Figure 1.1.: Moisture content over time for a general case of drying a moist material [1].

The period B – C shows an approximately linear reduction of the moisture over time. During this phase, the saturated surface area decreases gradually. The constant drying rate period ends at point C, which is known as the point of critical moisture content. During the B - C period, the moisture inside the material moves to the surface with a rate as great as the rate of evaporation from the surface. Therefore the surface of the wet material remains saturated with liquid water. This period is controlled by the heat transfer and moisture transfer, the surface area that is exposed to the drying agent and the temperature and humidity gradient between drying agent and wet material. When the saturated moisture at the surface is completely evaporated, phase C – D follows. During this phase there is no evaporation at the surface. The moisture is transported by diffusion, followed by a convective mass transfer at the solid surface. From point C onward, the surface temperature begins to rise until the dry-bulb temperature of the air is reached [1].

1.1.1. Drying Technologies

There are many different types of drying systems and equipment that are used for drying products in the food, pharmaceutical and other industries. Drying systems are generally engineered to maximize the drying rate and mass transfer at the lowest costs possible. The operating conditions and drying agent must be well chosen. During the design of a drying system, many details and aspects require careful selection, analysis and evaluation [1].

Drying systems can be classified based on multiple points of view such as the drying agent, the application type, the main drying processes, the process continuity (batch or continuous) and the heat transfer. A classification criteria of drying systems is shown in figure 1.2. In general, air is used as drying agent, but also steam or carbon dioxide can be used. Continuous dryers are mainly used in chemical and food industries. The

most common continuous dryers are fluid-bed and spray dryers, especially in the pharmaceutical industry. Depending on the product and industry, also rotary dryers, drum dryers, kiln dryers, flash dryers, tunnel dryers and others are used [2]. In direct dryers, the heat transfer between the surface of the moist material and the drying agent is accomplished by direct contact. In indirect dryers, a wall is placed between the heat transfer fluid and the moist material. Therefore, the moist material is only in contact with the hot surface and not the drying agent. The rate of drying for indirect drying depends on the contact of the moist material with hot surfaces. In addition, better control of the operating conditions can be obtained. Furthermore, indirect drying is probably the best option to handle sensitive materials and if inert gas solvents or condensing solvents must be recycled. The vaporized liquid can be removed independently from the heating medium. The classification of indirect-contact dryers is shown in figure 1.3.

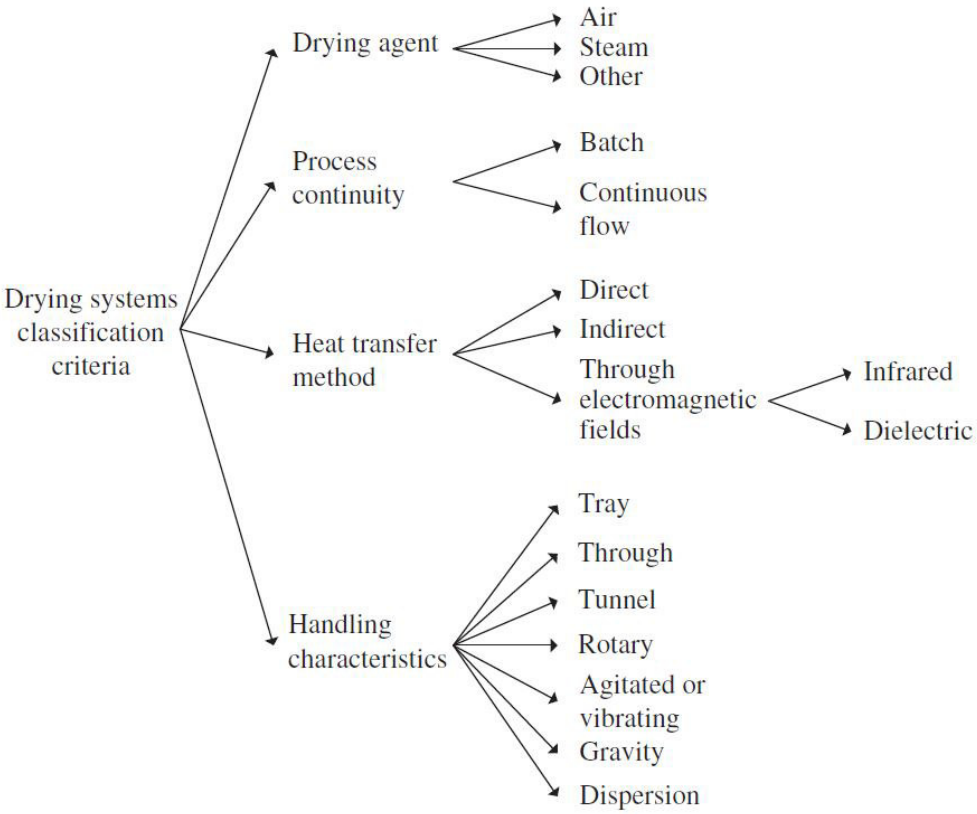

Figure 1.2.: Classification criteria of drying equipment and systems [1]

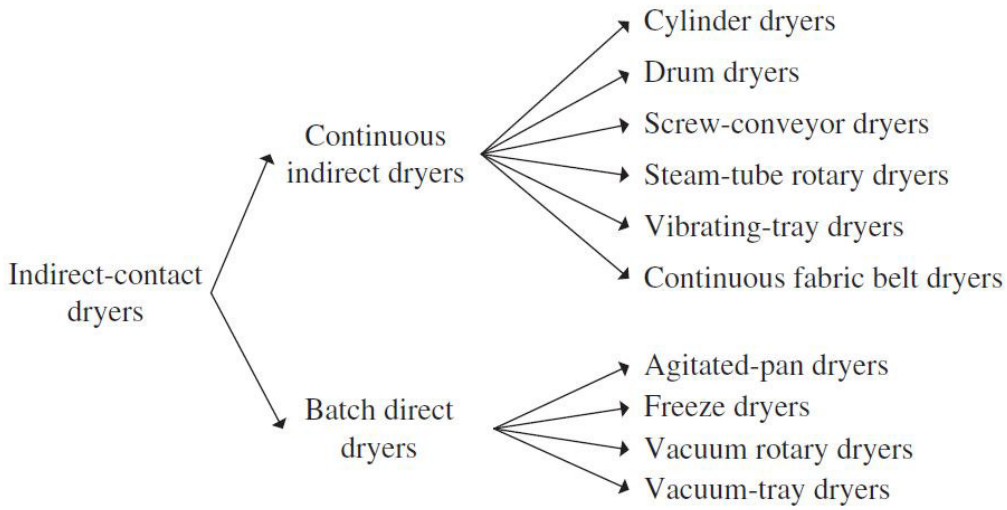

Figure 1.3.: Classification of indirect-contact dryers [1]

1.1.2. Mass Balance for Continuous Drying Processes

Continuous dryers are a closed system, therefore all the evaporated moisture from the product has to leave the dryer with the drying agent. An overall mass balance of a continuous dryer is shown in figure 1.4 and equation 1.1, where G and L are the mass flows of the drying air and the product to be dried, Y_1 and Y_2 are the water load of the air at the inlet and outlet of the dryer and X_1 and X_2 are the water load of the material to be dried at the inlet and outlet of the dryer.

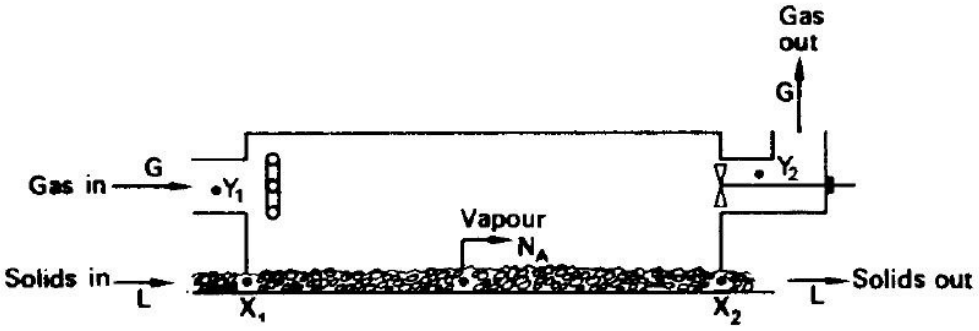

Figure 1.4.: Mass balance of a continuous drying process [5].

$$L \cdot (X_1 - X_2) = G \cdot (Y_2 - Y_1) \tag{1.1}$$

1.2. Moisture in Solid Materials and Gases

Moist materials can have different physical, chemical, structural, mechanical and other properties, depending on the state of water within the material. In wet powders, solid particles are bound by a liquid which can be in form of discrete liquid bridges or a continuous phase. Air inclusions between the particles also affect the flow properties of wet powders. Coulomb frictional forces at the particle contact points as well as the adhesive forces due to the surface tension of the liquid require high shear stresses to make wet powders flow. On the other hand, the binder liquid also reduces the coefficient of internal friction between the particles by acting as a lubricant on the particle surface [6, 7]. In general, a higher moisture content of a powder decreases its ability to flow [8]. One of the main causes is the increased thickness of the adsorbed liquid layer, which also increases the strength of liquid bridges between the particles [8]. The van der Waals forces are strengthened by adsorbed moisture because the thickness of the moisture layer decreases the inter-particle distance. On the other hand, electrostatic forces decrease with increasing moisture content because of the conductive properties of water.
Water in powders can be in different physical states:

- Adsorbed monolayer or multilayers on the surfaces of the particle
- Condensed water on the particle surface
- Physically absorbed water within the particle
- Chemisorbed water

The state and distribution of the water in the powder depends on different properties and the water content of the powder [9].

For drying processes, the moisture content of a material is generally determined based on the dry material $\acute{w}$, where $m_{\mathrm{H_2O}}$ is the mass of H_2O and m_{dry} is the mass of dry material (equation 1.2). In addition, the water content w can be related to the total mass m_{total} (equation 1.3) [1].

$$\acute{w} = \frac{m_{\mathrm{H_2O}}}{m_{dry}} \tag{1.2}$$

$$w = \frac{m_{\mathrm{H_2O}}}{m_{total}} = \frac{m_{\mathrm{H_2O}}}{(m_{\mathrm{H_2O}} + m_{dry})} \tag{1.3}$$

The moisture content based on dry and wet material is connected by equation 1.4 and 1.5.

$$w = \frac{\acute{w}}{1 + \acute{w}} \tag{1.4}$$

$$\acute{w} = \frac{w}{1 - w} \tag{1.5}$$

The relevant thermodynamic parameters for moisture and humidity in gases are:

- pressure (water vapor pressure or total gas pressure of a system)
- gas temperature
- the concentration

The transition between thermodynamic equilibrium states of the water vapor in a monoatomic gas can be described by the ideal gas law (equation 1.6).

$$P \cdot V = n \cdot R \cdot T = \frac{m \cdot R \cdot T}{M} \tag{1.6}$$

For water vapor in air, this equation can be rewritten as shown in equation 1.7.

$$P_{\mathrm{H_2O}} \cdot V_{\mathrm{H_2O}} = n_{\mathrm{H_2O}} \cdot R \cdot T = \frac{m_{\mathrm{H_2O}} \cdot R \cdot T}{M_{\mathrm{H_2O}}} \tag{1.7}$$

The total pressure of a mixture of gases is the sum of the partial pressures of all gas components. For water vapor in air this can be expressed by equation 1.8.

$$P_{total} = P_{air} + P_{\mathrm{H_2O}} \tag{1.8}$$

The amount of moisture or humidity of a gas can be expressed by the water load of the dry gas, which is the ratio of the mass of water vapor to the mass of dry gas. For water vapor in air, equation 1.9 can be used to calculate the water load of air.

$$Y = \frac{m_{\mathrm{H_2O}}}{m_{dry\,air}} = \frac{P_{\mathrm{H_2O}}}{(P_{total} - P_{\mathrm{H_2O}})} \cdot \frac{M_{\mathrm{H_2O}}}{M_{air}} = \frac{\varphi \cdot P^s_{\mathrm{H_2O}}}{(P_{total} - \varphi \cdot P^s_{\mathrm{H_2O}})} \cdot \frac{M_{\mathrm{H_2O}}}{M_{air}} \tag{1.9}$$

The relative humidity is the ratio of the partial pressure of the vapor in the air to the saturation vapor pressure at a given gas temperature. The relative humidity is normally expressed as a percentage (equation 1.10).

$$\varphi = \frac{P_{\mathrm{H_2O}}}{P^s_{\mathrm{H_2O}}} \cdot 100\% \tag{1.10}$$

1.3. Particle Size Analysis

The particle size is of central importance in many areas of technology such as pharmaceuticals (drugs and excipients), foods (grain, flour, sugar), materials technology (ceramics, abrasives) and building materials (sand and cement). Nearly all solid materials in common use are at some point in a powder or granular form. The main reason for analysing the particle size is its influences on the physical properties and flowability as well as the way they behave in various production processes [10].
Some influences of particle size on the behavior of pharmaceuticals are [10]:

- The particle size influences the dissolution. Small particles dissolve faster than large ones. This is important for determining the behavior of the drug in the body and also in various manufacturing processes.
- The flow properties of powders are strongly dependent on particle size and shape. Since most powders are transported from one place to another by flowing, the control of the flow behavior is very important. Generally, coarse, roughly spherical particles flow much more easily than small or elongated particles.
- The deposition of airborne particles on surfaces depends on the particle size. This is of considerable significance in the study of aerosol formulations and their deposition in the various regions of the lung.
- The stability of dispersions (suspensions, emulsions) depends on the size of the dispersed material. The forces between colloidal particles depend on their dimensions, and the settling rates of larger particles depend on their size and density.

The size for spherical particles can be described by a length, such as the diameter. In practical applications, it is unlikely that the particles are spherical. Usually equivalent diameters are used to represent the diameter of a sphere, which behaves as the real (non-spherical) particle. As an example, the volume equivalent sphere is the sphere which has the same volume as the irregular particle and is characterized by the volume equivalent diameter. Geometrical and physical properties can be used to describe an equivalent diameter. There are different possibilities to define equivalent diameters and many of them have their origins in some practical particle sizing measurement, such as the Stokes equivalent diameter. All of the equivalent diameters have different values for a given irregular particle. To obtain a good description of the particle system, the equivalent diameter should be selected based on the relevant property of the particle [10].

There are many measurement techniques available to analyse the size of bulk solids and powders, such as [11]:

- Sieve analysis
- Air elutriation analysis
- Photoanalysis
- Sedimentation techniques
- Laser diffraction

1.3.1. Laser Diffraction

In the classical setup of a laser diffraction (LD) sensor the particles interact with the laser light in a parallel laser beam. The intensity of the light scattered by a particle is directly proportional to the particle size and can be calculated with the Fraunhofer or Mie diffraction theory [12]. Large particles scatter light with high intensity through low angles and small particles scatter light with low intensity through high angles [13, 14]. In all laser diffraction systems for particle size measurement a radial variation of the intensity pattern of the diffracted light is recorded [15]. The optical setup of the HELOS laser diffraction sensor is shown in figure 1.5.

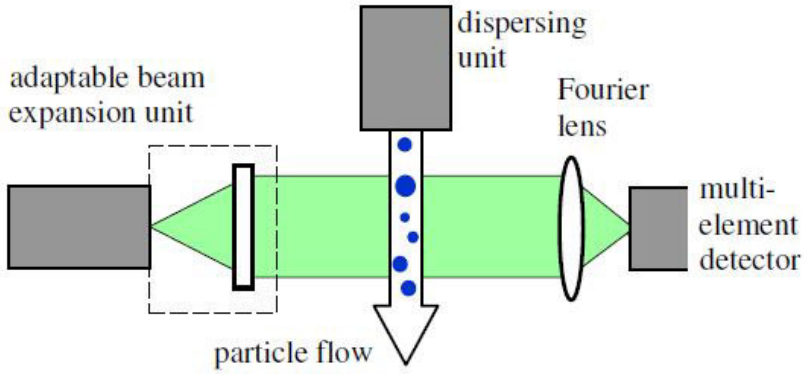

Figure 1.5.: Optical set-up of the HELOS laser diffraction sensor [16].

Diffraction is a valid approximation if the particles are opaque and their shapes are sufficiently represented by their two-dimensional projection areas. For non-spherical particles the LD method reports a size distribution in which the predicted diffraction pattern for the volumetric sum of spherical particles matches the measured diffraction pattern [15]. It is generally difficult to interpret the relationship between the obtained diffraction pattern and the equivalent size distribution in the case of non-spherical particles [16].

Fine powders tend to form agglomerates which behave very differently compared to dispersed particles. Therefore it is essential to disperse the particles before they are measured. For successful dispersion of the particles, sufficient separating forces have to be applied to overcome the inter-particle forces, such as van der Waals forces, electrostatic forces and forces due to liquid bridges. The relative strength of these forces increases with decreasing particle size, therefore finer powders are more difficult to handle [17].
Two different principles are usually applied to disperse particle: Wet and dry dispersion. During dry dispersion, the sample being analyzed is injected into a compressed air stream within a venturi nozzle. The pressure drop across the venturi nozzle is adjusted to apply enough energy to cause dispersion without breaking the particles. The dispersion pressure must be carefully adjusted to ensure complete de-agglomerate without primary particle breakage [17]. The goal is to maximize dispersion while minimizing attrition.
Wet dispersion requires the particles to be dispersed in a suitable liquid. The particles

are dispersed (de-agglomeration) in the liquid by wetting of the surface of the particle and a gentle shear force through stirring.

1.3.2. Particle Size Distribution

A particle size distribution (PSD) can be displayed as a table or a diagram (see figure 1.6) [18]. In the simplest case, the measured particle sizes are divided into size intervals and the particles are sorted into the corresponding size classes.

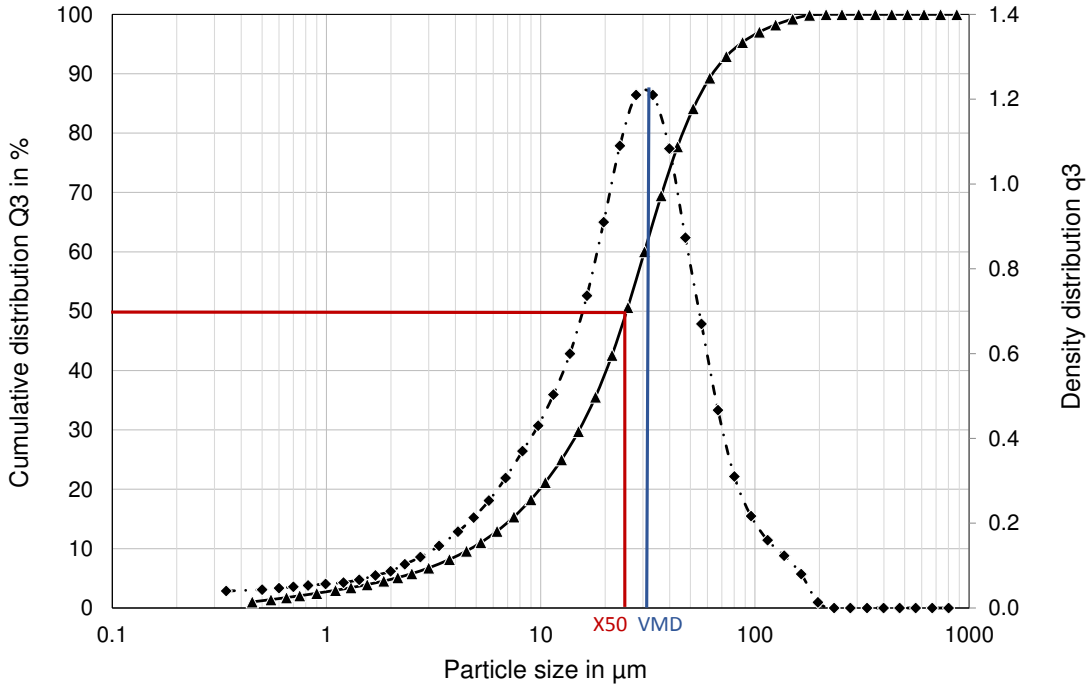

Figure 1.6.: Density distribution q3 and cumulative distribution Q3 of raw Ibuprofen particles.

The fractions in the different size classes are summed and normalized to 100%, resulting in the cumulative distribution $Q(x)$. For a given particle size, x, the Q-value represents the percentage of the particles finer than x. There are four different quantity measure of a distribution [11]:

- $Q_0(x)$, $q_0(x)$: number distribution
- $Q_1(x)$, $q_1(x)$: length distribution
- $Q_2(x)$, $q_2(x)$: area (surface) distribution
- $Q_3(x)$, $q_3(x)$: volume or mass distribution

The normalization of the fraction $\Delta Q_{r,i}$ to the size of the corresponding interval Δx_i leads to the density distribution $\bar{q}_{r,i}$ expressed by equation 1.11.

$$\bar{q}_{r,i} = \frac{\Delta Q_{r,i}}{\Delta x_i} \tag{1.11}$$

If the cumulative distribution $Q_r(x)$ is differentiable, the density distribution function $q_r(x)$ can be calculated as the first derivative of $Q_r(x)$ vs. x expressed by equation 1.12.

$$q_r(x) = \frac{dQ_r(x)}{dx} \tag{1.12}$$

On the other hand, the cumulative distribution can be calculated by integrating the density distribution function $q_r(x)$ from x_{min} to x_{max} expressed by equation 1.13.

$$Q_r(x) = \int_0^x q_r(x) \cdot dx \tag{1.13}$$

Particle size distributions are often plotted on a logarithmic abscissa. While the $Q_r(x)$ values remain the same, care has to be taken for the transformation of the distribution density $q_r(x)$. The corresponding areas under the density distribution curve has to remain 1 or 100%, independent of the transformation of the abscissa. The transformation has to be performed with equation 1.14, or for class i with equation 1.15. Also the value for the density distribution $\bar{q}_r^*$ for the class $\log(x_{l,i}), \log(x_{u,i})$ is located at the geometric mean of the class (see equation 1.16).

$$q_r^*(\log(x)) = \frac{dQ_r(x)}{d\log(x)} \tag{1.14}$$

$$\bar{q}_r^*(\log(x_{l,i}), \log(x_{u,i})) = \frac{\Delta Q_{r,i}}{\log(\frac{x_{u,i}}{x_{l,i}})} \tag{1.15}$$

$$\bar{x}_i = \sqrt{x_{u,i} \cdot x_{l,i}} \tag{1.16}$$

The volume mean diameter (VMD) can be calculated with equation 1.17 or 1.18.

$$VMD = \sum_{i=1}^{n} \bar{x}_i \cdot q_{r,i} * \Delta x_i = \sum_{i=1}^{n} \bar{x}_i \cdot \Delta Q_{r,i} \tag{1.17}$$

$$VMD = \int_{x_{min}}^{x_{max}} x \cdot q_r(x) \cdot dx \tag{1.18}$$

1.4. Flow Properties of Powders

Powders and bulk solids have to be handled or stored in nearly all industries, from nano-scale powders and pharmaceutical substances to products like cement, coal, and ore, from dry materials like fly ash to moist bulk solids like filter cake and clay. All these materials have to be transported, or handled otherwise [19]. The flow properties of powders through a given process can change, often resulting in blockages or poor quality products [20, 21]. Therefore the characterization of powders and bulk solids regarding their flow properties plays an important role for product development and optimization [19, 20].
It is still not possible to accurately predict the flow behavior of a powder from knowledge of particle size, shape or moisture content [22]. Powder rheometers can provide fast, repeatable and sensitive measurements with a high degree of automation [20]. Their primary purpose is the characterization of flow properties and measure data to design equipment for storage, transportation or general handling of bulk solids. Flowability measurements are also needed to compare the flowability of similar or competing bulk solids [23]. Although there are numerous characterization techniques and tests available, the right one has to be selected for the specific application [24].

The flowability of fine powders (below 30 µm) depends largely on the adhesive forces between individual particles. Adhesive forces are the main source of poor flowability, caking and agglomeration [24]. Adhesive forces are caused by different mechanisms such as van der Waals interactions, electrostatic forces and liquid bridges between particles. The van der Waals forces are based on electric dipoles of atoms and molecules. Their intensity depends on the particle size and distance as well as on the materials of the interacting surfaces. Electrostatic forces are based on different electric potentials of particle surfaces. In moist bulk solids, liquid bridges between the particles are usually the most important adhesive forces. Due to the surface tension of the liquid, the particles are attracted to each other. The influence of adhesive forces on flow behavior increases with decreasing particle size [19].

The flow properties of bulk solids and powders depend on the following parameters, amongst others:

- particle size distribution
- particle shape
- water content (moisture)
- temperature
- chemical composition

It is not possible to determine the flow behavior of bulk solids and powders as a function of all of these parameters. Therefore it is necessary to determine the flow properties in appropriate testing devices [19].
There are various methods available to measure the powder flow such as the angle of repose, bulk density, tapped density, Carr's index, Hausner ratio, cohesivity determination, shear cell test, compressibility test, dielectric imaging, atomic force microscopy,

penetrometry and many others. All these methods have different drawbacks and limitations including their reproducibility, performance conditions, and predictability [25].

2. Materials and Methods

2.1. Materials

2.1.1. Ibuprofen 25

For all drying test runs Ibuprofen was used as model substance. Ibuprofen is a chiral propionic acid derivate and belongs to the class of non-steroidal anti-inflammatory drugs. In the Biopharmaceutics Classification System (BCS) it belongs to Class II, which means high permeability and low solubility.
Ibuprofen is used to treat inflammatory conditions such as rheumatoid arthritis, osteoarthritis, ankylosing spondyolitis, mild to moderate pain, dysmenorrhoea, vascular headache and fever [26].

Ibuprofen was obtained from BASF SE (Ludwigshafen, Germany) with a mean particle size of about 25 µm. It is a white, slightly transparent, crystalline powder with a melting point of 75 to 78 °C and a molecular weight of 206.28 g/mol. The bulk and the tapped density are approximately 0.3 and 0.47 kg/m^3.
The structural formula is shown in figure 2.1, the empirical formula is $C_{13}H_{18}O_2$.

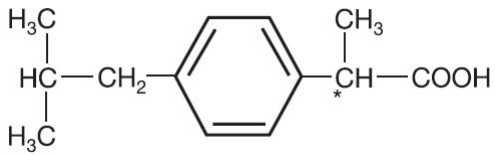

Figure 2.1.: Structural formula of Ibuprofen [26]

2.1.2. Sodium Pyrophosphate Tetrabasic

Sodium pyrophosphate tetrabasic (SPT) was used as a surfactant to lower the surface tension of water, which was used to moisturize the raw Ibuprofen for the drying test runs. Ibuprofen is hydrophobic [27] and therefore a lower surface tension results in a better wettability [28] of the surface of the Ibuprofen particles.

Sodium pyrophosphate tetrabasic (purity $\geq$ 95 %) was obtained from Sigma-Aldrich (St. Louis, Missouri, USA). Its structural formula is shown in figure 2.2, the empirical formula is $Na_4O_7P_2$.

For test runs V5 and V6 8 g/l of SPT was added to the water and dissolved under continuous stirring with a spoon. For all other test runs (V7 - V19) pure water was used to moisten the raw Ibuprofen. It was possible to achieve a homogeneous mixture

of water and Ibuprofen without addition of SPT with a high shear mixer.

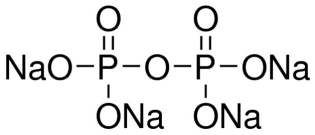

Figure 2.2.: Structural formula of Sodium pyrophosphate tetrabasic [29]

2.1.3. Tween 80

Tween 80 is a synthetic, non-ionic surfactant and emulsifier. It is water-soluble and was used to prepare samples of Ibuprofen for particle size measurements with wet dispersion with the Helos KR laser diffraction sensor (see chapter 2.2.6.1).

Tween 80 was obtained from Sigma-Aldrich (St. Louis, Missouri, USA). Its structural formula is shown in figure 2.3, the empirical formula is $C_{64}H_{124}O_{26}$.

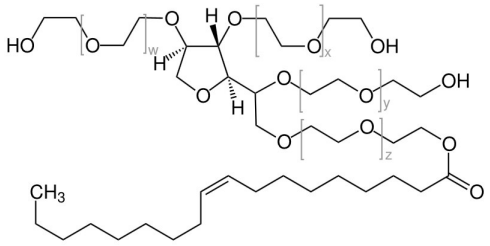

Figure 2.3.: Structural formula of Tween 80 https://de.wikipedia.org/wiki/Polysorbat_80 (28.06.2017)

2.1.4. Iron(III)oxide

Iron(III) oxide (Fe_2O_3) is a ferromagnetic, dark red solid. Fe_2O_3 is often used as a non-toxic pigment. It was obtained from Sigma-Aldrich (St. Louis, Missouri, USA) and was used as tracer in all residence time test runs (V1 to V4). Its molecular weight is 159.69 g/mol.

2.1.5. Water

Deionized water was used to moisturize the raw Ibuprofen for the drying test runs. It was also used in combination with Tween 80 to disperse the Ibuprofen particles for particle size measurements in wet dispersion mode in a cuvette.

For the heating of the dryer mantle and shaft as well as for cooling of the condenser normal tap water was used. The water for heating of the dryer was heated in a Thermo Haake® C10 heating circulator from Thermo Electron Corp (Waltham, Massachusetts, USA) to 55°C for V10 to V19 and 60 °C for V5 to V9. The temperature of the cooling water for the condenser was about 19°C to 20°C for all test runs.

2.1.6. Compressed Air

Compressed and dry air from the compressed air system was used as drying agent for all test runs. The air pressure was adjusted with a pressure regulator and the air flow rate was set with a DK800 PV variable area flowmeter from Krohne (Duisburg, Germany). The air was blown into the dryer on the bottom side of the rotary valve through a 90° fitting, shown in figure 2.4. The air flow should also prevent a fill-up of the rotary valve chambers with Ibuprofen particles.

Figure 2.4.: Top view on the air inlet under the rotary valve at the dryer inlet.

2.2. Methods

2.2.1. Feed Material Preparation

For all drying test runs raw Ibuprofen was moisturized with deionized water. To disperse the deionized water in the hydrophobic Ibuprofen powder a UMC 5 high shear mixer from Stephan (Hameln, Germany), shown in figure 2.5, was used.

The bowl of the Stephan mixer was weighed on a precision scale (Mettler Toledo MS8001TS/00) with an accuracy of 0.1 g. 500 to 1000 g of raw Ibuprofen was filled into the bowl. The appropriate weight of water was calculated, based on the dry mass of Ibuprofen (equation 2.2) for test run V5 to V9 and based on the total mass of wet Ibuprofen (equation 2.1) for test run V10 to V19. Both calculated water content values, w and $\acute{w}$, for all test runs are shown in table 2.1. The raw Ibuprofen was mixed with the added water with an agitator speed of 2250 rpm (75% of maximal rpm) for one minute and three seconds (three seconds to speed up the rotating knives), while continuously turning the hand mixing baffle with about 30 rpm. The prepared wet Ibuprofen was then stored in sealable barrels to minimize the evaporation of water.

Figure 2.5.: Stephan Mixer UMC 5. http://www.foodmachinedeals.com/en/detail/2 (28.06.2017)

$$w = \frac{m_{\mathrm{H_2O}}}{m_{total}} = \frac{m_{\mathrm{H_2O}}}{(m_{\mathrm{H_2O}} + m_{Ibu})} \tag{2.1}$$

$$\acute{w} = \frac{m_{\mathrm{H_2O}}}{m_{Ibu}} \tag{2.2}$$

Table 2.1.: Water contents of wet Ibuprofen of each test run. V5 - V9: Preperation based on dry mass of Ibuprofen ($\acute{w}$). V10 - V19: Preperation based on total mass of wet Ibuprofen (w). 8g SPT per 1 kg of water was dissolved in the added water for test run V5 and V6.

Test run	w [kg/kg$_{total}$]	ẃ [kg/kg$_{dry}$]	SPT [g/kg$_{H2O}$]
V5	9.1%	10%	8.0
V6	9.1%	10%	8.0
V7	16.7%	20%	-
V8	9.1%	10%	-
V9	23.1%	30%	-
V10	10%	11.1%	-
V11	10%	11.1%	-
V12	10%	11.1%	-
V13	10%	11.1%	-
V15	30%	42.9%	-
V18	10%	11.1%	-

2.2.2. Temperature Tests

After test run V9 a temperature experiment has been carried out to investigate the temperature deviation between the temperatures measured by the temperature sensors of the thermostats and the real temperatures inside the dryer. During test run V6 and V7 molten Ibuprofen was observed at the dryer outlet due to overheating of the equipment, although the temperature of the outlet was set to 60°C. The melting point of Ibuprofen (75.0 - 77.5°C) was exceeded.

The temperatures of the lid, filter and outlet were controlled with three electronic line sensing thermostats (Raychem AT-TS-14). Due to the closed design of the dryer it was not possible to place the temperature sensors of the thermostats at the correct positions inside the dryer. Therefore, the temperature sensors to control the temperature of the lid and outlet were placed on the top side of the lid and the sensor of the filter was placed inside a hole in the filter housing. The outlet was isolated and mantled, therefore it was not possible to place the sensor for the outlet heating in a meaningful way.

To measure the real temperatures inside the dryer, thermocouples (type K) from Reckmann (Hagen, Germany) were fixed with aluminum tape on specific locations as shown in figure 2.6 (a,b,c). The thermocouple of the outlet was fixed with aluminum tape in the middle of the inner wall of the outlet pipe. There is no picture of the thermocouple in the outlet-pipe because the thermocouple location was difficult to access with the camera.

The temperature sensor of the thermostat for the filter and lid were placed at the same position as in the previous test runs (V5 - V9) and were fixed with aluminum tape. To improve temperature regulation of the outlet, the sensor for the outlet was fixed with aluminum tape inside the housing of the outlet pipe, direct on the outer wall of the pipe as shown in figure 2.6 (d).

The shaft and housing of the dryer were heated with water at 55°C and a volume flow of 65 l/h each. The first temperature set points were 40 °C for the filter, 45°C for the lid and 35°C for the outlet. The system was heated up for one hour to achieve constant temperatures. After one hour the temperature of the outlet was changed to 40°C via the thermostat. After two hours the temperature of the lid was changed to 50°C and after three hours the temperature of the filter was changed to 45°C. The temperatures inside the dryer (outlet, lid, filter and shaft)were measured with thermocouples and were recorded with a Testo 176 T4 datalogger from Testo (Lenzkirch, Germany).

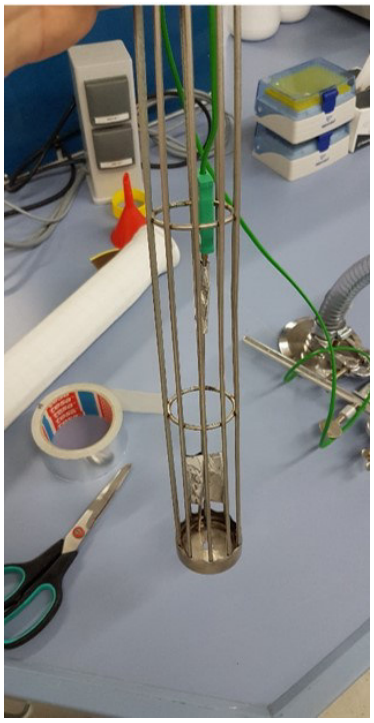

(a) Filter

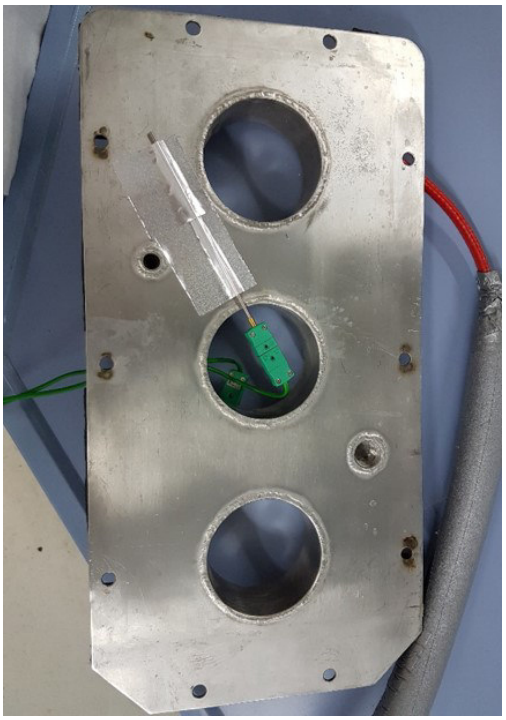

(c) Lid

(b) Shaft

(d) Outlet

Figure 2.6.: Placement of the thermocouple to measure the temperature (a) inside the filter, (b) on the outer wall of the shaft, (c) on the inner side of the lid and (d) the inner side of the outlet.

2.2.3. Paddle dryer prototype

In this work a continuously operated, indirect heated paddle dryer prototype from Hosokawa Micron (Doetinchem, Netherlands) (figure 2.7) was optimized for drying wet powders. Paddles dryers are suitable for paste-like and granular materials. In general, paddle dryers are heated with steam, but the dryer used in this work was heated with hot water (housing and shaft) and electricity (lid, filter and outlet). A horizontal rotating shaft, with paddles mounted on it, mixed and transported the material through the dryer. The solvent (water) was condensed and collected in a flask.

Figure 2.7.: Drying test run set up of the dryer prototype (Hosokawa)

2.2.4. Drying Experiments

All drying experiments were carried out using the dryer prototype from Hosokawa Micron (Doetinchem, Netherlands). Wet Ibuprofen was fed with a KT20 feeder with a K-SFS-24 scale and fine concave twin-screws (0.1 - 9 dm^3/h) from Coperion K-tron (Stuttgart, Germany) into the rotary valve of the dryer. After passing the rotary valve, the wet material fell into the dryer where it was transported through the dryer by the paddles on the rotating shaft. The shaft speed of the dryer was adjusted with a Flender gear. At the end of the dryer the material was ejected by the paddles into the outlet pipe. The dried material was collected in the product bin.
Compressed air at room temperature was used as drying agent. The pressure of the air was adjusted with a pressure regulator and the air flow was set with a DK800 PV variable area flowmeter From Krohne (Duisburg, Germany). The air was blown into the dryer under the rotary valve through a 90° fitting as shown in figure 2.4, to prevent a fill-up of the rotary valve chambers with Ibuprofen powder. The air flow through the dryer was introduced in co-current mode to the wet Ibuprofen and absorbed the evaporated water from the material. The humid air left the dryer through a filter, to prevent any Ibuprofen particles from leaving the dryer with the air flow. The humid air was cooled in the condenser and the condensate was collected in a flask. The condensate mass was weighed with a MS8001SE precision balance from Mettler Toledo (Columbus, Ohio, USA). Figure 2.9 (a) shows the measurement of the temperature and water load of the exhaust air at the outlet of the flask with a MI70 measurement indicator and a HMP75 humidity and temperature probe, both from Vasaila (Vantaa, Finland) in figure 2.9 (a). The average velocity of the wet exhaust air was measured for 1 min (right before the individual stop) at the condenser outlet with a Testo 425 thermal anemometer from Testo (Lenzkirch, Germany) shown in figure 2.9 (c).

The housing and shaft of the dryer were heated with hot water using a Thermo Haake® C10 heating circulator. The water flow through the shaft and housing was regulated separately with two DK800 N variable area flowmeters from Krohne (Duisburg, Germany). The temperature of the heating water was measured at the inlet and outlet of the shaft and housing with Typ-K thermocouples (± 2.2°C precision) and recorded with a Testo 176-T4 datalogger. The lid, outlet and filter were heated electrical with heating cables and regulated with three electronic line sensing thermostats (Raychem AT-TS-14) with temperature sensors. The temperature right after the filter was measured with a Typ-K thermocouple and a PCE-T390 thermometer from PCE (Meschede, Germany) (see 2.9 (b)) to be able to calculate the relative humidity of the air after the filter (position of maximal water load of the air).

The test run set up of the dryer and auxiliary devices are show in figure 2.7. The flow sheet of the dryer together with all auxiliary devices (PID-diagram) is shown in figure 2.8.

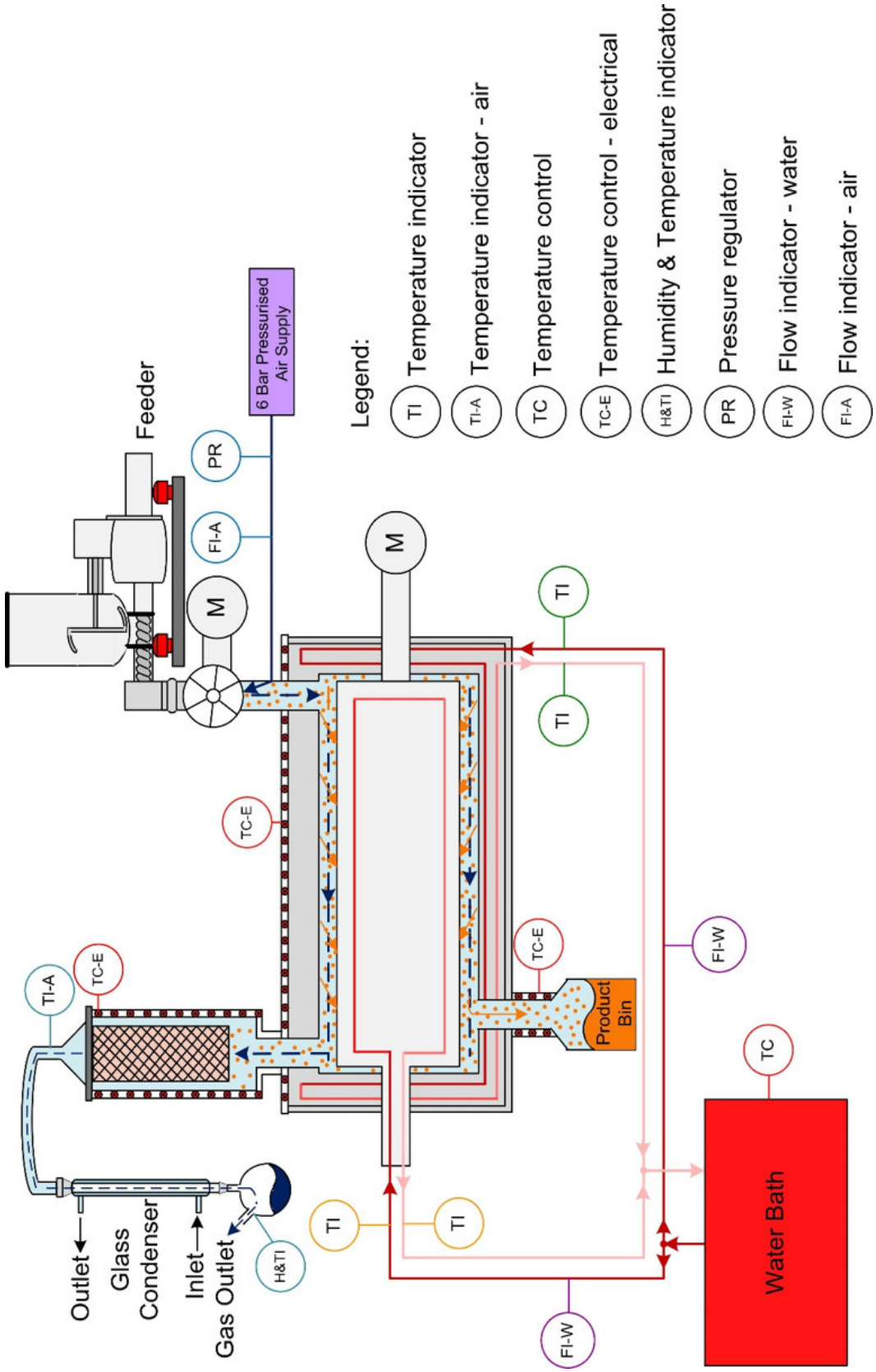

Figure 2.8.: Flow sheet of the test run set up of the dryer prototype (Hosokawa)

(a)

(b)

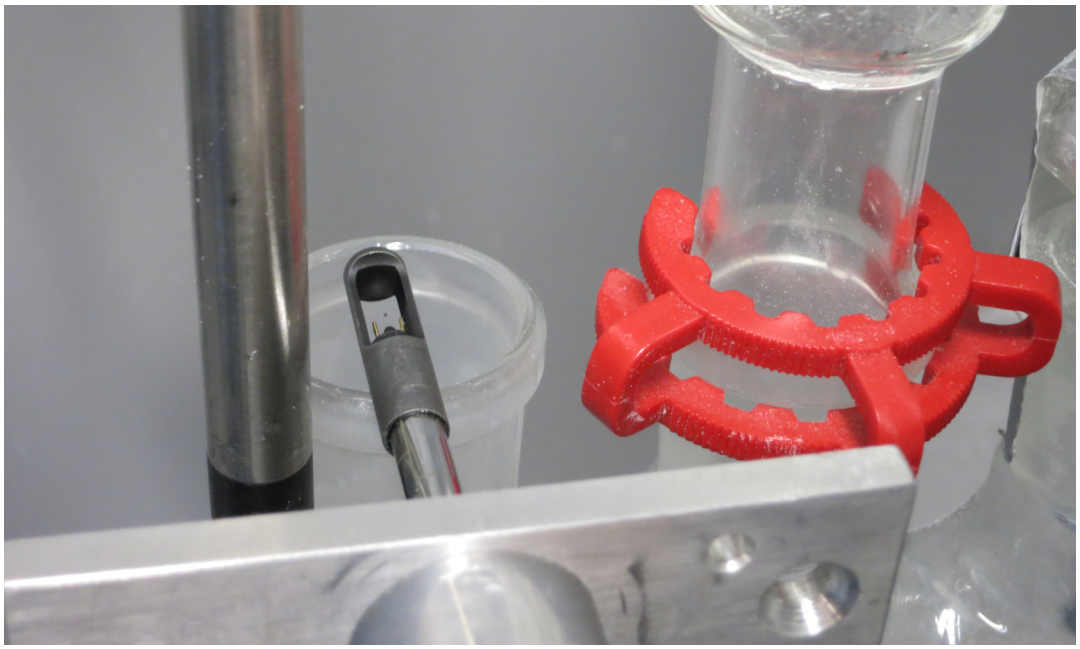

(c)

Figure 2.9.: (a): Measurement of water load and temperature of the wet exhaust air with a measurement indicator (Vaisala MI70) and a humidity and temperature probe (Vaisala HMP75). (b): Temperature measurement of hot exhaust air after the filter. (c): Measurement of the average velocity of the wet exhaust air, at the condenser outlet, with the thermal anemometer (Testo 425).

All experimental settings of test run V5 to V19 are shown in table 2.2.

Table 2.2.: Experimental settings for test run V5 to V19

Test run	Feed material	Water content w [wt.%]	Feed flow $\dot{m}_{Feed,in}$ [kg/h]	Shaft speed n [rpm]	Air flow $\dot{V}$ [Nm³/h]	Temperature [°C]				Water flow	
						Lid	Filter	Outlet	Water	Shaft $\dot{m}_{H2O}$ [l/h]	Housing $\dot{m}_{H2O}$ [l/h]
V5	Ibuprofen	9.0%	5.0 and 2.5	60	-	60	60	60	60	148	
V6	Ibuprofen	8.8%	2.5	60	-	60	30	60	60	148	
V7	Ibuprofen	16.0%	2.5	60	3.7	60	40	60	60	148	
V8	Ibuprofen	8.4%	2.5	60	3.7	60	40	35	60	148	
V9	Ibuprofen	22.9%	2.5	60	3.7	60	40	35	60	148	
V10	Ibuprofen	7.1%	1.25	60	3.7	50	40	40	55	70	70
V11	Ibuprofen	7.7%	2.5	120	3.7	50	40	40	55	65	65
V12	Ibuprofen	9.4%	1.25	120	3.7	50	40	40	55	65	65
V13	Ibuprofen	9.5%	1.25	60	1.8	50	40	40	55	65	65
V15	Ibuprofen	29.7%	1.25	60	3.7	50	40	40	55	65	65
V16	Ibuprofen	19.3%	1.25	60	3.7	50	40	40	55	65	65
V17	Ibuprofen	10.2%	1.25	60	3.7	50	40	40	55	65	65
V18	Ibuprofen	8.9%	1.25	60	1.4	50	40	40	55	varied	varied
V19	Ibuprofen	9.5%	1.25	60	1.8	50	40	40	55	2.5	2.5

After a transient time of one to two hours to reach steady state (depending on the feed flow rate), the drying test runs were stopped at specific times to note the fed mass of wet Ibuprofen ($m_{wet,in,i}$), weigh the mass of dried Ibuprofen that left the dryer ($m_{dried,out,i}$), weigh the mass of condensate ($m_{cond,i}$) and to take samples of the dried material to calculate the hold-up as well as the water content of the dried product over time. The hold-up of the dryer was calculated with equation 2.3 where $m_{\mathrm{H_2O}\,in\,air,i}$ is the mass of water that left the dryer with the humid air at the outlet, $m_{\mathrm{H_2O}\,lost\,air,i}$ is the mass of water that left the dryer with the lost air and i is the number of stops.

$$Hold\text{-}up = \sum_{i=1}^{N} m_{wet,in,i} - m_{dried,out,i} - m_{cond,i} - m_{\mathrm{H_2O}\,in\,air,i} - m_{\mathrm{H_2O}\,lost\,air,i} \tag{2.3}$$

The mass of water that left the dryer with the humid air $m_{\mathrm{H_2O}\,in\,air,i}$ was calculated with equation 2.4, where $Y_{air,out,i}$ is the average measured water load of the humid air at the outlet of the dryer, $\dot{m}_{air,out,i}$ is the measured mass flow of drying air at the outlet of the dryer and t_i is the time between the two stops.

$$m_{\mathrm{H_2O}\,in\,air,i} = Y_{air,out,i} \cdot \dot{m}_{air,out,i} \cdot \frac{t_i}{60\ (min/h)} \tag{2.4}$$

The mass flow of drying air at the outlet $\dot{m}_{air,out,i}$ was calculated with equation 2.5. The velocity of the humid exhaust air ($v_{air,out,i}$) was measured at ambient conditions for wet air. The velocity was first multiplied with the outlet area A_{out} (diameter: 3 cm) and 3600 s/h to obtain the volume flow in m^3/h. The Volume flow was then converted to standard conditions for dry air (1.013 bar and 273.15 K) and multiplied with the density ($\rho_{air,norm}$) to obtain the mass flow. P_{H2O} was calculated with the Antoine equation with the temperature of the wet air at the outlet.

$$\dot{m}_{air,out,i} = v_{air,out,i} \cdot A_{out} \cdot 3600\ (s/h) \cdot \frac{(P_{lab} - \varphi_i \cdot P_{\mathrm{H_2O}})}{P_{norm}} \cdot \frac{T_{norm}}{T_{air,out}} \cdot \rho_{air,norm} \tag{2.5}$$

It was not possible to measure the water load of the lost air, therefore it was assumed that the water load of the lost air is the same as the water load of the air after the filter. The water load of air after the filter ($Y_{after\ filter}$) was calculated with equation 2.7, where m_{evap} is the total evaporated water (condensate and water in air) of the whole test run, calculated with equation 2.8 and t_{total} is the total experiment time.
The water in the lost air was calculated with equation 2.6

$$m_{\mathrm{H_2O}\,lost\,air,i} = Y_{after\ filter} \cdot (\dot{m}_{air,in,i} - \dot{m}_{air,out,i}) \cdot \frac{t_i}{60\ (min)} \tag{2.6}$$

$$Y_{after\ filter} = \frac{m_{evap} \cdot 60\ (min/h)}{\dot{m}_{air,out} \cdot t_{total}} \tag{2.7}$$

$$m_{evap} = \sum_{i=1}^{n}(m_{cond,i} + m_{\mathrm{H_2O}\,in\,air,i}) \tag{2.8}$$

In test runs V5 to V9 the velocity, temperature and water load of the humid exhaust air was not measured, therefore it was not possible to calculate the mass of water in air and lost air. The mass of water that left the dryer with the air (for test run V5 to V9 air means air at the outlet of the dryer and the lost air) was estimated with equation 2.9, where w_{feed} is the water content of the wet Ibuprofen, $w_{dried,i}$ is the water content of the dried Ibuprofen and $m_{cond,i}$ is the mass of condensate.

$$m_{\mathrm{H_2O}\,in\,air,i} = m_{wet,in,i} \cdot (w_{wet} - w_{dried,i}) - m_{cond,i} \tag{2.9}$$

The mass flow of the wet Ibuprofen $\dot{m}_{wet,in}$ was either recorded with the XAMControl software from Evon (Gleisdorf, Austria), or calculated by the mass difference and time between two stops (equation 2.10). The mean mass flow of dried Ibuprofen $\dot{m}_{dried,out}$ was calculated with 2.11. For the calculation of the mean mass flow of dried Ibuprofen only mass flow values after reaching a steady state were used.

$$\dot{m}_{wet,in} = \frac{1}{n} \cdot \sum_{i=1}^{n} \frac{m_{wet,in,i} \cdot 60\ (min/h)}{t_i} \tag{2.10}$$

$$\dot{m}_{dried,out} = \frac{1}{n} \cdot \sum_{i=1}^{n} \frac{m_{dried,out,i} \cdot 60\ (min/h)}{t_i} \tag{2.11}$$

The mass flow of the humid exhaust air $\dot{m}_{humid\,air,out}$ was calculated with equation 2.12, where $\rho_{humid\,air}$ is the density of the humid air at the outlet. $\rho_{humid\,air}$ was calculated with equation 2.13, where $P_{\mathrm{H_2O}}$ is the vapor pressure of water at the measured outlet temperature and φ is the averaged measured relative humidity of the exhaust air of the whole test run.

$$\dot{m}_{humid\,air,out} = \frac{1}{n} \cdot \sum_{i=1}^{n} v_{air,out,i} \cdot A_{out} \cdot 3600\ (s/h) \cdot \rho_{humid\,air} \tag{2.12}$$

$$\rho_{humid\,air} = \rho_{vapor} + \rho_{air}$$

$$\rho_{humid\,air} = \frac{M_{\mathrm{H_2O}} \cdot \varphi \cdot P_s}{R \cdot T} + \frac{M_{air} \cdot (P - \varphi * P_s)}{R \cdot T}$$

$$\rho_{humid\,air} = \frac{1}{R \cdot T} \cdot (M_{\mathrm{H_2O}} \cdot \varphi \cdot P_{\mathrm{H_2O}} + M_{air} \cdot (P - \varphi * \mathrm{H_2O})) \tag{2.13}$$

The mean mass flows of the condensate $\dot{m}_{cond}$, water in air $\dot{m}_{\mathrm{H_2O}\,in\,air}$ and water in lost air $\dot{m}_{\mathrm{H_2O}\,lost\,air}$ were calculated with equation 2.14 to 2.16 for the whole test run.

$$\dot{m}_{cond} = \frac{1}{n} \cdot \sum_{i=1}^{n} \frac{m_{cond,i} \cdot 60\ (min/h)}{t_i} \tag{2.14}$$

$$\dot{m}_{\mathrm{H_2O}\,in\,air} = \frac{1}{n} \cdot \sum_{i=1}^{n} \frac{m_{\mathrm{H_2O}\,in\,air,i} \cdot 60\ (min/h)}{t_i} \tag{2.15}$$

$$\dot{m}_{\mathrm{H_2O}\,lost\,air} = \frac{1}{n} \cdot \sum_{i=1}^{n} Y_{after\ filter,i} \cdot (\dot{m}_{air,in,i} - \dot{m}_{air,out,i}) \cdot \frac{t_i}{60\ (min)} \tag{2.16}$$

The mean mass flow of the measured evaporated water $\dot{m}_{evap,meas}$ consisted of the measured water in the humid exhaust air $\dot{m}_{\mathrm{H_2O}\,in\,air}$ as well as the measured condensate flow $\dot{m}_{cond}$ and was calculated with equation 2.17.

The mean mass flow of evaporated water $\dot{m}_{evap,th}$ was also calculated theoretical with the fed mass of wet Ibuprofen and the water content of wet and dried material (equation 2.18).

$$\dot{m}_{evap,meas} = \dot{m}_{cond} + \dot{m}_{\mathrm{H_2O}\,in\,air} \tag{2.17}$$

$$\dot{m}_{evap,th} = \frac{\sum_{i=1}^{n} m_{wet,in,i} \cdot (w_{wet} - w_{dried,i}) \cdot 60\ (min)}{t_{total}} \tag{2.18}$$

For test runs V10 to V19 mass balances of Ibuprofen, water and air were calculated. The mass balance with all in- and outgoing masses is shown in figure 2.10.

The mass balances were calculated based on the total mass of each substance that entered or left the dryer during the whole test run. All of the Ibuprofen entered the dryer through the feeder and left the dryer as dried product. The difference between the total in- and outgoing mass remained in the dryer (hold-up). All of the water entered the dryer with the wet Ibuprofen and left the dryer with the exhaust and lost air, the condensate and also the dried product (residual moisture of the product). The water content of the hold-up was the calculated by subtracting the total amount of outgoing water from the total amount of ingoing water. All of the air was blown into the dryer at the inlet and left the dryer with the humid exhaust air and lost air.

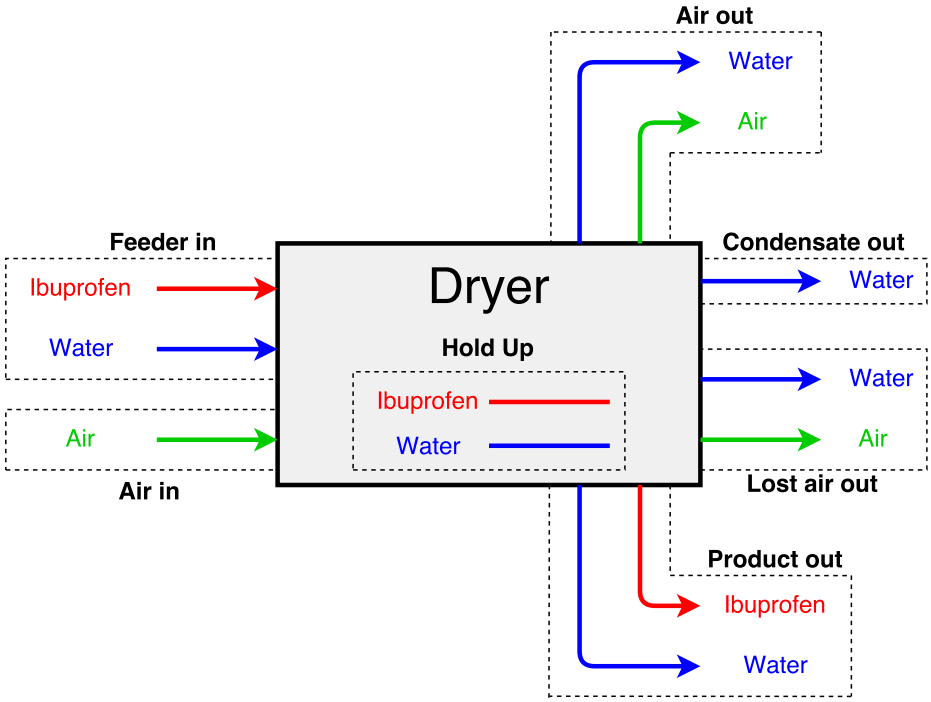

Figure 2.10.: Schematic representation of the mass balance of the dryer with all ingoing and outgoing masses

2.2.5. Water Content

The water content of wet (feed) and dried (after drying) Ibuprofen was measured gravimetrically (triple determination). Samples of 5 to 7 g were put on a petri dish and weighed with one of the following analytical scales: BP 121S from Sartorius (Göttingen, Germany),AW 224 from Sartorius or SI-243A from Denver Instruments (Bohemia, NY, USA). All analytical scales had the same accuracy of 0.1 mg.

The samples were dried in a VD 115 vacuum drying chamber from Binder (Tuttlingen, Germany) at 50°C for at least 24 hour. Vacuum was generated with a PC 500 series chemistry vacuum pump from Vacuubrand (Wertheim, Germany) and set to 63 mbar. The water content was then calculated based on the mass difference before and after drying in the vacuum chamber with equation 2.19.

$$w = \frac{m_{wet} - m_{dry}}{m_{wet}} \tag{2.19}$$

2.2.6. Particle Size Distribution

Particle size distribution measurements were made to investigate the influence of mixing (moisturizing of the raw Ibuprofen with water in a high shear mixer), drying (flow through the dryer) and the water content on the particle size of the powder. Raw (supplier), wet (after mixer) and dried (after drying) Ibuprofen, with a water content w of up to 30 wt.%, was investigated.

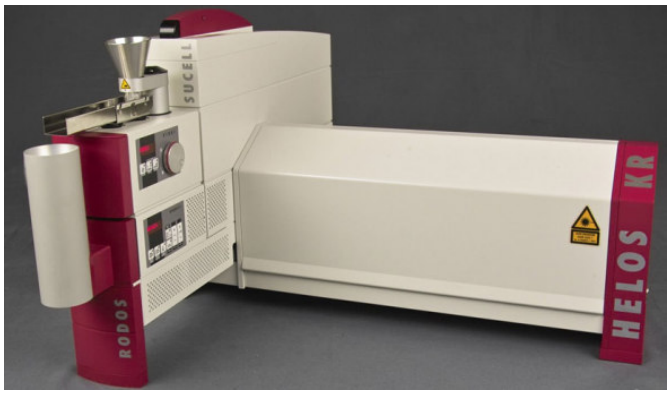

Figure 2.11.: Laser diffraction sensor HELOS/BR for dry dispersion. http://www.sympatec.com/EN/LaserDiffraction/HELOS.html (28.06.2017)

2.2.6.1. Wet Dispersion

For the wet particle size distribution measurement a laser diffraction sensor (Sympatec HELOS/BR) with a cuvette chassis platform and a 50 ml cuvette was used. The cuvette was filled with 50 ml deionized water and placed on the cuvette chassis platform. The stirrer speed was set to 1000 rpm. Before each measurement a reference measurement was done.

About 10 ml Tween 80 were added to 500 ml of deionized water and stirred with a magnetic stirrer (Phoenix Instruments RSM-10HP) at 750 rpm until all of the Tween 80 was dissolved. The Ibuprofen sample was put on a disposable weighing pan made of polystyrene. The Tween 80 solution was added to the Ibuprofen sample with a pasteur pipette and mixed with a spatula until a paste-like mixture was achieved. This was done to moisten the surface of the Ibuprofen particles and break agglomerates, for a better dispersion of the particles in water.

A small amount of the Ibuprofen paste was added to the water in the cuvette with a spatula until an optical concentration of 20 to 30 %. The particles were measured with a measuring range of R2 (0.45 - 87.5 µm) and R5 (4.5 - 875 µm) and combined to a single particle size distribution. The evaluation of the particle size distributions was done with FREE (Fraunhofer Enhanced Evaluation).

2.2.6.2. Dry Dispersion

For the dry particle size distribution measurement a Laser diffraction sensor (Sympatec HELOS/BR) with a dry feeder (VIBRI/L), dry disperser (RODOS/L) in the lower part and a special adaptation SUCELL/L on the upper part was used (figure 2.11). The Ibuprofen particles were measured at 0.5, 1.0, 1.5 and 2.0 bar (air injection pressure). After each pressure change of the system the "auto-adjust depression" function was executed. Before each measurement a reference measurement was done.

One tablespoon of the Ibuprofen sample was fed into the funnel of the feeder. The particles were measured with a measuring range of R2 (0.45 - 87.5 µm) and R5 (4.5 - 875 µm) and combined to a single particle size distribution. The evaluation of the particle size distributions was done with FREE (Fraunhofer Enhanced Evaluation).

2.2.7. Particle Shape (optical)

Both (wet and dry) particle size measurements with laser diffraction are not able to provide any information of the shape of the particles. Particle breakage or abrasion through mixing or drying would change the shape of the particles. To investigate a possible influence of mixing and drying on the particles, a high speed image analysis sensor (Sympatec QICPIC/R) with a dry feeder (VIBRI/L), dry disperser (RODOS/L) in the lower part and a special adaptation SUCELL/L on the upper part was used (figure 2.12). The primary measuring information of image analysis method is the contour (shape) of a particle (two-dimensional).

Figure 2.12.: High speed image analysis sensor system QICPIC/R. http://www.sympatec.com/EN/ImageAnalysis/QICPIC-R.html (28.06.2017)

To quantify the shape of the particles the sphericity (equation 2.21) and the aspect ratio (equation 2.20) of raw, wet and dried Ibuprofen was calculated and compared.

$$S = \frac{PM_s}{PM_{real}} = \frac{2 \cdot \sqrt{\pi \cdot A_s}}{PM_{real}} \tag{2.20}$$

PM_s is the perimeter of the surface equivalent circle and PM_{real} is the perimeter of the real particle.

$$AR = \frac{F_{min}}{F_{max}} \tag{2.21}$$

F_{min} is the minimal and F_{max} the maximal Feret diameter of a particle.

2.2.8. Microscopy

Samples of raw, wet and dried Ibuprofen particles were observed under a microscope (Leica DM4000 M)(shown in figure 2.14) to investigate if mixing or drying had influence on the particle shape and surface texture due to abrasion or breakage of Ibuprofen particles. Pictures of raw, wet and dried Ibuprofen of test run V10 were recorded at 5x and 20x magnification. In addition, pictures of wet and dried Ibuprofen, which was dried for 48 h in a vacuum drying chamber at 60°C and 63 mbar, were recorded.
The samples were placed on a microscopy slide with a spatula. To break the particle clusters (see figure 2.13) a second microscopy slide was placed on top of the sample and was carefully moved horizontal to spread the particles. After spreading the top microscopy slide was removed. All pictures were taken without the top microscopy slide.

All pictures were taken using dark-field microscopy with a light intensity of 224. The aperture diaphragm was set to 3. For 5x magnification an exposure time of 130 ms was used. Gain was set to 1.0, saturation to 70 and gamma to 0.50. At 20x magnification the gamma value was changed to 0.50. For post processing of pictures with 5x magnification the black content was set to 28 and the white level to 240. For pictures with 20x magnification the black content was set to 11 and the white level to 220.

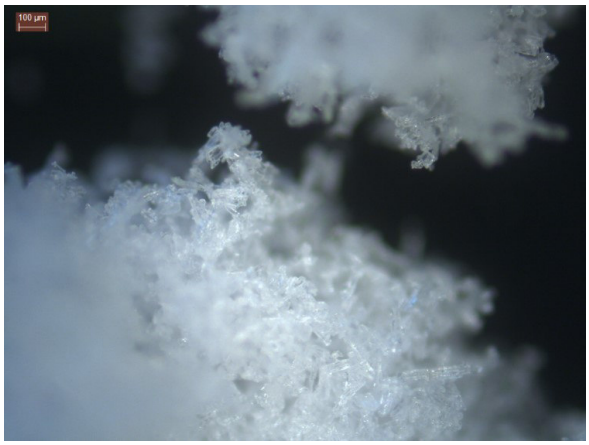

Figure 2.13.: Ibuprofen cluster of raw material before the distribution of the particles on the microscopy slide.

Figure 2.14.: Leica DM4000 M microscope. http://www.leica-microsystems.com/de/produkte/lichtmikroskope/industrie-materialanalyse/aufrechte-mikroskope/details/product/leica-dm4000-m/ (28.06.2017)

2.2.9. Powder Rheology

To characterize the influence of the drying and mixing process as well as the water content of the powder on the flow behavior, the flowability of the powder was determined with different test programs of a powder tester (Freeman technology FT4 powder rheometer) shown in figure 2.15.
Due to the complexity of granular materials there is no single test method to completely characterize the physical properties of a powder [24, 30].

The stability, variable flow rate, compressibility as well as the shear cell test of the raw, wet and dried ibuprofen were analyzed, using the standard test programs of the FT4. For all tests the 50 mm split vessel from Freeman Technology was used. The stability and variable flow rate and compressibility tests were done twice and three times for the shear cell test. The results of the individual tests were averaged.

Figure 2.15.: Freeman Technology FT4 powder rheometer. http://www.freemantech.co.uk/_powders/ft4-powder-rheometer-universal-powder-tester (28.06.2017)

2.2.9.1. Basic Flowability Energy (BFE), Specific Energy (SE), Stability and Variable Flow Rate

The stability and variable flow rate program of the FT4 was used to measure the BFE, SE, Stability Index (SI) and Flow Rate Index (FRI). The BFE is a key parameter that is highly sensitive and differentiating in relation to small differences in flow properties [31]. The SE is a measure of how easily a powder will flow in an unconfined or low stress environment. It is calculated from the energy needed to establish a particular flow pattern in a conditioned, precise volume of powder. The flow pattern of this measurement is an upward clockwise motion of the blade, which generates a gentle lift and low stress flow. The SE is calculated from the work done in moving the blade through the powder from bottom to top of the vessel. Gravity dominates in this test, so to compensate for varying bulk densities the flow energy is expressed as specific energy and normalised by the mass of powder. The SE depends primarily on the shear forces acting between particles. Cohesion is often the most influential property in low stress environments [31].

In this test the powder was conditioned with a rotating blade to homogenize the powder sample. The homogenised sample was split to level the sample volume at 90 ml as shown in figure 2.16. With the mass and volume of the split sample the conditioned

bulk densitiy ρ_b can be calculated (equation 2.26). The sample was then conditioned and tested seven times. The flow pattern of the test cycle is a downward anti-clockwise motion of the blade with a tip speed of 100 mm/s, generating a compressive, relatively high stress flow mode in the powder (figure 2.17 (a)). The BFE was calculated (equation 2.22) from the work done by moving the blade through the powder from the top to the bottom of the vessel[32].

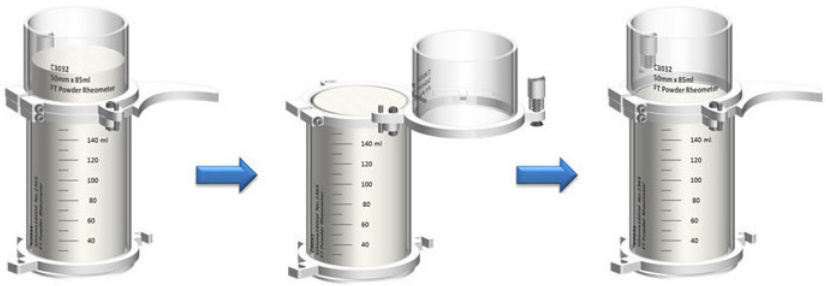

Figure 2.16.: Level procedure of the 50 mm split vessel. http://www.freemantech.co.uk/_powders/powder-testing-bulk-properties (28.06.2017).

The upward flow pattern is a clockwise motion of the blade, generating gentle lifting and low stress flow of the powder (figure 2.17 (b)). The SE was calculated (equation 2.23) from the work done in moving the blade through the powder from the bottom of the vessel to the top. To see if the powder is going to change as a result of being made to flow, the stability index (SI) was calculated with equation 2.24.

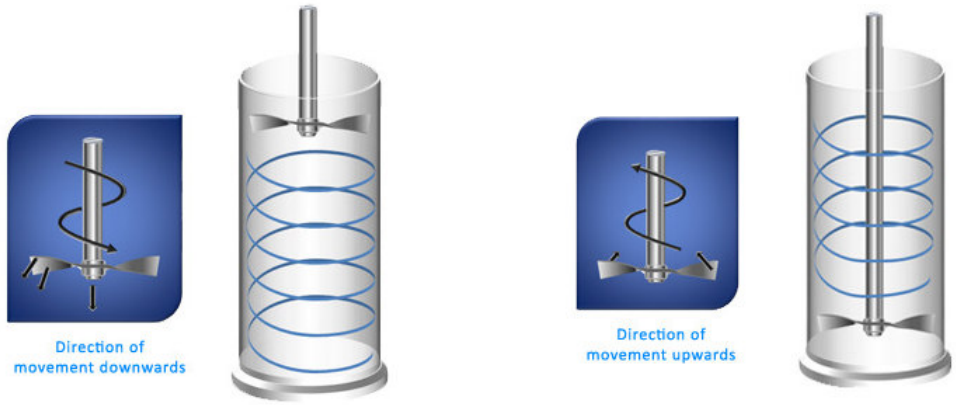

(a) (b)

Figure 2.17.: (a): Downward blade movement. (b): Upwards blade movement. http://www.freemantech.co.uk/_powders/powder-testing-confined-and-unconfined-powder-flow (28.6.2017).

After the stability test four additional test cycles, with varying tip speed (100, 70, 40 and 10 mm/s), were executed. To evaluate the sensitivity of a powder to flow rate changes, the flow rate index (FRI) was calculated with equation 2.25. It is common

that cohesive powders are more sensitive to changes in flow rate than non-cohesive or granular materials, mainly as a result of the higher air content in the cohesive materials [33].

$$BFE = E_{Test\,7}\ (mJ) \tag{2.22}$$

$$SE = \frac{(E_{Test\,6\,(up)} + E_{Test\,7\,(up)})/2}{m_{split}} \tag{2.23}$$

$$SI = \frac{E_{Test\,7}}{E_{Test\,1}} \tag{2.24}$$

$$FRI = \frac{E_{Test\,11}}{E_{Test\,8}} \tag{2.25}$$

$$\rho_b = \frac{m_{split}}{V_{split}} \tag{2.26}$$

2.2.9.2. Compressibility

The Compressibility is a bulk property measurement and describes the characteristics of how density changes as a function of applied normal stress. It is influenced by many factors such as particle size distribution, cohesivity, particle stiffness, shape and surface texture [34]. The Compressibility is not a direct measure of the flowability of a powder, but is a useful indicator whether a powder has a cohesive flow behavior or not [31].

In the compressibility test three conditioning cycles with a blade were executed to homogenize the powder sample, followed by splitting to level the sample at 90 ml. With a vented piston the sample was compressed under increasing normal stress up to 15 kPa (figure 2.18). The compressibility was calculated with equation 2.27 where V_0 is the initial volume of the powder and V_{end} is the volume of the powder after applying a specific normal stress i.

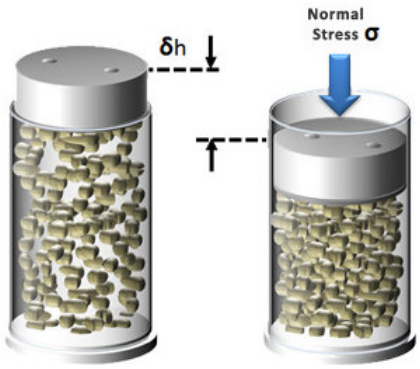

Figure 2.18.: The measurement of Compressibility. http://www.freemantech.co.uk/_powders/powder-testing-bulk-properties (28.6.2017).

$$C = \frac{V_0 - V_{end}}{V_0} \tag{2.27}$$

To compare the results of compressibility of raw, wet and dried Ibuprofen, the compressibility without water was calculated with equation 2.28 to 2.31 for wet and dried Ibuprofen from the original compressibility and a conversion constant f (equation 2.32).

The volume in the compressibility equation was first split into the wet and dried volume. Due to the incompressibility of water the volume of water before and after compression stays the same.

$$C = \frac{V_0 - V_c}{V_0} = \frac{(V_{0,b} + V_{0,w}) - (V_{c,b} + V_{c,w})}{(V_{0,b} + V_{0,w})} = \frac{(V_{0,b} - V_{c,b})}{(V_{0,b} + V_{0,w})} \tag{2.28}$$

The above term can be rewritten as:

$$\frac{(V_{0,b} - V_{c,b})}{(V_{0,b} + V_{0,w})} = \frac{(V_{0,b} - V_{c,b})}{V_{0,b}} \cdot \frac{1}{1 + \frac{V_{0,w}}{V_{0,b}}} \Rightarrow C = \acute{C} \cdot f \tag{2.29}$$

With

$$V_{0,w} = \frac{m_{total} \cdot w}{\rho_w} \tag{2.30}$$

$$V_{0,b} = \frac{m_{total} \cdot (1 - w)}{\rho_b} \tag{2.31}$$

f can be expressed by

$$f = \frac{1}{1 + \frac{V_{0,w}}{V_{0,b}}} = \frac{1}{1 + \frac{w \cdot \rho_b}{(1-w) \cdot \rho_w}} \tag{2.32}$$

- C Compressibility
- $\acute{C}$ Compressibility without water
- V_0 Total volume before compression
- V_{end} Total volume after compression
- $V_{0,b}$ Total volume of Ibuprofen before compression
- $V_{0,w}$ Total volume of water before compression
- $V_{c,b}$ Total volume of Ibuprofen after compression
- $V_{c,w}$ Total volume of water after compression
- f Conversion constant to convert the compressibility with without water
- m_{total} Total mass of tested sample
- ρ_b Bulk density of Ibuprofen
- ρ_w Density of water
- w Water content

2.2.9.3. Shear Cell Test

In the shear cell test the powder was first conditioned and pre-sheared to achieve a consistent and homogenised powder sample. The homogenised sample was split to level the sample volume at 90 ml. Then the sample was put under a constant normal stress of 9.0 kPa to compact the sample using the vented piston. With the shear head the sample was pre-sheared under the same normal stress (9.0 kPa) until a constant shear stress for 20 seconds was reached to increase repeatability between the tests. The powder sample was then placed under a lower normal stress and sheared again, until incipient failure occurs. The process of pre-shearing and shearing was repeated for all normal stresses (7.0, 6.0, 5.0, 4.0 and 3.0 kPa). The principal schematic of the shear cell test is shown in figure 2.19 (a). The shear cell of the FT4 powder rheometer is shown in figure 2.19 (b). The measured shear stresses defined the points on the yield locus of the powder.

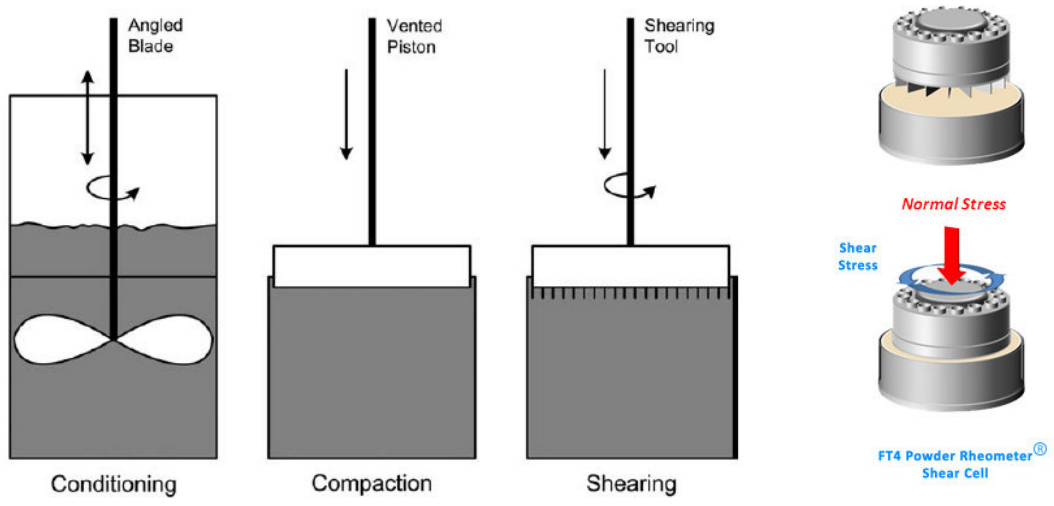

Figure 2.19.: (a): Schematic of the shear cell test using the FT4 Powder Rheometer [24]. (b): FT4 powder rheometer shear cell. http://www.freemantech.co.uk/_powders/powder-testing-shear-cells (28.06.2017).

The linear equation with the slope a (equation 2.33) of the yield locus was calculated via linear regression of the measured shear points. By extrapolating the yield locus to zero normal stress the cohesion τ_0 was obtained at the intersection point of the yield locus and the shear stress axis (ordinate). All following equations are taken from [11].

$$\tau = \tau_0 + a \cdot \sigma \tag{2.33}$$

The internal angle of friction ϕ_i was calculated with equation 2.34.

$$\phi_i = \arctan(a) \tag{2.34}$$

The unconfined yield strength σ_c was calculated wit equation 2.35.

$$\sigma_c = 2 \cdot \tau_0 \cdot \tan(\frac{\pi}{4} + \frac{\phi_i}{2}) \tag{2.35}$$

The center of Mohr´s circle for pre-shearing σ_M was calculated with equation 2.36 where $\sigma_{xx,st}$ and $\tau_{xy,st}$ are the normal and shear stress at the pre-shear point at steady state.

$$\sigma_M = [\sigma_{xx,st} \cdot (1+a^2) + a \cdot \tau_0] - \sqrt{[\sigma_{xx,st} \cdot (1+a^2) + a \cdot \tau_0]^2 - [(\sigma_{xx,st}^2 + \tau_{xy,st}^2) \cdot (1+a^2) - \tau_0^2]} \tag{2.36}$$

The radius of the Mohr´s circle for pre-shearing σ_R was calculated with equation 2.37.

$$\sigma_R = \frac{a}{\sqrt{1+a^2}} \cdot (\sigma_M + \frac{\tau_0}{a}) \tag{2.37}$$

The principal normal stress σ_1 was calculated with equation 2.38.

$$\sigma_1 = \sigma_M + \sigma_R \tag{2.38}$$

At the intersection point of the yield locus and the Mohr´s circle for pre-shearing, the end points of the yield locus σ_E and τ_E was calculated with equation 2.39 and 2.40.

$$\sigma_E = \frac{a}{1+a^2} \cdot (\frac{\sigma_M}{a} - \tau_0) \tag{2.39}$$

$$\tau_E = \tau_0 + \frac{a}{1+a^2} \cdot (\sigma_M - a \cdot \tau_0) \tag{2.40}$$

The angle of the effective yield locus ϕ_e can be calculated with equation 2.41.

$$\phi_e = \arcsin(\frac{\sigma_R}{\sigma_M}) \tag{2.41}$$

A representative example of the graphic evaluation of the yield locus is shown in figure 2.20.

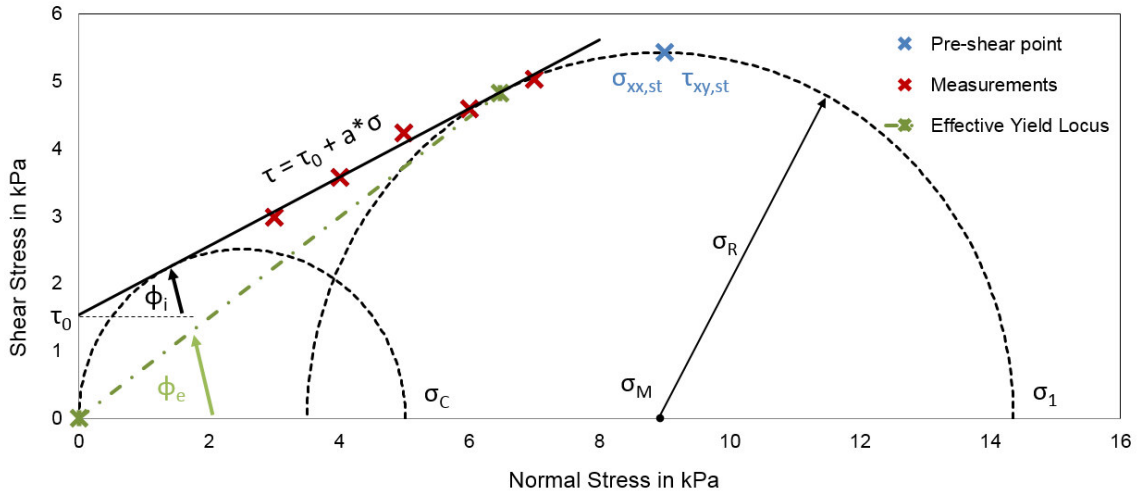

Figure 2.20.: Graphical evaluation of the yield locus of test run V7

The flowability was characterised numerical with the flow function ffc, calculated with the unconfined yield strength σ_c and the major principal stress or consolidation stress σ_1 (equation 2.38) [35]. Large numbers of ffc stands for high flowability and vice versa. The flow behavior can be classified as shown in figure 2.21 [35, 36].

$$ffc = \frac{\sigma_1}{\sigma_c} \tag{2.42}$$

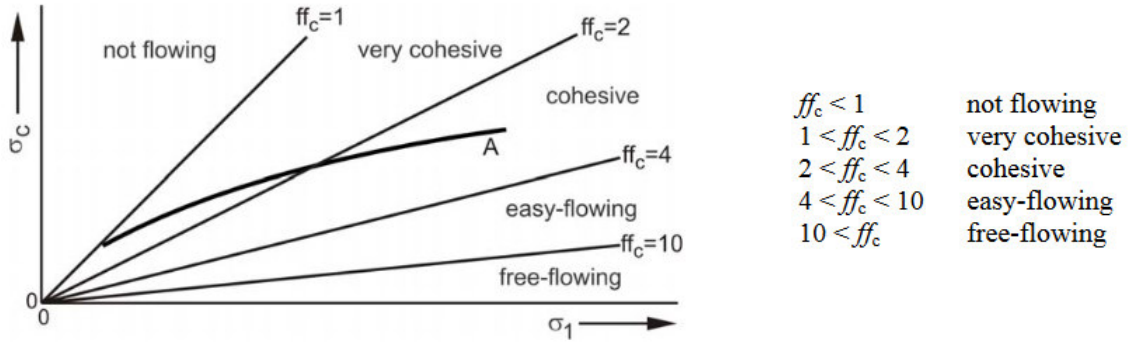

Figure 2.21.: Classification of the flow function [35, 36].

2.2.9.4. Tapped Density, Carr Index and Hausner Ratio

The Hausner ratio and Carr Index measurements are very popular for powder characterization because of their simplicity and rapidity of the measurement [37, 38].

The tapped density was measured (triple determination) with a tapping density and apparent volume tester from Pharma-Test (PT-TD200), shown in figure 2.22. About 200 ml of a Ibuprofen sample was filled in the standard test cylinder (250 ml). The volume after 500 strokes and another 750 strokes was determined per eye.

Tapped density, Carr Index and Hausner Ratio were determined for V7, V8 and V9 only. Raw and wet Ibuprofen samples, with a water content of 8.43, 15.95 and 22.87 wt.%, were tested to indicate the flowability of the powders and determine its dependence on the water content. Both, Carr Index and Hausner Ratio were calculated from compressibility data. They are a good indicator of the flowability of the tested powder [39]. A Carr index greater than 25 is considered to be an indication of poor flowability, and below 15, of good flowability[40]. Bulk and tapped density was calculated with equation 2.43 and 2.44 where the subscript t stands for tapped and b for bulk. The Hausner Ratio was calculated with equation 2.46 and the Carr Index with equation 2.45.

$$\rho_b = \frac{m}{V_b} \tag{2.43}$$

$$\rho_t = \frac{m}{V_t} \tag{2.44}$$

$$CI = 100 \cdot \frac{V_b - V_t}{V_b} \tag{2.45}$$

$$H = \frac{\rho_t}{\rho_b} \tag{2.46}$$

This simple test to characterise the cohesiveness of a material has some drawbacks. The result of the measurement depends strong on the operator. The filling method influences the initial volume of the material in the test cylinder. The volume measurements by naked eyes induce strong errors of the measured volume. The compaction dynamics between the initial and the final measurements are completely missed [38].
In addition, the test is measuring a form of compressibility, which does not always relate to cohesive forces. It has also been shown that the tapped bulk density measurements are extremely sensitive to the apparatus and the number of taps [41].

Figure 2.22.: Pharma-Test PT-TD200 tapping density and apparent volume tester. http://www.pharma-test.de/pt-td200/ (28.06.2017)

Table 2.3 shows the relations between both Hausner ratio and Carr index and the flow character of the powder.

Table 2.3.: Empirical relations between both Hausner ratio and Carr index and the flow character of the powder [42].

Flow character	Carr Index in %	Hausner Ratio
Excellent	< 10	1.00 - 1. 11
Good	10 - 15	1.12 - 1.18
Fair	16 - 20	1.19 - 1.25
Passable	21 - 25	1.26 - 1.34
Poor	26 - 31	1.35 - 1.45
Very poor	32 - 37	1.46 - 1.59
Very, very poor	> 38	> 1.60

3. Results and Discussion

3.1. Drying Experiments

3.1.1. V5 - V9

V5 was the first test run with wet Ibuprofen. The paddle configuration of test run V2 and V4 (five scrapers and three long one-peak paddles per side) was used. In a first trial 5 kg/h were fed into the dryer. Due to a feeding problem the experiment was stopped after 45 minutes. The feeder screws were changed from the fine (0.1 - 9 dm^3/h) to the coarse (0.3 - 20 dm^3/h) concave twin-screws. The mass flow was set to 2.5 kg/h. The test run was continued for 18 minutes until the rotary valve got filled up with Ibuprofen powder. The rotary valve was cleaned with a vacuum cleaner and the product bin was changed. The test run was then continued for another 80 minutes without problems.

For the last 80 minutes an average feed flow of 2.23 kg/h wet Ibuprofen with a measured water content of 8.2 wt.% was fed into the dryer. In 80 minutes a hold-up of 1.12 kg was reached. The weight of the product was only measured at the beginning and at the end, therefore it was not possible to determine steady state and the mass flow of dried Ibuprofen. A water content of 0.03 wt.% was measured for dried Ibuprofen. A condensate mass flow of 65.0 g/h was measured. 111.2 g/h water left the dryer with the humid air. As described in chapter 2.2.4 the measured mass flow of evaporated water in air (air + lost air) was calculated based on the calculated evaporated water (see equation 2.9 and 2.15) for test run V5 to V9. This was done because the water load of the humid exhaust air and the air flow of the humid exhaust air were not measured during this test runs and therefore a calculation of the measured evaporated water was not possible. All results of test run V5 are given in table 3.1.
At the end of test run V5 Ibuprofen deposits were found in the condenser and condensate. The material also accumulated inside the dryer.

Before test run V6 the paddle configuration was changed to 20 double-peak paddles. The paddles were glued on the shaft in three spiral rows with an offset of 120° as shown in figure 3.1 (a). The half shell covers were closed with two top covers as shown in figure 3.1 (b). This setup was tested prior to this work and showed good material transportation and a low hold-up. The experiment time was increased to reach steady state.

45 minutes after the start of the drying test run molten Ibuprofen dripped out of the product outlet into the product bin. The thermostat sensors of the filter and the lid were interchanged and were placed correctly 55 minutes after the start.

Table 3.1.: Results and set values of drying test runs V5 - V9.

			V5	V6	V7	V8	V9
Set	Water content (feed)	[wt.%]	8.2%	8.8%	16.0%	8.4%	22.9%
	Mass flow (feed)	[kg/h]	2.23	2.38	2.49	2.50	2.49
	Shaft speed	[rpm]	60	60	60	60	60
	Air flow (inlet)	[Nm³/h]	-	-	3.7	3.7	3.7
Results	Hold-up	[kg]	1.12	1.86	1.09	1.21	1.00
	Experiment time	[min]	80	145	182	195	180
	Steady state (dried Ibuprofen)	[min]	-	-	90.0	-	90.0
	Mass flow (dried)	[kg/h]	-	-	2.23	-	2.27
	Water content (dried)	[wt.%]	0.03%	0.7%	9.6%	3.0%	16.7%
	Evaporated water (calc)	[g/h]	176.2	196.2	150.0	123.7	151.1
	Evaporated water (measured)	[g/h]	176.2	196.2	150.0	123.7	151.1
	Mass flow condensate	[g/h]	65.0	37.7	53.7	29.0	40.5
	Mass flow water in air	[g/h]	111.2	158.5	96.3	94.7	110.6

During the 145 minutes long test run an average feed flow of 2.38 kg/h wet Ibuprofen with a measured water content of 8.8 wt.% was fed into the dryer. After 65 minutes the hold-up and condensate was measured every 20 minutes. A hold-up of 1.86 kg was reached at the end of the test run. The hold-up and the mass flows of wet and dried Ibuprofen over time are shown in figure 3.2. The decrease of the mass flow of wet Ibuprofen around minute 80 was due to bridging of the material in the feeder reservoir. No steady state was reached and therefore it was not possible to calculate the mass flow of dried Ibuprofen. An average water content of 0.7 wt.% was measured for dried Ibuprofen. The water content over time is shown in figure 3.3. A condensate mass flow of 37.7 g/h was measured. 158.5 g/h water left the dryer with the humid air. The calculated evaporated water was 196.2 g/h. All results of test run V6 are given in table 3.1.

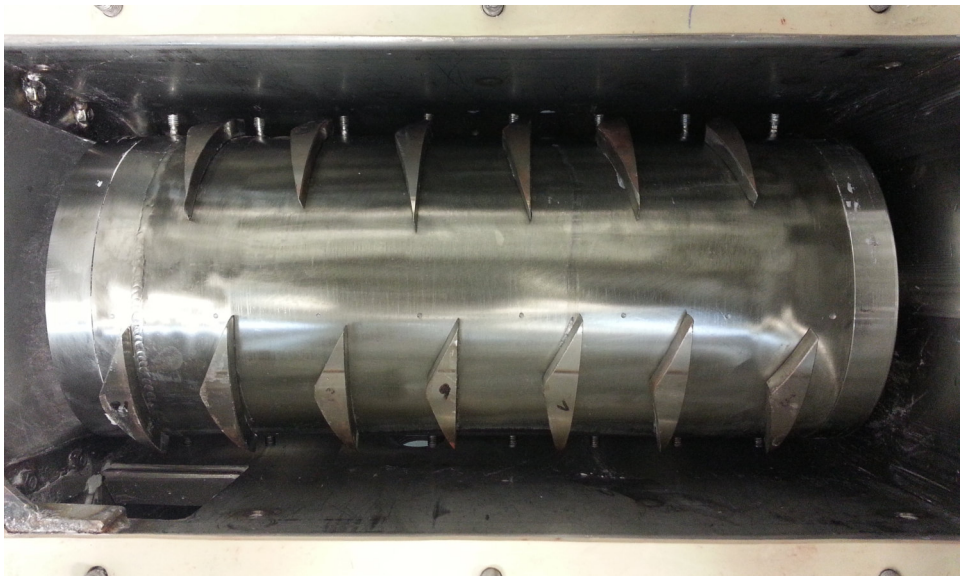

(a)

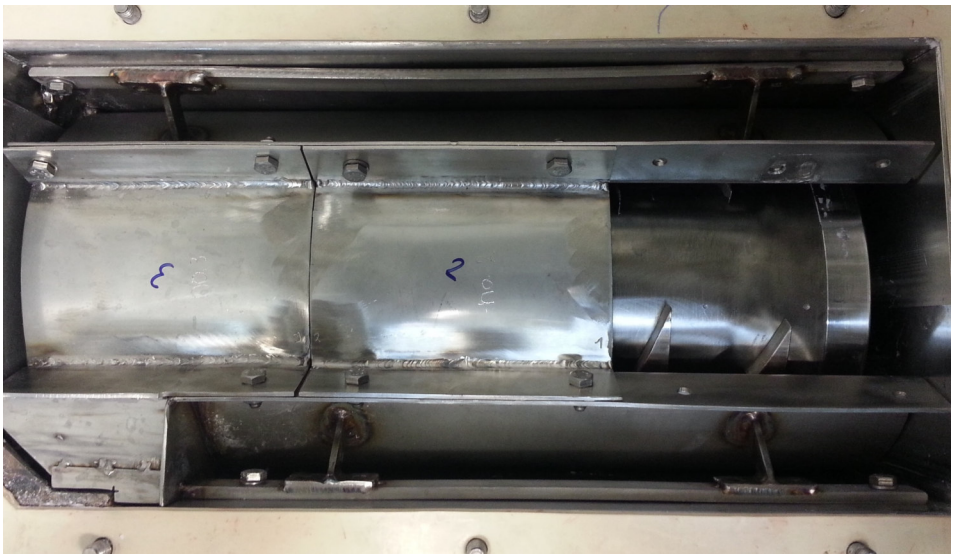

(b)

Figure 3.1.: (a): Paddle configuration of V6 to V9. 20 double-peak paddles glued on the shaft in three spiral rows with an offset of 120°. (b): Closed half shell covers of test run V6.

Ibuprofen deposits were found in the condenser and condensate. The rotary valve was partly filled up with Ibuprofen deposits, but none of the chambers was completely filled (see figure 3.4). The material inside the dryer at the end of test run V6 is shown with and without the top half shell covers in figure 3.5 (a) and (b). Material was accumulated on top of the half shell covers and at the inlet of the dryer. At the outlet of the dryer the material was compacted against the wall due to the bad ejection into the outlet pipe. Material deposits were observed on the shaft and half shells, but there was still enough space in between for the material transport (see figure 3.5 (b)).

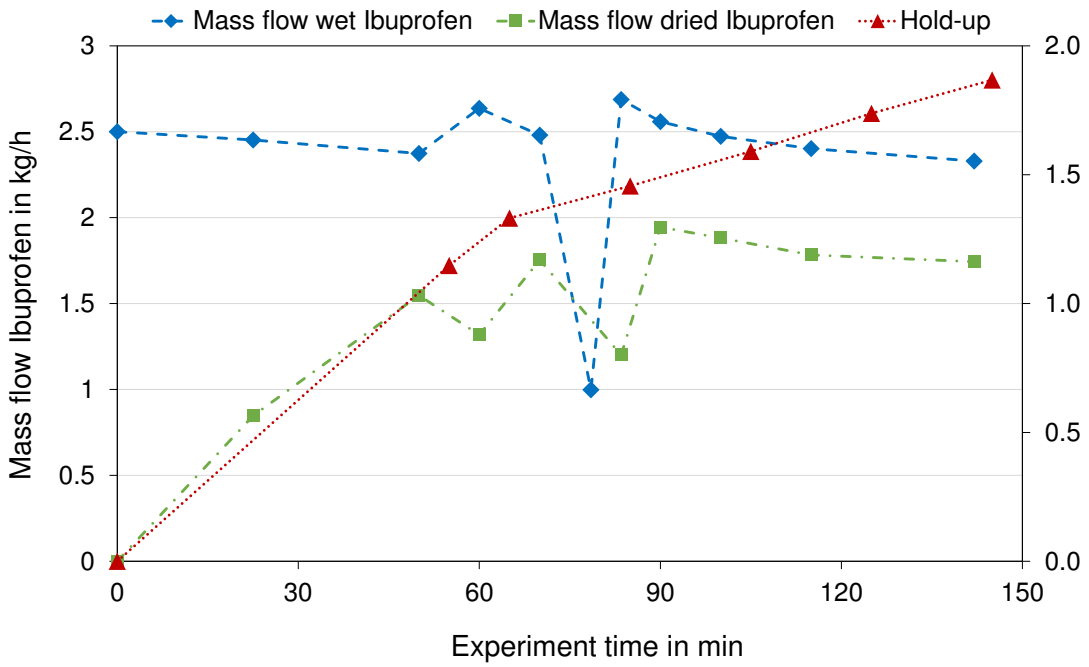

Figure 3.2.: Mass flow of wet and dried Ibuprofen as well as hold-up over experiment time of test run V6.

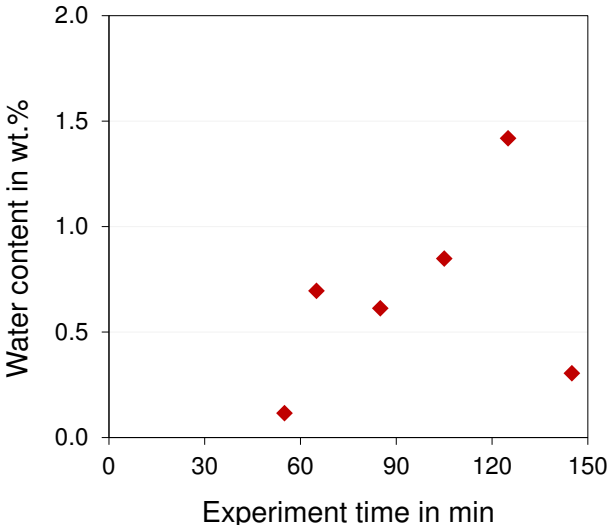

Figure 3.3.: Water content of test run V6 over experiment time.

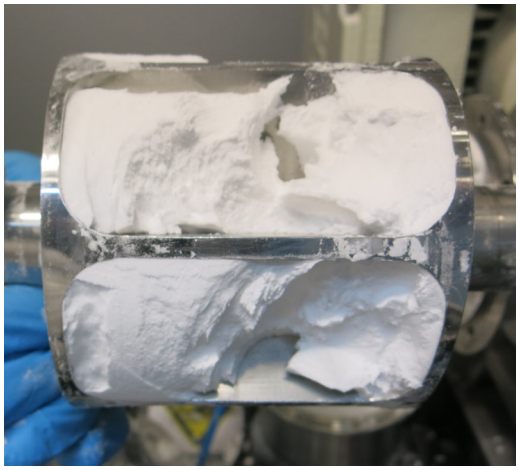

Figure 3.4.: Material deposits in the chambers of the rotary valve at the end of test run V6.

(a)

(b)

Figure 3.5.: Material inside the dryer at the end of the test run V6 with (a) top half shell covers and (b) without top half shell covers.

In test run V7 to V9 the water content of the feed material was varied. The experiment time was raised to three hours because no steady state was reached for the previous test runs. The pressure of the ingoing air flow was set to 2 bar by a pressure regulator and the air flow rate was regulated to 2.7 Nm^3/h with a variable area flowmeter.

After 60 minutes molten Ibuprofen was found in the product bin and outlet pipe. The outlet pipe was totally blocked with crystallised Ibuprofen which had to be removed. Afterwards, the thermostat of the outlet pipe was set from 60°C to 35°C to prevent overheating of the outlet.
During the 182 minutes long test run an average feed flow of 2.49 kg/h wet Ibuprofen with a measured water content of 16.0 wt.% was fed into the dryer. A hold-up of 1.09 kg was reached at the end of the test run. The hold-up and the mass flows of wet and dried material over time are shown in figure 3.6. No steady state of the hold-up was reached. The steady state of the mass flow of dried product was reached after about 90 minutes. At the end of the test run the mass flow of wet Ibuprofen decreased because the feeder was empty. This also led to a decreased mass flow of dried Ibuprofen. The last datapoint of the mass flow of wet and dried Ibuprofen were excluded for all further calculations. An average mass flow of 2.23 kg/h dried Ibuprofen left the dryer. An average water content of 9.6 wt.% was measured for dried Ibuprofen. The water

content over time is shown in figure 3.7. A condensate mass flow of 53.7 g/h was measured. 96.3 g/h water left the dryer with the humid air. All results of test run V7 are given in table 3.1.

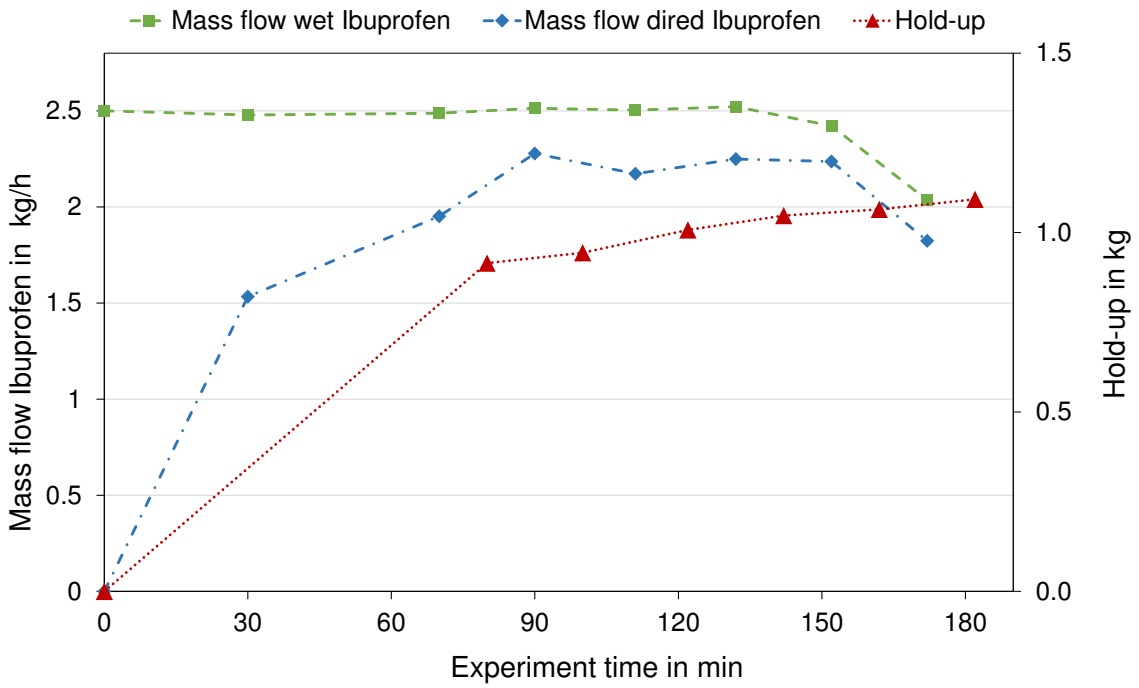

Figure 3.6.: Mass flow of wet and dried Ibuprofen as well as hold-up over experiment time of test run V7.

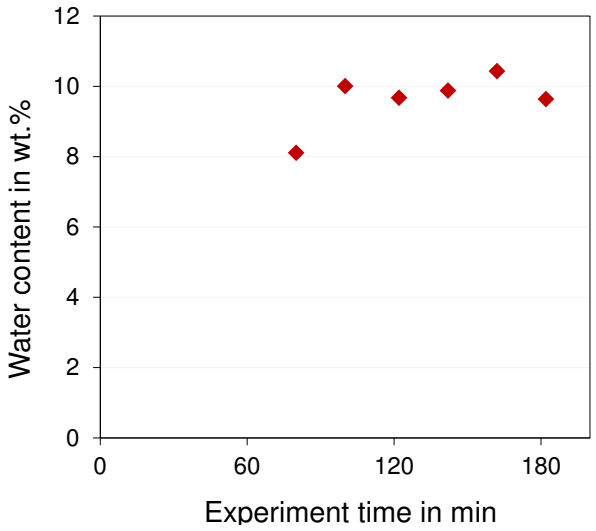

Figure 3.7.: Water content of test run V7 over experiment time.

During the 195 minutes long test run V8 an average feed flow of 2.50 kg/h wet Ibuprofen with a measured water content of 8.4 wt.% was fed into the dryer. A hold-up of 1.21 kg was reached at the end of the test run. The hold-up and the mass flows of wet and dried material over time are shown in figure 3.8. No steady state was reached and therefore it was not possible to calculate the mass flow of dried product. At the end of the test

run the mass flow of wet Ibuprofen decreased because the feeder was empty. This also led to a decreased mass flow of dried Ibuprofen. The last datapoint of the mass flow of wet and dried Ibuprofen were excluded for all further calculations. An average water content of 3.0 wt.% was measured for dried Ibuprofen. The water content of the dried Ibuprofen over time is shown in figure 3.9. A condensate mass flow of 29.0 g/h was measured. 94.7 g/h water left the dryer with the humid air. All results of test run V8 are given in table 3.1.

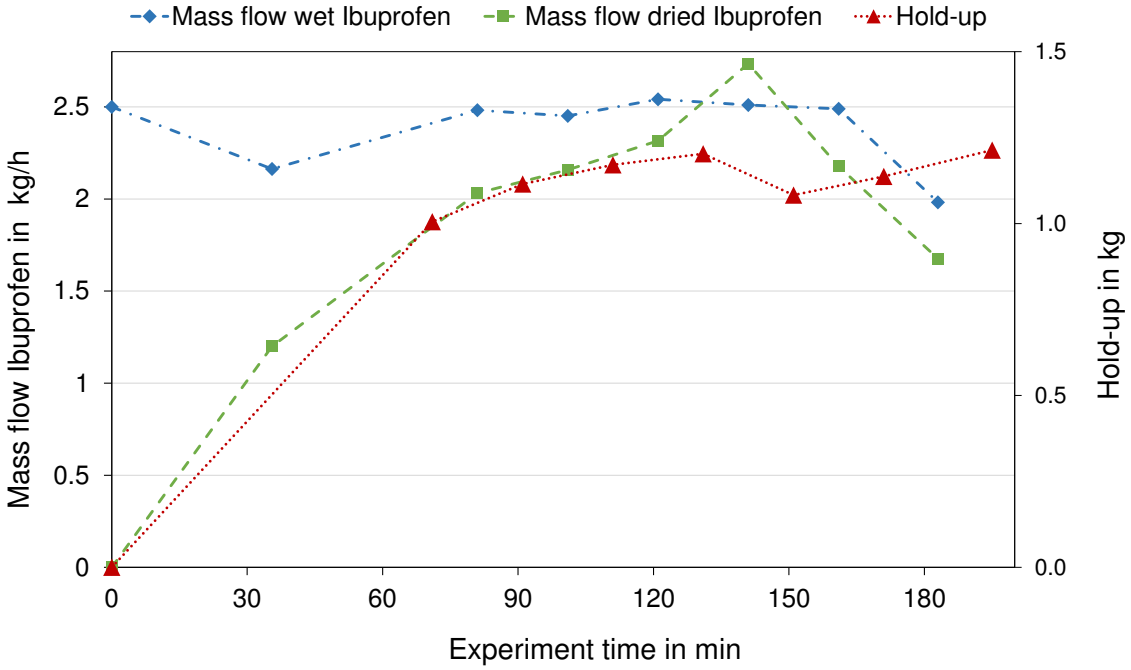

Figure 3.8.: Mass flow of wet and dried Ibuprofen as well as hold-up over experiment time of test run V8.

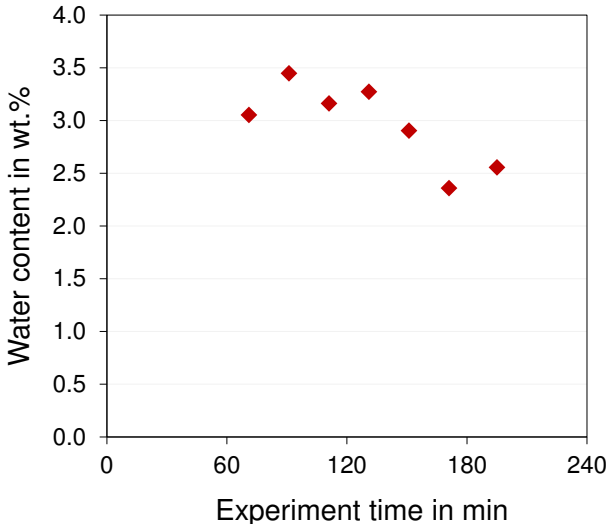

Figure 3.9.: Water content of test run V8 over experiment time.

During the 180 minutes long test run V9 an average feed flow of 2.49 kg/h wet Ibuprofen with a measured water content of 22.9 wt.% was fed into the dryer. A hold-up of 1.00 kg was reached at the end of the test run. The steady steady state of the hold-up was reached at about 120 minutes. The hold-up and the mass flows of wet and dried material over time are shown in figure 3.10. The steady state of the mass flow of dried product was reached after about 90 minutes. An average mass flow of 2.27 kg/h dried Ibuprofen left the dryer with an average water content of 16.7 wt.%. The water content over time is shown in figure 3.11. A condensate mass flow of 40.5 g/h was measured. 110.6 g/h water left the dryer with the humid air. All results of test run V9 are given in table 3.1.

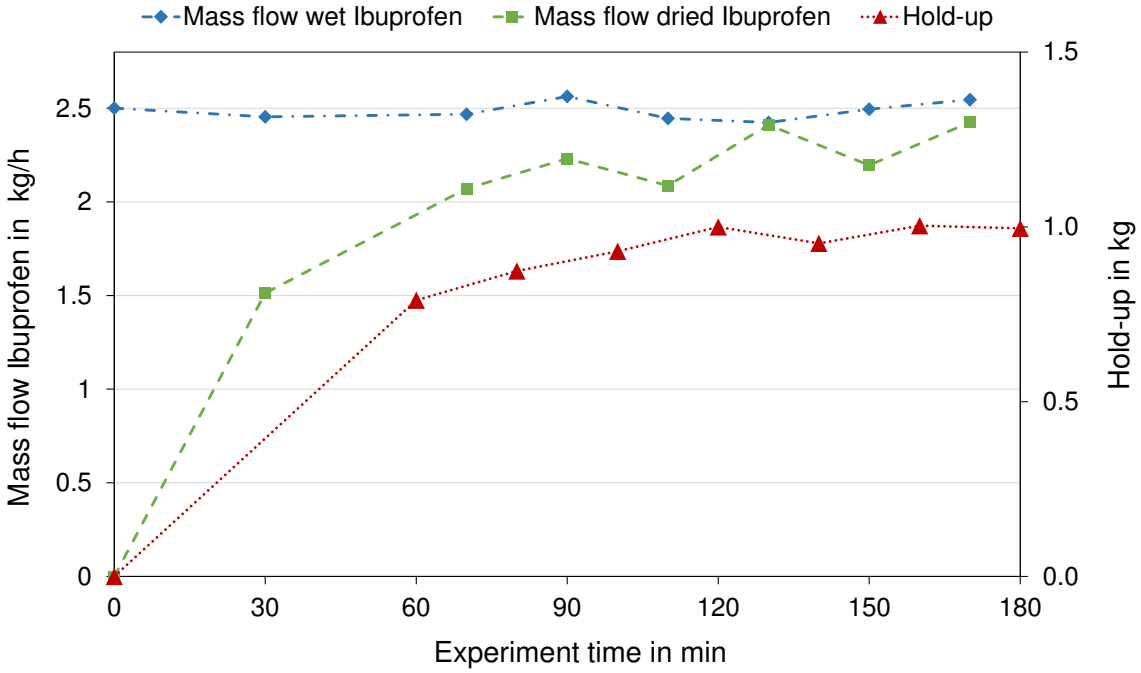

Figure 3.10.: Mass flow of wet and dried Ibuprofen as well as hold-up over experiment time of test run V9.

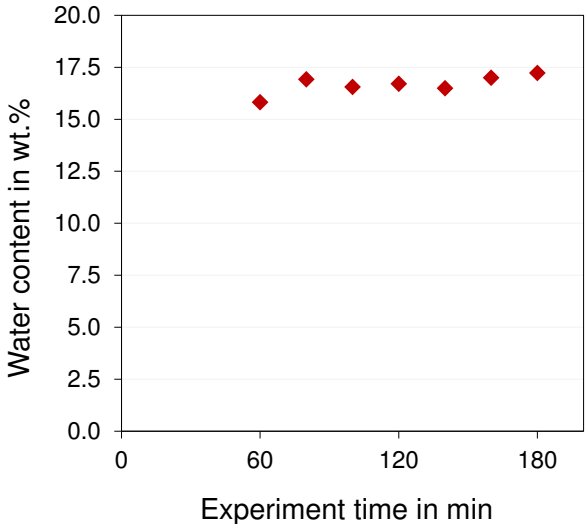

Figure 3.11.: Water content of test run V9 over experiment time.

The material inside the dryer at the end of each test run is shown with the top half shell covers for test run V7 (figure 3.14 (b)) and without the top half shell covers for test run V8 and V9 (figure 3.14 (a) and (c)). No picture was recorded from the inside of the dryer without the top half shell covers for test run V7. Material deposits were found on top of the half shell covers at the end of all three test runs. The material accumulation seemed to decrease with increased water content of the feed material as shown in figure 3.14. Also the hold-up was smaller for test runs with high water content of the feed material.
In all test runs Ibuprofen deposits were found in the condenser, but not in the condensate (see figure 3.15). Ibuprofen deposits were observed in the rotary valve and in the connection pipe between rotary valve and dryer. This deposits also seemed to decrease with increasing water content of the feed material as shown in figure 3.12 and 3.13. In all three test run the material was compacted to the wall at the outlet of the dryer due to the bad ejection into the outlet pipe.

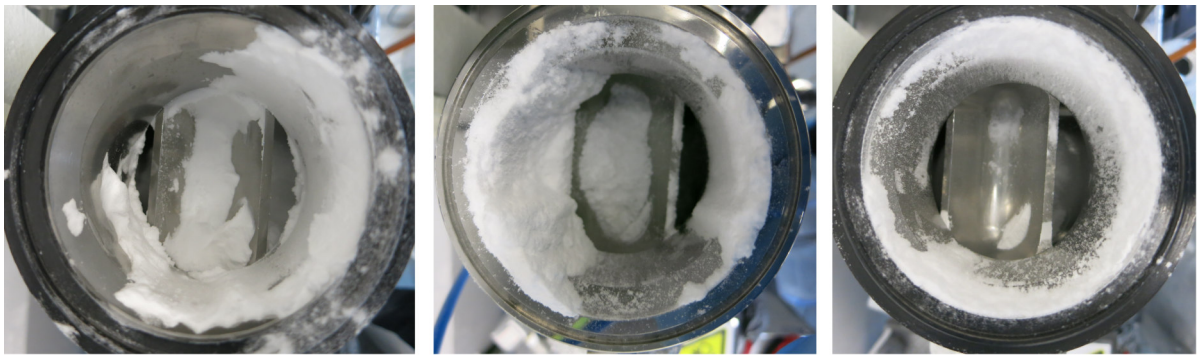

Figure 3.12.: Top view on the rotary valve at the end of each test run. Left: V8 (8.4 wt.% H_2O), mid: V7 (16.0 wt.% H_2O), right: V9 (22.9 wt.% H_2O).

Figure 3.13.: Top view on the inlet of the dryer at the end of each test run. Left: V8 (8.4 wt.% H_2O), mid: V7 (16.0 wt.% H_2O), right: V9 (22.9 wt.% H_2O).

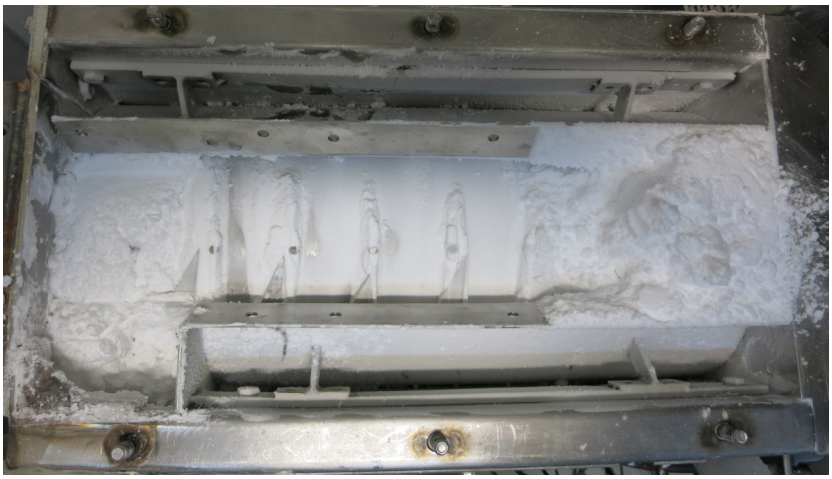

(a)

(b)

(c)

Figure 3.14.: (a): Material inside the dryer at the end of the test run V8 (8.4 wt.% H_2O) without top half shell covers. (b): Material inside the dryer at the end of the test run V7 (16.0 wt.% H_2O) with top half shell covers. (c): Material inside the dryer at the end of the test run V9 (22.9 wt.% H_2O) without top half shell covers.

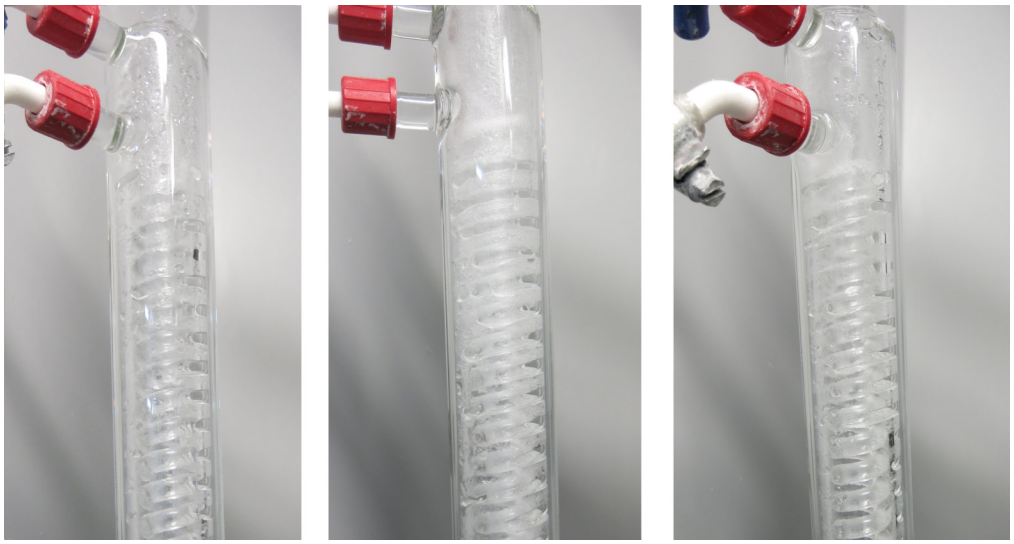

Figure 3.15.: Ibuprofen deposits in the condenser at the end of each test run. Left: V8 (8.4 wt.% H_2O), mid: V7 (16.0 wt.% H_2O), right: V9 (22.9 wt.% H_2O).

3.2. Temperature Tests

Two temperature test runs were carried out to investigate the temperature deviation between the measured temperatures by the temperature sensors of the thermostats and the real temperatures inside the dryer. In the first test run the temperature of the outlet was set to 35 and 45°C. The temperature fluctuated between 37 and 59°C for a set temperature of 35°C and between 47 and 78°C for a set temperature of 45°C. To reduce this high temperature fluctuations of the outlet-temperature, the sensor of the thermostat was placed directly on the electric heating cable. Due to this adjustment the temperature fluctuation decreased, but was still higher than the fluctuations of the filter and lid temperature (see figure 3.16).
Due to improper sensor position of the thermostat sensor of the lid and filter, the sensor placement was adjusted. This led to a better match of the set (thermostat) and the actual temperature inside the dryer, measured with the thermocouples as shown in figure 3.16 (compare temperature differences between set and measured temperature of the filter and lid, before and after the sensor adjustment).

The temperature regulation of the filter and lid worked well with the correct sensor placement. For the lid a set temperature of 50°C led to a measured temperature between 48 and 51°C. For the filter a set temperature of 45°C led to a measured temperature between 54 and 56°C. This deviation of set and measured temperature was caused by the sensor placement inside the filter housing (isolation). Product outlet temperatures were measured between 48 and 57°C for a set temperature of 40°C. The big deviation of set and measured temperature as well as the large temperature fluctuations, despite an optimal sensor placement direct on the heating cable, was most likely caused by a damaged or malfunctioning thermostat.
The set shaft temperature of 55°C (set at the Thermo Haake heating circulator) was reached after about 60 minutes and remained constant for the whole test run.

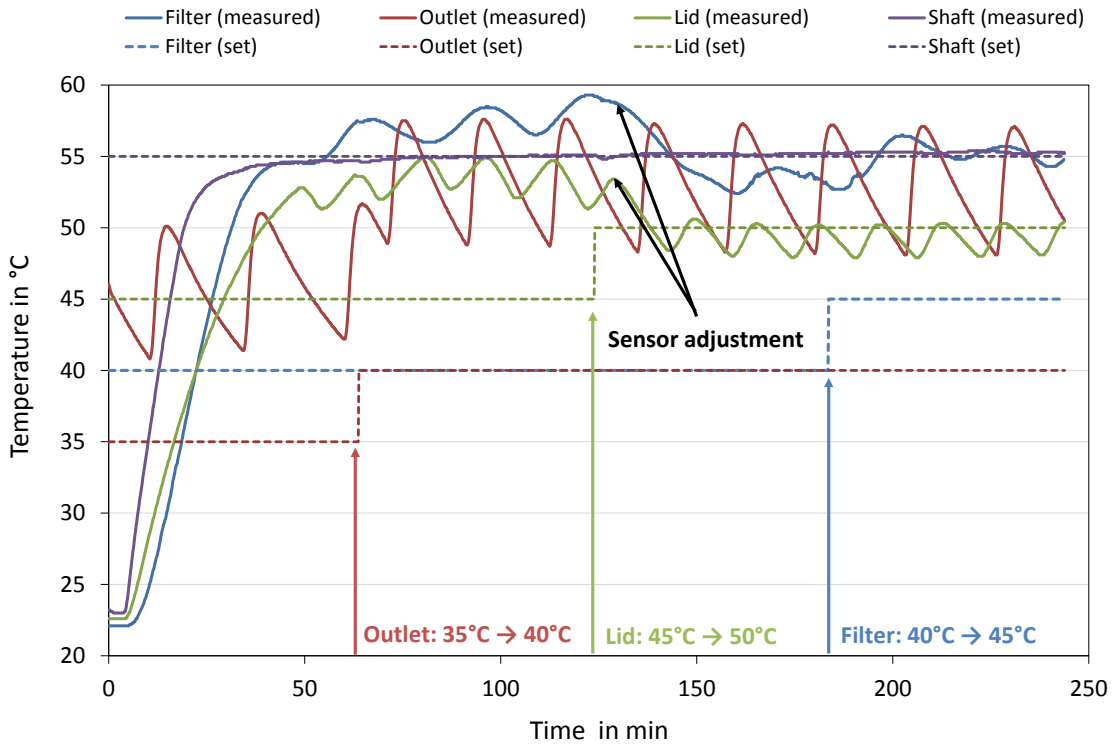

Figure 3.16.: Results of temperature test run. Dashed lines represents the set temperature on the thermostats. The solid lines represents the actual temperature measured by the thermocouples. Temperature changes and sensor adjustments are marked by arrows.

3.2.0.1. Summary of Test Runs V5 to V9 and equipment improvements

- The feed mass flow of wet Ibuprofen was reduced from 5 kg/h to 2.5 kg/h. A mass flow of 5 kg/h was too high to be handled by the dryer and resulted in blockages of the outlet and therefore a fill up of the dryer after a short time.
- To reduce the hold-up, the dead volume of the dryer has to be reduced.
- Material was compacted to the wall on the outlet side of the dryer due to bad ejection into the outlet pipe. The paddle configuration at the outlet was optimised.
- Water content had influence on the flowability of the powder and therefore on the material accumulation and the material deposits inside the dryer.
- Big fluctuations of the condensate mass flow despite constant system settings.
- Molten Ibuprofen was found at the outlet with a set temperature of 60 °C. Temperature measurements and sensor adjustments were done as described in chapter 2.2.2. The temperature of filter, outlet and lid inside the dryer has to be measured and compared to the set values of the thermostats.
- To enable proper calculation of the water mass flow in the humid exhaust air, the humidity and air flow rate of the exhaust air has to be measured.
- To calculate the relative humidity of the air with maximal water load (assumed to be right after the filter), the temperature of the humid air after the filter has to be measured.
- The steady state of the hold-up was only reached for test run V9. The experiment time has to be further increased.

3.2.1. Modifications of the Dryer and Additional Measurements

After test run V9 the drying process was modified based on the obtained informations of all previous test runs. To prevent material compaction to the wall on the outlet side of the dryer, the paddle configuration was changed. Four scrapers were glued on the shaft at the outlet with an offset of 90° as shown in figure 3.17. The scrapers were angled to enforce a counter flow at the outlet to improve the ejection of the material into the outlet pipe.

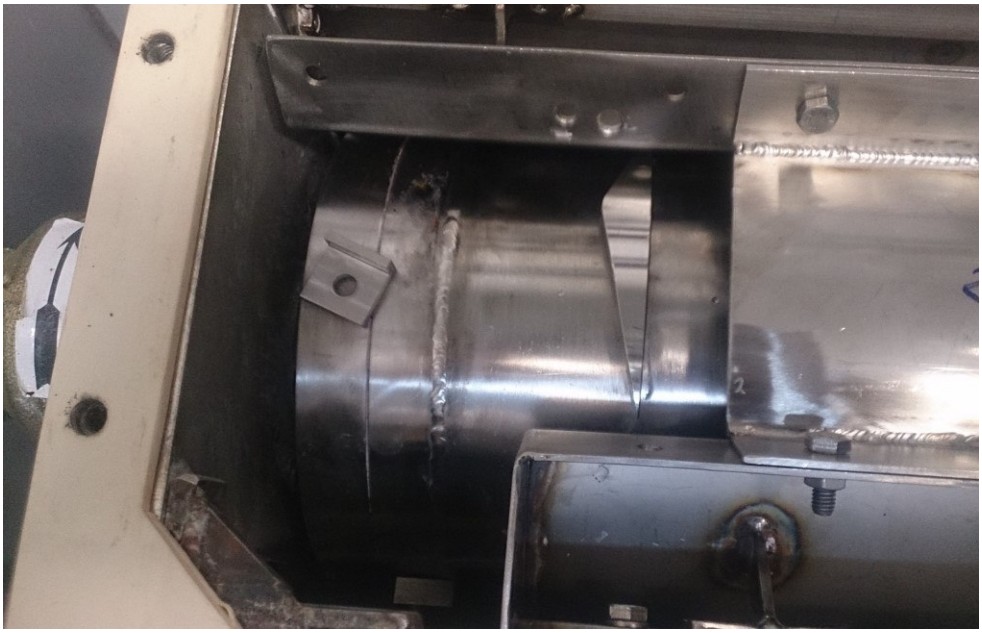

Figure 3.17.: Modification of the paddle configuration. Four scrapers with an offset of 90°.

To reduce the dead volume between the lid and the top half shell covers a foam insert was used. Holes for the humid air were drilled in the half shell cover under the filter as shown in figure 3.18.

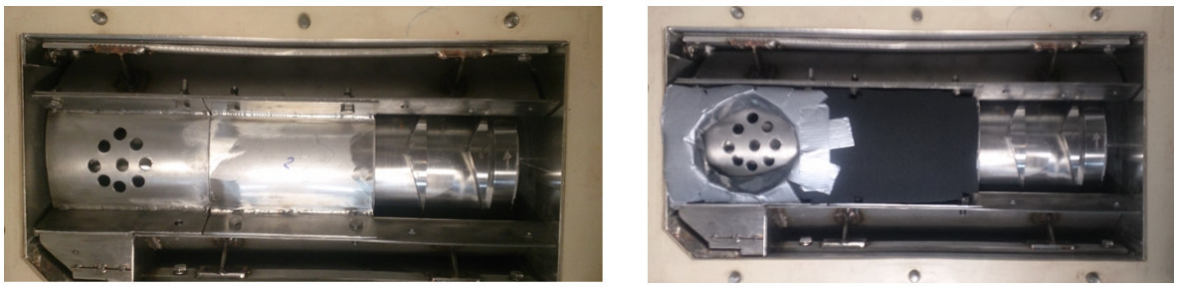

Figure 3.18.: Left: Air holes in the top half shell cover under the filter inlet. Right: Foam insert to reduce the dead volume of the dryer.

To reduce material deposits on the inlet and the rotary valve, the inner surface was covered with self-adhesive teflon-tape as shown in figure 3.19.

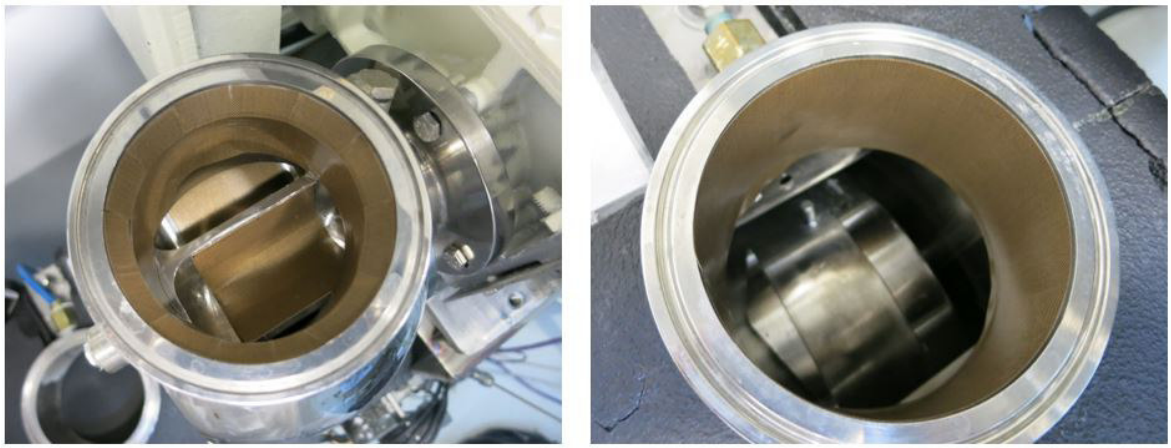

Figure 3.19.: Teflon tape on the inner surface of the inlet and rotary valve.

Two variable area flow meters were installed to regulate the heating of the shaft and the housing of the dryer separately. The variable area flow meters with the heating circulator are shown in figure 3.20. The water temperature of the in- and outlets of the shaft and housing were measured with typ-K thermocouples and recorded with a Testo data logger.

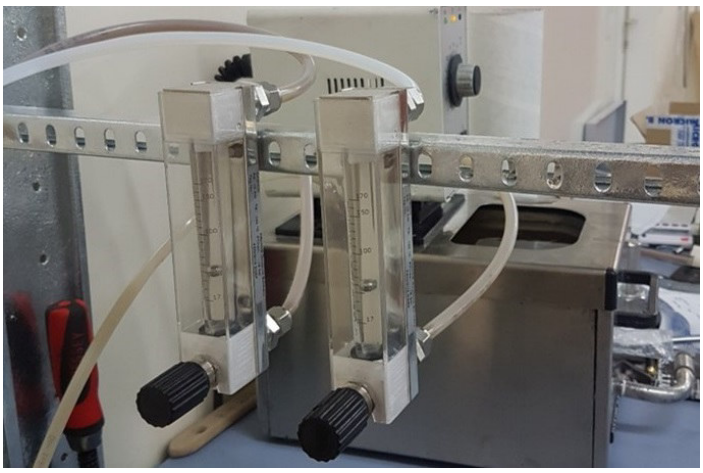

Figure 3.20.: Variable area flow meters to regulate the mass flow of hot water through the shaft and housing of the dryer.

A removable isolation for the product bin was installed to reduce the heat loss and condensation at the inner wall of the product bin (see figure 3.22).
The temperature right after the filter outlet was measured with a typ-K thermocouple as shown in figure 3.21. This temperature was used to calculate the relative humidity of the humid air at the filter outlet.

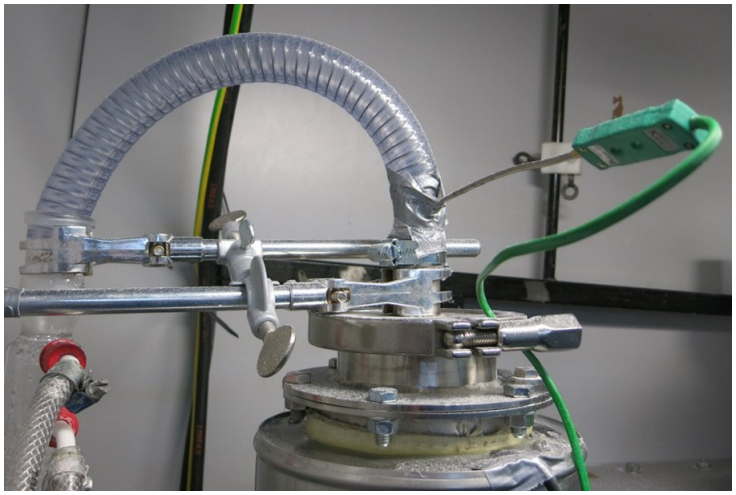

Figure 3.21.: Temperature measurement of the humid air after the filter with a typ-K thermocouple.

Figure 3.22.: Isolation of the product bin.

The temperature, relative humidity and velocity of the humid exhaust air were measured as described in chapter 2.2.4. The measurement devices and their position are shown in figure 3.23 and 3.24.

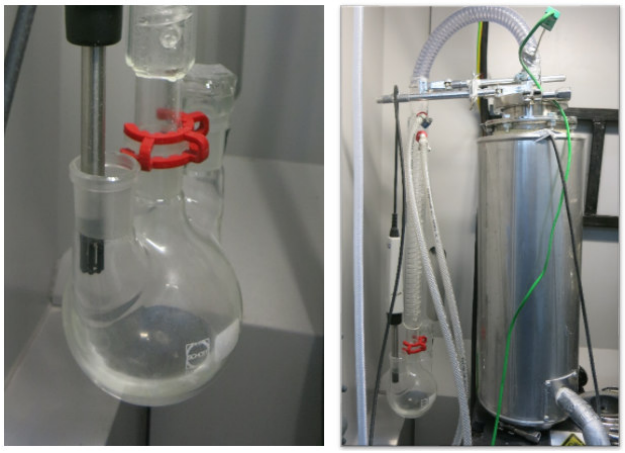

Figure 3.23.: Measurement of relative humidity and temperature of the humid exhaust air at the dryer outlet.

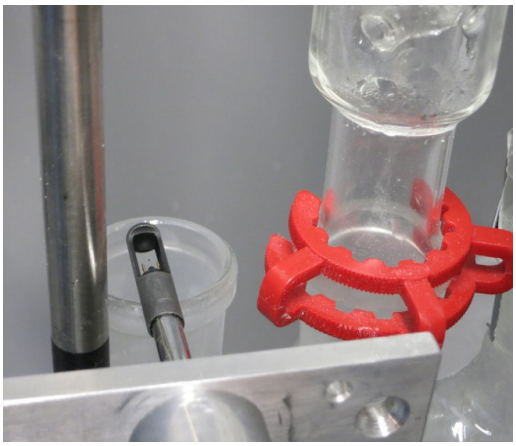

Figure 3.24.: Velocity measurement of the humid exhaust air.

3.2.2. V10 - V13

In test run V10 to V13 the mass flow of wet Ibuprofen, the shaft speed and the air flow rate were varied to investigate the influence of this parameters on the drying performance. In test run V11 the mass flow of wet Ibuprofen and the shaft speed were doubled, in test run V12 only the shaft speed was doubled and in test run V13 the air flow rate was halved, compared to V10.

During the 286 minutes long test run V10 an average feed flow of 1.25 kg/h wet Ibuprofen with a measured water content of 7.1 wt.% was fed into the dryer. The wet Ibuprofen was prepared with 10.0 wt.% H_2O. The big deviation between prepared and measured water content was probably due to bad sampling. A hold-up of 1.43 kg was reached at the end of the test run. The hold-up was still slightly increasing at the end of the test run. With the mass balance of the dryer a hold-up water content of -6.93 wt% was calculated. This means that more water left the dryer than entered the dryer, which is not possible. This was probably due to the low measured water content of the feed material. The mass balance of test run V10 is shown in table 3.2. The hold-up and the mass flows of wet and dried material over time are shown in figure 3.26. The steady state of the mass flow of dried product was reached after about 140 minutes. An average mass flow of 1.11 kg/h dried Ibuprofen left the dryer with an average water content of 1.3 wt.%. The water content over time is shown in figure 3.25. A condensate mass flow of 25.8 g/h was measured. 52.0 g/h water left the dryer with the humid air. The calculated mass flow of evaporated water was 74.7 g/h compared to a measured mass flow of 77.8 g/h. 2.9 Nm^3/h of drying air with an average measured water load of 13.8 g/kg and a relative humidity of 88.7 % left the dryer at the air outlet. The humid air after the filter had a water load of 20.9 g/kg with an average relative humidity of 30.5 % and an average temperature of 47.4°C. 22% of the air flow was lost between inlet and outlet. The calculated mass flow of water in the lost air was 21.4 g/h. All results of test run V10 are given in table 3.3.

Table 3.2.: Mass balance of test run V10.

		Ibuprofen [kg]	Water [kg]	Drying air [kg]	Total [kg]
In	Feeder	5.59	0.425	0.0	6.02
	Air	0.0	0.0	22.60	22.60
Out	Product	4.06	0.051	0.0	4.11
	Condenser	0.0	0.123	0.0	0.12
	Air	0.0	0.248	17.72	17.97
	Lost air	0.0	0.102	4.88	4.98
	Hold-up	1.53	-0.099	0.0	1.43

No Ibuprofen was found in the condensate and condenser. Ibuprofen was transported through the air holes of the half shell cover. The space between half shell cover and filter was filled with loose Ibuprofen as shown in figure 3.27. In addition, material deposits were also observed on the inner wall of the filter housing as shown in figure 3.27.
The foam insert prevented a fill up of the space between the top half shell covers and the lid. Material accumulations occurred on the inlet and outlet of the dryer as shown

in figure 3.28 (a). Even though additional paddles were installed to improve material ejection, still compacted material at the outlet of the dryer was observed (see figure 3.28 (b)). The space between shaft and half shell remained free for material transport as shown in figure 3.28 (c).

Table 3.3.: Results and set values of drying test runs V10 - V13.

			V10	V11	V12	V13
Set	Water content (feed)	[wt.%]	7.1%	7.7%	9.4%	9.5%
	Mass flow (feed)	[kg/h]	1.25	2.50	1.25	1.25
	Shaft speed	[rpm]	60	120	120	60
	Air flow (inlet)	[Nm³/h]	3.7	3.7	3.7	1.8
Results	Hold-up	[kg]	1.43	3.44	2.99	1.40
	Experiment time	[min]	286	240	200	300
	Steady state (dried Ibuprofen)	[min]	140	-	-	100
	Mass flow (dried)	[kg/h]	1.11	-	-	1.13
	Water content (dried)	[wt.%]	1.3%	3.7%	0.3%	2.8%
	Evaporated water (calc)	[g/h]	74.7	112.2	116.6	84.2
	Evaporated water (measured)	[g/h]	77.8	93.8	88.4	74.7
	Mass flow condensate	[g/h]	25.8	48.5	45.5	48.0
	Mass flow water in air	[g/h]	52.0	45.3	43.0	26.7
	Mass flow water in lost air	[g/h]	21.4	37.2	46.2	18.2
	Air flow (outlet)	[Nm³/h]	2.9	2.6	2.4	1.5
	Lost air flow	[%]	22%	29%	35%	20%
	Water load of air	[g/kg]	13.8	13.1	13.2	14.0
	Relative humidity (outlet)	[%]	88.7%	91.6%	90.6%	95.3%
	Water load of lost air	[g/kg]	20.9	27.6	28.4	39.2
	Relative humidity (filter)	[%]	30.5%	39.4%	40.4%	62.5%

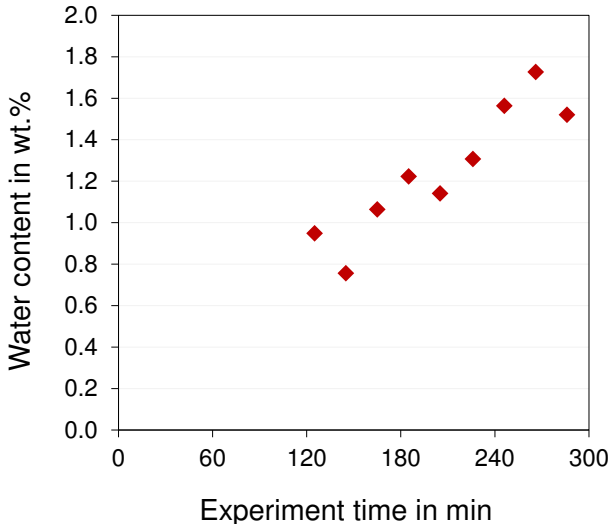

Figure 3.25.: Water content of test run V10 over experiment time.

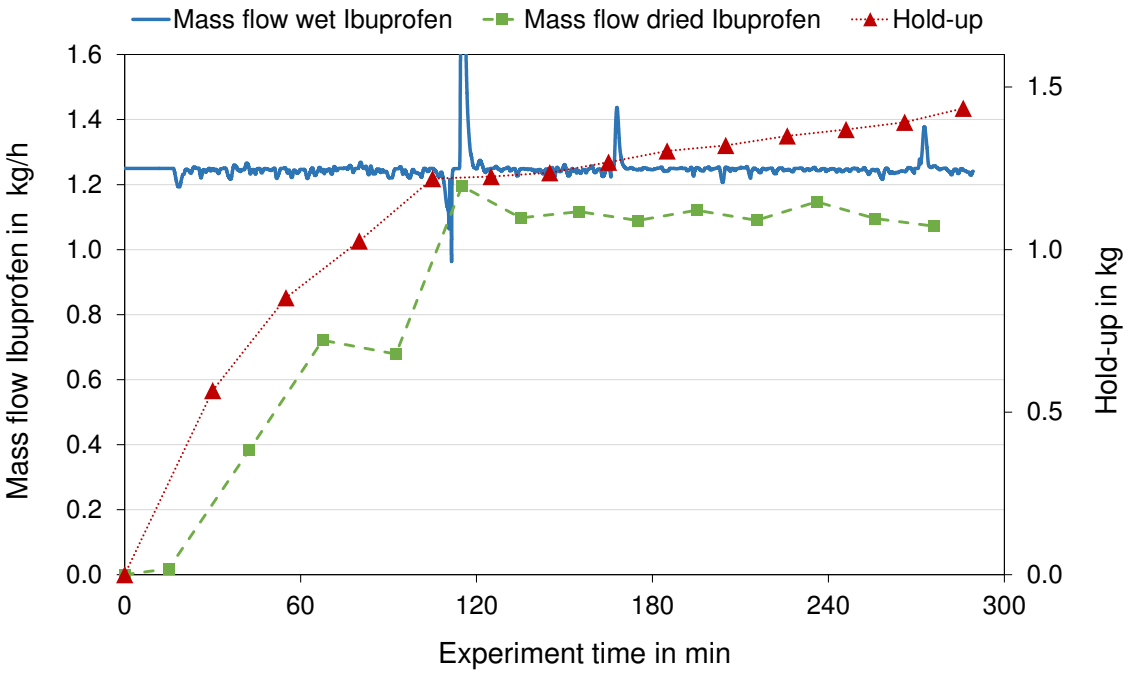

Figure 3.26.: Mass flow of wet and dried Ibuprofen as well as hold-up over experiment time of test run V10.

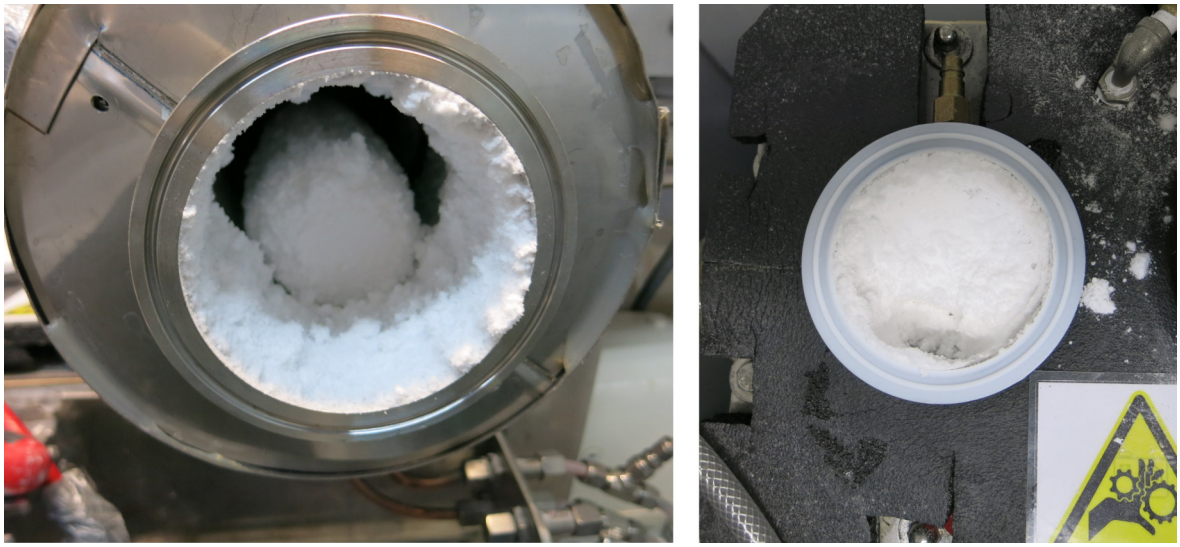

Figure 3.27.: Left: View on the bottom side of the filter. Material deposits on the inner wall of the filter housing. Right: View on the filter connection of the lid.

(a)

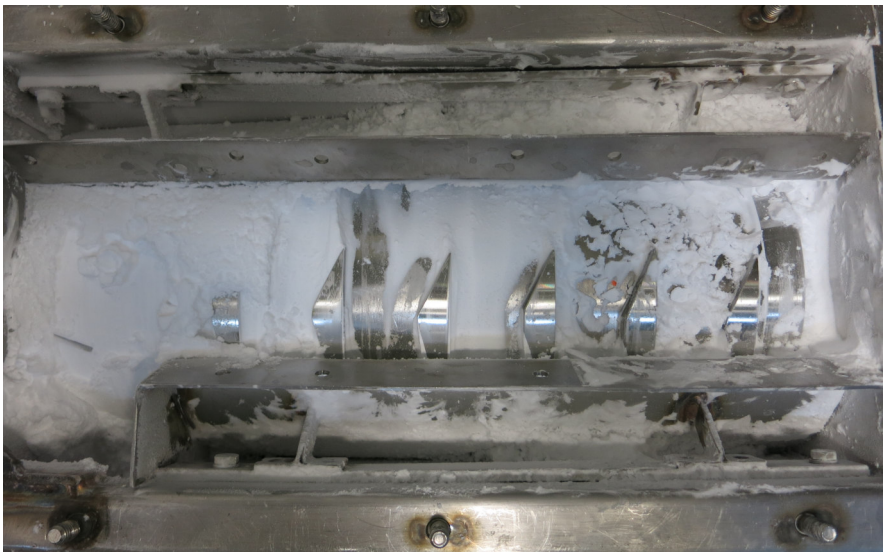

(b)

(c)

Figure 3.28.: (a): Material inside the dryer at the end of the test run V10 with top half shell covers. (b): Material inside the dryer at the end of the test run V10 without top half shell covers. The inlet part was already clean with a vacuum cleaner. (c): Hollow space between half shell and shaft.

During the 240 minutes long test run V11 2.50 kg/h of wet Ibuprofen with a measured water content of 7.7 wt.% was fed into the dryer. The wet Ibuprofen was prepared with 10.0 wt.% H_2O. The big deviation between prepared and measured water content was probably due to bad sampling, bad mixing of water and Ibuprofen powder or a combination of both. Due to blockages of the outlet pipe, caused by the high shaft speed, an unsteady mass flow of dried Ibuprofen occurred. A hold-up of 3.44 kg was reached at the end of the test run. With the mass balance of the dryer a hold-up water content of 1.03 wt% was calculated. The mass balance of test run V11 is shown in table 3.4. At the end of the test run, the dryer and the majority of the filter was filled up with Ibuprofen which is shown in figure 3.31. The hold-up and the mass flows of wet and dried material over time are shown in figure 3.29. Due to data loss the first 53 minutes of the mass flow of wet Ibuprofen were missing. No steady state was reached. The dried Ibuprofen left the dryer with an average water content of 3.7 wt.%. The water content was also very unsteady over time as shown in figure 3.30. A condensate mass flow of 48.5 g/h was measured. 45.3 g/h water left the dryer with the humid air. The calculated mass flow of evaporated water was 112.2 g/h compared to a measured mass flow of 93.8 g/h. 2.6 Nm^3/h of drying air with an average measured water load of 13.1 g/kg and a relative humidity of 91.6 % left the dryer at the air outlet. The humid air after the filter had a water load of 27.6 g/kg with an average relative humidity of 39.4 % and an average temperature of 47.6°C. Due to the blocked filter 29% of the air flow was lost between inlet and outlet. The calculated mass flow of water in the lost air was 37.2 g/h. All results of test run V11 are given in table 3.3.

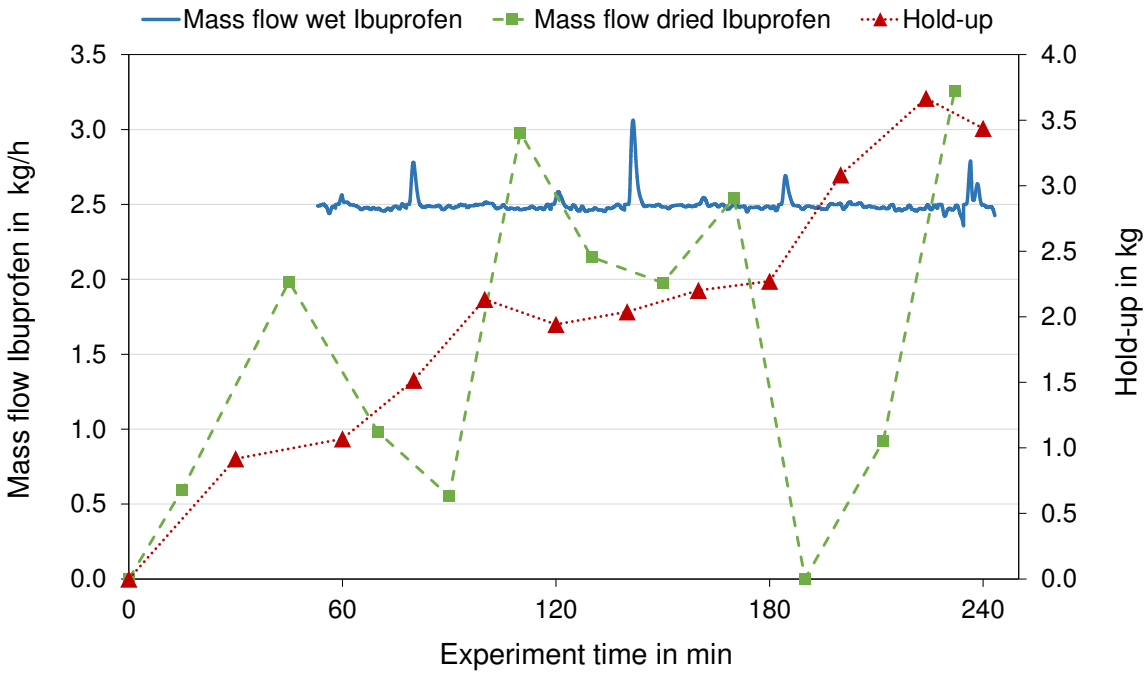

Figure 3.29.: Mass flow of wet and dried Ibuprofen as well as hold-up over experiment time of test run V11.

Table 3.4.: Mass balance of test run V11.

		Ibuprofen [kg]	Water [kg]	Drying air [kg]	Total [kg]
In	Feeder	9.43	0.790	0.0	10.22
	Air	0.0	0.0	18.96	18.96
Out	Product	6.03	0.231	0.0	6.26
	Condenser	0.0	0.194	0.0	0.19
	Air	0.0	0.181	13.57	13.75
	Lost air	0.0	0.149	5.40	5.55
	Hold-up	3.40	0.035	0.0	3.44

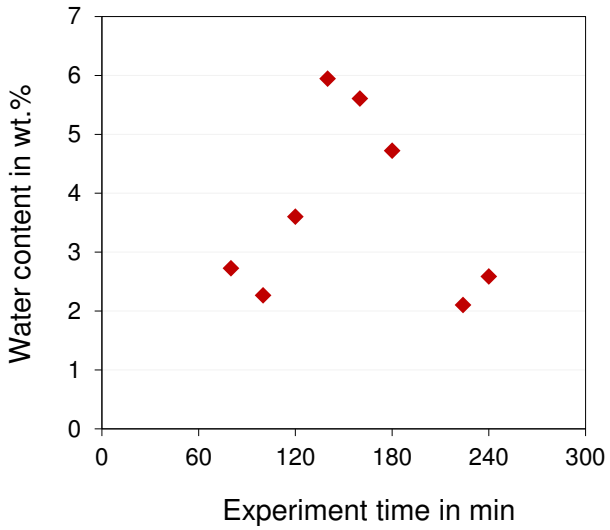

Figure 3.30.: Water content of test run V11 over experiment time.

No Ibuprofen was found in the condensate and condenser. Due to blockages of the outlet the dryer filled up with Ibuprofen and the material was pressed through the air holes into the filter. At the end of the test run the filter was completely filled up with Ibuprofen as shown in figure 3.31.
Also the dryer was completely filled up with Ibuprofen as shown in figure 3.33. The inlet and outlet of the dryer were already cleaned with a vacuum cleaner before the picture was taken. The material was compacted on the shaft and on the half shell covers (see figure 3.34), but there was still enough space in between for the material transport (see figure 3.32).

Figure 3.31.: View on the bottom side of the filter housing. The interior of the filter housing was completely filled up with Ibuprofen.

Figure 3.32.: Hollow space between half shell and shaft.

Figure 3.33.: Material inside the dryer at the end of the test run V11 with top half shell covers. Inlet and outlet part of the dryer were already cleaned with a vacuum cleaner.

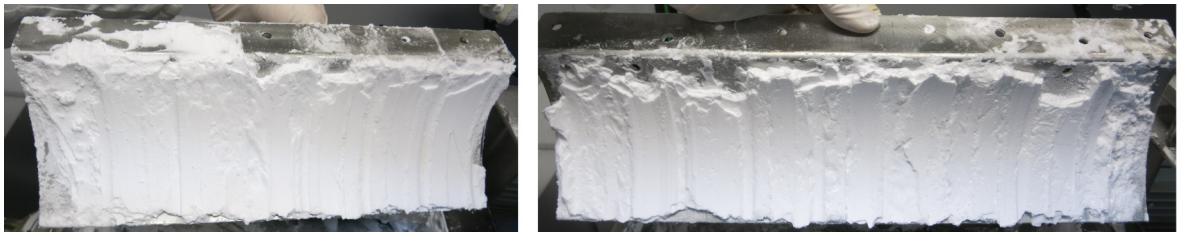

Figure 3.34.: Compacted material on the half shell covers.

During the 200 minutes long test run V12 1.25 kg/h of wet Ibuprofen with a measured water content of 9.4 wt.% was fed into the dryer. Due to blockages of the outlet pipe at about 170 minutes, caused by the high shaft speed, the experiment had to be stopped after 200 minutes. A hold-up of 2.99 kg was reached at the end of the test run. With the mass balance of the dryer a hold-up water content of -1.58 wt% was calculated. This means that more water left the dryer than entered the dryer, which is not possible. Possible reasons for this were a wrong measured mass flow of water in air and lost air. Also the assumption that the water load of the lost air is the same as the water load after the filter involves error potential. The mass balance of test run V12 is shown in table 3.5. The hold-up and the mass flows of wet and dried material over time are shown in figure 3.35. The dried Ibuprofen left the dryer with an average water content of 0.3 wt.%. Two data points of the water content over time are given in figure 3.36. A condensate mass flow of 45.5 g/h was measured. 43.0 g/h water left the dryer with the humid air. The calculated mass flow of evaporated water was 116.6 g/h compared to a measured mass flow of 88.4 g/h. 2.4 Nm^3/h of drying air with an average measured water load of 13.2 g/kg and a relative humidity of 90.6 % left the dryer at the air outlet. The humid air after the filter had a water load of 28.4 g/kg with an average relative humidity of 40.4 % and an average temperature of 47.7°C. Due to the blocked filter 35% of the air flow was lost between inlet and outlet. The calculated mass flow of water in the lost air was 46.2 g/h. All results of test run V12 are given in table 3.3.

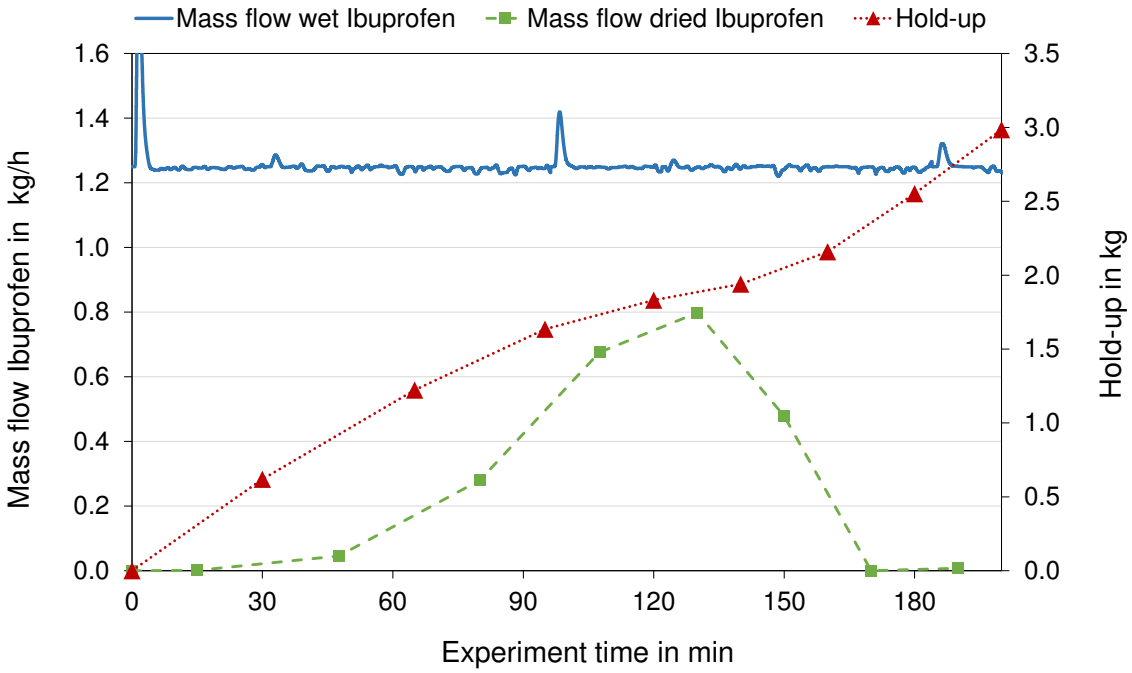

Figure 3.35.: Mass flow of wet and dried Ibuprofen as well as hold-up over experiment time of test run V12.

Table 3.5.: Mass balance of test run V12.

		Ibuprofen [kg]	Water [kg]	Drying air [kg]	Total [kg]
In	Feeder	3.91	0.404	0.0	4.31
	Air	0.0	0.0	15.80	15.80
Out	Product	0.87	0.003	0.0	0.88
	Condenser	0.0	0.152	0.0	0.15
	Air	0.0	0.143	10.38	10.52
	Lost air	0.0	0.154	5.42	5.58
	Hold-up	3.03	-0.047	0.0	2.99

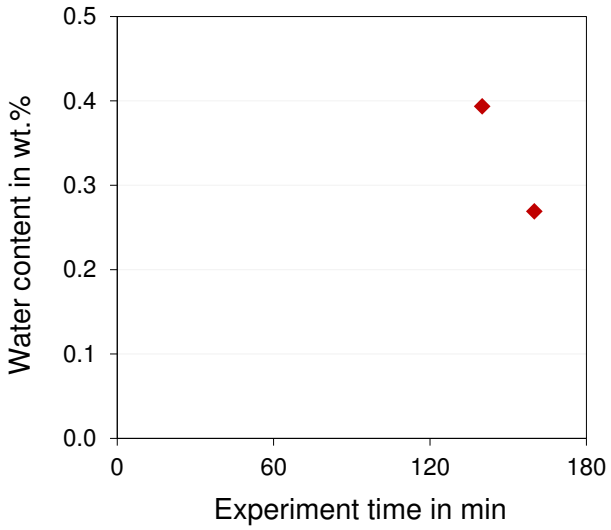

Figure 3.36.: Water content of test run V12 over experiment time.

No Ibuprofen was found in the condensate and condenser. Due to blockages of the outlet the dryer filled up with Ibuprofen and the material was pressed through the air holes into the filter. The filter was completely filled up with Ibuprofen, except a small hole for the air flow, as shown in figure 3.37. The small hole was also found in the material deposit in the filter connection pipe (see figure 3.38).
The dryer was completely filled up with Ibuprofen as in test run V11. The connection pipe between rotary valve and lid was also filled up with Ibuprofen, shown in figure 3.39.

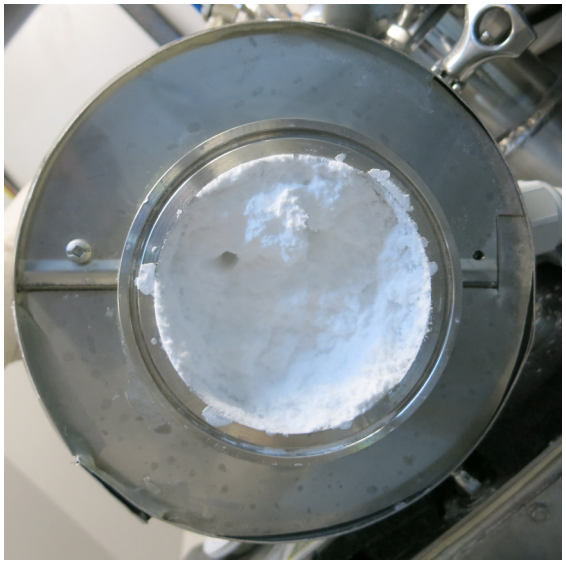

Figure 3.37.: View on the bottom side of the filter housing. The interior of the filter housing was completely filled up with Ibuprofen. Air circulation through a small hole in the material deposits.

Figure 3.38.: View on the material deposits in the filter connection pipe.

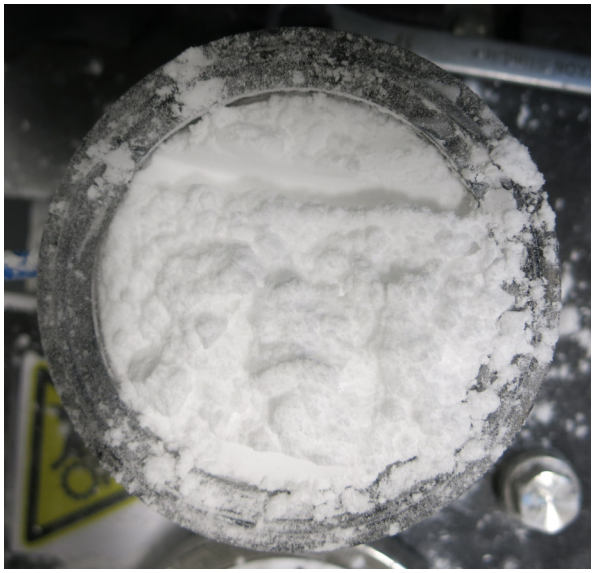

Figure 3.39.: Top view on the material deposits in the connection pipe between rotary valve and lid.

During the 300 minutes long test run V13 1.25 kg/h of wet Ibuprofen with a measured water content of 9.5 wt.% was fed into the dryer. A hold-up of 1.40 kg was reached at the end of the test run. The hold-up was still slightly increasing at the end of the test run. With the mass balance of the dryer a hold-up water content of 1.23 wt% was calculated. The mass balance of test run V13 is shown in table 3.6. The hold-up and the mass flows of wet and dried material over time are shown in figure 3.40. The steady state of the mass flow of dried product was reached after about 100 minutes. An average of 1.13 kg/h of dried Ibuprofen left the dryer with an average water content of 2.8 wt.%. The water content over time is shown in figure 3.41. A condensate mass flow of 48.0 g/h was measured. 26.7 g/h water left the dryer with the humid air. The calculated mass flow of evaporated water was 84.2 g/h compared to a measured mass flow of 74.7 g/h. 1.5 Nm^3/h of drying air with an average measured water load of 14.0 g/kg and a relative humidity of 95.3 % left the dryer at the air outlet. The humid air after the filter had a water load of 39.2 g/kg with an average relative humidity of 62.5 % and an average temperature of 45.1°C. 20% of the air flow was lost between inlet and outlet. The calculated mass flow of water in the lost air was 18.2 g/h. All results of test run V13 are given in table 3.3.

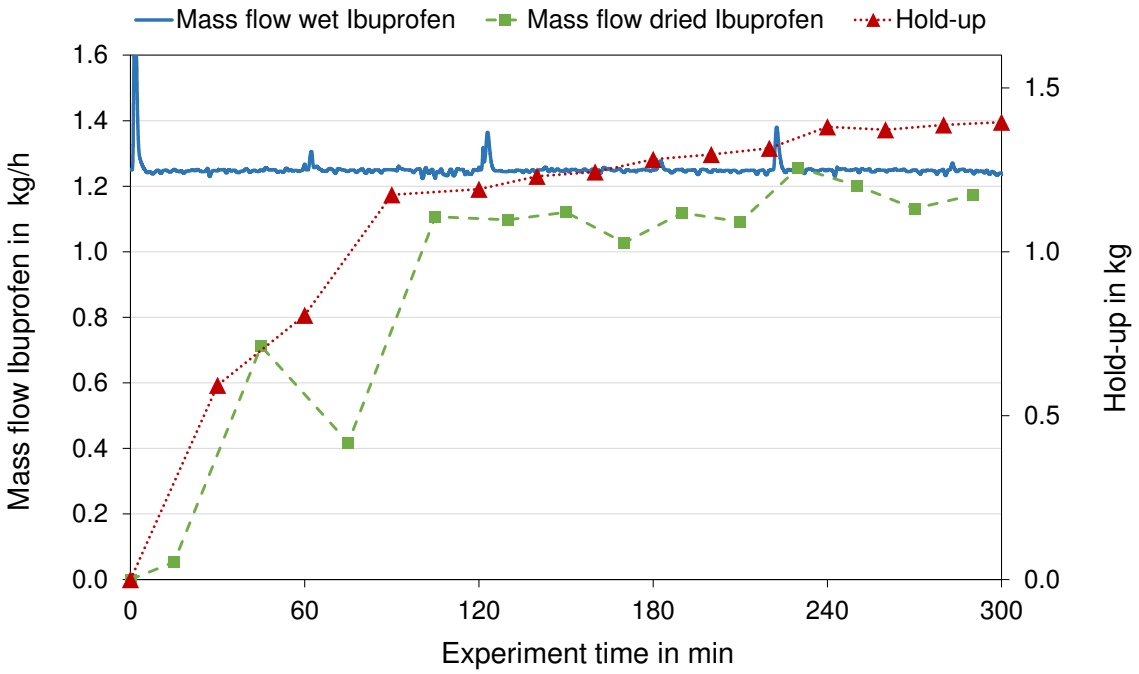

Figure 3.40.: Mass flow of wet and dried Ibuprofen as well as hold-up over experiment time of test run V13.

Table 3.6.: Mass balance of test run V13.

		Ibuprofen [kg]	Water [kg]	Drying air [kg]	Total [kg]
In	Feeder	5.80	0.608	0.0	6.41
	Air	0.0	0.0	11.85	11.85
Out	Product	4.42	0.127	0.0	4.55
	Condenser	0.0	0.240	0.0	0.24
	Air	0.0	0.133	9.53	9.67
	Lost air	0.0	0.091	2.32	2.41
	Hold-up	1.38	0.017	0.0	1.40

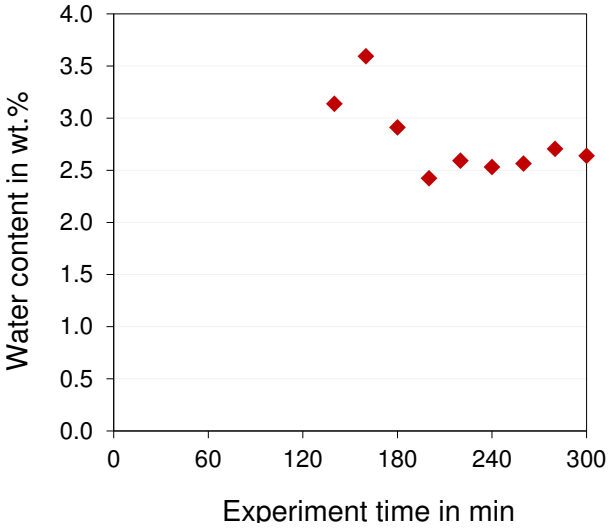

Figure 3.41.: Water content of test run V13 over experiment time.

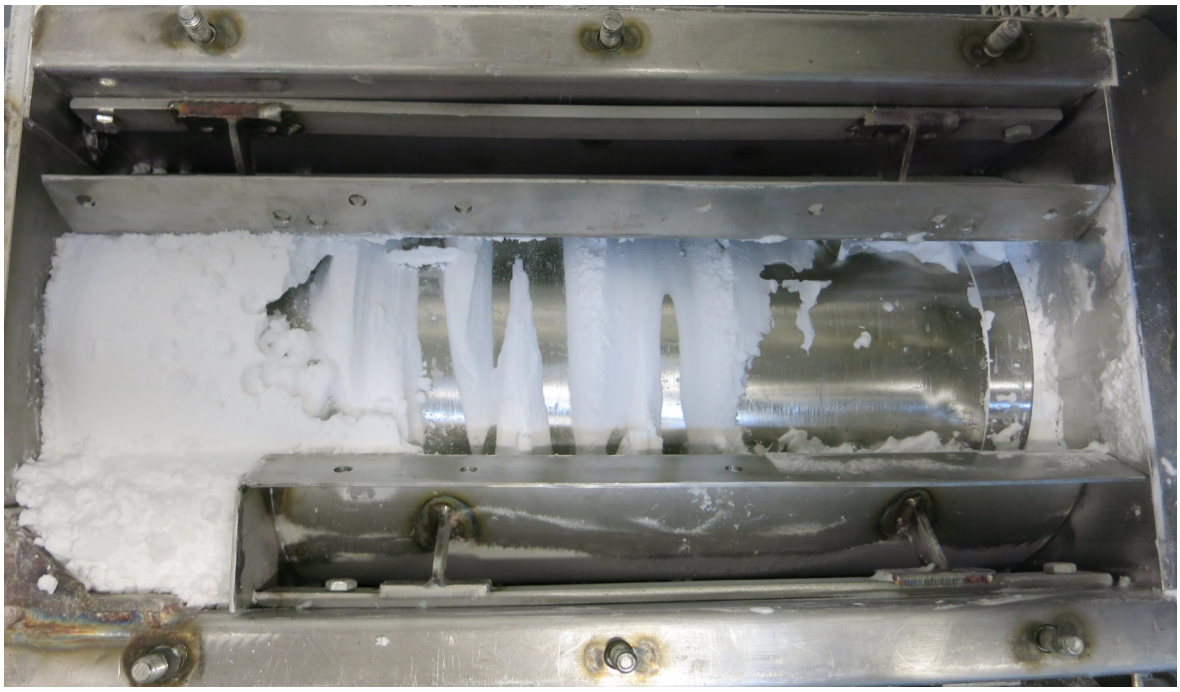

Figure 3.42.: Material inside the dryer at the end of test run V13 without top half shell covers. The material deposit on the inlet was already cleaned with a vacuum cleaner.

No Ibuprofen was found in the condensate and condenser. A small amount of Ibuprofen was transported through the air holes of the half shell cover due to material accumulation on the outlet side of the dryer. The space between half shell cover and filter was mainly free and no Ibuprofen deposits were found in the filter as shown in figure 3.43. Material accumulations occurred at the inlet (see figure 3.45) and outlet of the dryer. The accumulated material was compressed at the outlet side of the dryer shown in figure 3.42. The space between shaft and half shell covers remained free for the material transport as shown in figure 3.44.

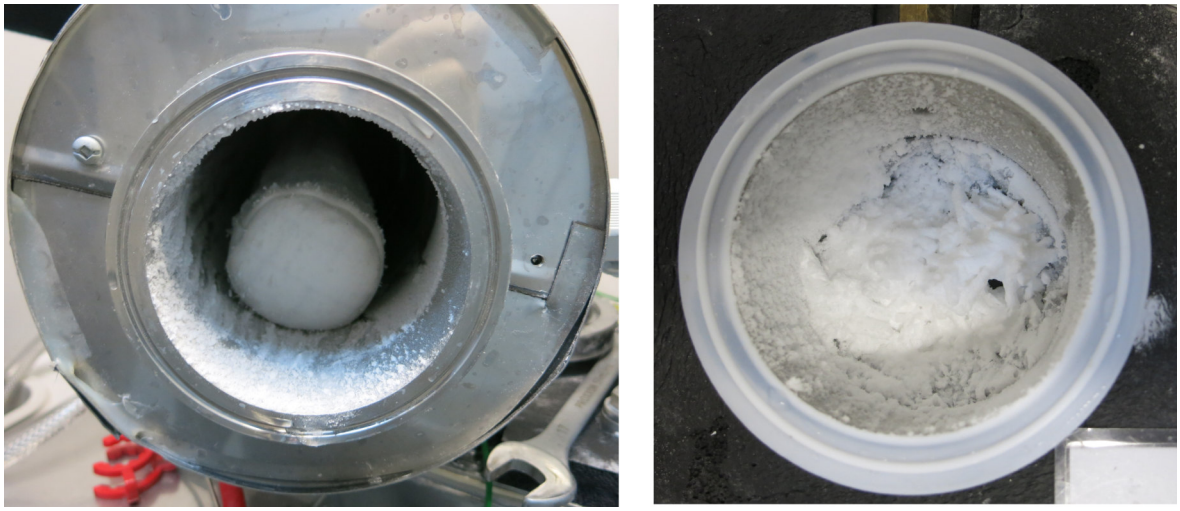

Figure 3.43.: Left: View on the bottom side of the filter. Right: View on the filter connection of the lid.

Figure 3.44.: Hollow space between half shell and shaft.

Figure 3.45.: Top view on the material deposit in the connection pipe between rotary valve and lid.

3.2.2.1. Summary of Test Runs V10 to V13

- A shaft speed of 120 rpm led to a blockage of the outlet with both, a feed mass flow of 1.25 kg/h and 2.5 kg/h. The material was thrown on the inner walls of the dryer and compacted there.
- A lower air flow rate led to a slightly higher water content of the product, a lower mass flow of water in air as well as higher relative humidity at the outlet and after the filter.
- A shaft speed of 120 rpm led to slightly higher mass flows of evaporated water.
- The big deviation between prepared and measured water content of test run V10 and V11 was probably due to bad sampling.
- A negative hold-up water content was calculated for test run V10 and V12. Possible reasons for this were an incorrect measured water content of the feed material or product, an inaccurate measurement of the water load or velocity of the humid exhaust air and a wrong assumption of the water load of the lost air.
- No significant improvement of the material flow at the outlet was realized through the additional ejection paddles.

3.2.3. V15 - V17

Test runs V15 to V17 were carried out as refeed experiment with three drying cycles. The dried product of test run V15 was used as feed material for test run V16 and the dried product of V16 was used as feed material for test run V17.

In test run V15 1.25 kg/h of wet Ibuprofen with a measured water content of 29.7 wt.% was fed into the dryer for 300 minutes. A hold-up of 0.79 kg was obtained after 300 minutes. No constant hold-up was reached till the end of the test run. The steady state of the mass flow of dried product was reached after about 90 minutes. An average mass flow of 1.03 kg/h dried Ibuprofen left the dryer with an average water content of 19.3 wt.%. A condensate mass flow of 67.1 g/h was measured. 53.5 g/h water left the dryer with the humid air. The calculated mass flow of evaporated water was 129.4 g/h compared to a measured mass flow of 120.5 g/h. 2.8 Nm^3/h of drying air with an average measured water load of 14.5 g/kg and a relative humidity of 95.7 % left the dryer at the air outlet. The humid air after the filter had a water load of 32.7 g/kg with an average relative humidity of 48.2 % and an average temperature of 46.9°C. 23 % of the air flow was lost between inlet and outlet. The calculated mass flow of water in the lost air was 34.6 g/h.

After test run V15 the feeder reservoir was emptied and cleaned and the dried product of test run V15 was filled in the feeder reservoir.
In the following test run V16 1.25 kg/h of wet Ibuprofen (product of test run V15) with a measured water content of 19.3 wt.% was fed into the dryer for 180 minutes. The hold-up increased from 0.79 kg at the end of test run V15 to 1.08 kg at the end of test run V16 (see figure 3.47). An average mass flow of 0.96 kg/h dried Ibuprofen left the dryer with an average water content of 10.2 wt.%. A condensate mass flow of 93.6 g/h was measured. 53.8 g/h water left the dryer with the humid air. The calculated mass flow of evaporated water was 114.2 g/h compared to a measured mass flow of 147.4 g/h. In test run V16 the measured mass flow of evaporated water raised to 147.4 g/h, because the hold-up in the dryer was still wet. The water of the hold-up of test run V15 and the water of the feed material was evaporated. 2.8 Nm^3/h of drying air with an average measured water load of 14.6 g/kg and a relative humidity of 98.7 % left the dryer at the air outlet. The humid air after the filter had a water load of 40.5 g/kg with an average relative humidity of 59.8 % and an average temperature of 46.6°C. 24 % of the air flow was lost between inlet and outlet. The calculated mass flow of water in the lost air was 44.7 g/h.

After test run V16 the feeder reservoir was emptied and cleaned again and the dried product of test run V16 was filled in the feeder reservoir for test run V17.
In test run V17 1.19 kg/h of wet Ibuprofen with a measured water content of 10.2 wt.% was fed into the dryer for 90 minutes. The hold-up increased from 1.08 kg at the end of test run V16 to 1.17 kg at the end of test run V17. At the end of test run V17 the hold-up decreased slightly (see figure 3.47). An average mass flow of 0.95 kg/h dried Ibuprofen left the dryer with an average water content of 2.1 wt.%. A condensate mass flow of 80.1 g/h was measured. 55.6 g/h water left the dryer with the humid air. The calculated mass flow of evaporated water was 96.0 g/h compared to a measured mass flow of 135.6 g/h. In test run V17 the amount of evaporated water decreased compared to V16, because the water content of the hold-up decreased as well. 3.0 Nm^3/h of dry-

ing air with an average measured water load of 14.4 g/kg and a relative humidity of 98.2 % left the dryer at the air outlet. The humid air after the filter had a water load of 35.5 g/kg with an average relative humidity of 57.6 % and an average temperature of 44.9°C. 20 % of the air flow was lost between inlet and outlet. The calculated mass flow of water in the lost air was 32.8 g/h.

With the mass balance of the dryer an average hold-up water content of -5.55 wt% was calculated. This means that more water left the dryer than entered the dryer, which is not possible. Possible reasons for this were a wrong measured mass flow of water in air and lost air. The mass balance of test run V15 to V17 is shown in table 3.8. The water content over time for the whole refeed test run is shown in figure 3.46. All results are given in table 3.7.

Table 3.7.: Results and set values of drying test runs V15 - V17.

			V15	V16	V17
Set	Water content (feed)	[wt.%]	29.7%	19.3%	10.2%
	Mass flow (feed)	[kg/h]	1.25	1.25	1.19
	Shaft speed	[rpm]	60	60	60
	Air flow (inlet)	[Nm³/h]	3.7	3.7	3.7
Results	Hold-up	[kg]	0.79	1.08	1.17
	Experiment time	[min]	300	180	90
	Steady state (dried Ibuprofen)	[min]	90	-	-
	Mass flow (dried)	[kg/h]	1.03	0.96	0.95
	Water content (dried)	[wt.%]	19.3%	10.2%	2.1%
	Evaporated water (calc)	[g/h]	129.4	114.2	96.0
	Evaporated water (measured)	[g/h]	120.5	147.4	135.6
	Mass flow condensate	[g/h]	67.1	93.6	80.1
	Mass flow water in air	[g/h]	53.5	53.8	55.6
	Mass flow water in lost air	[g/h]	34.6	44.7	32.8
	Air flow (outlet)	[Nm³/h]	2.8	2.8	3.0
	Lost air flow	[%]	23%	24%	20%
	Water load of air	[g/kg]	14.5	14.6	14.4
	Relative humidity (outlet)	[%]	95.7%	98.7%	98.2%
	Water load of lost air	[g/kg]	32.7	40.5	35.5
	Relative humidity (filter)	[%]	48.2%	59.8%	57.6%

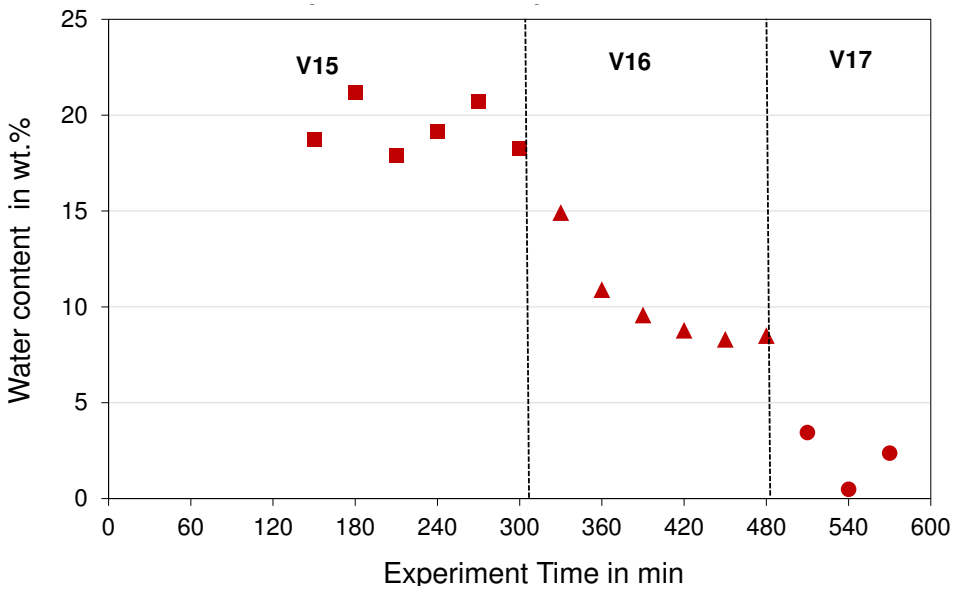

Figure 3.46.: Water content of refeed test runs V15 to V17 over experiment time.

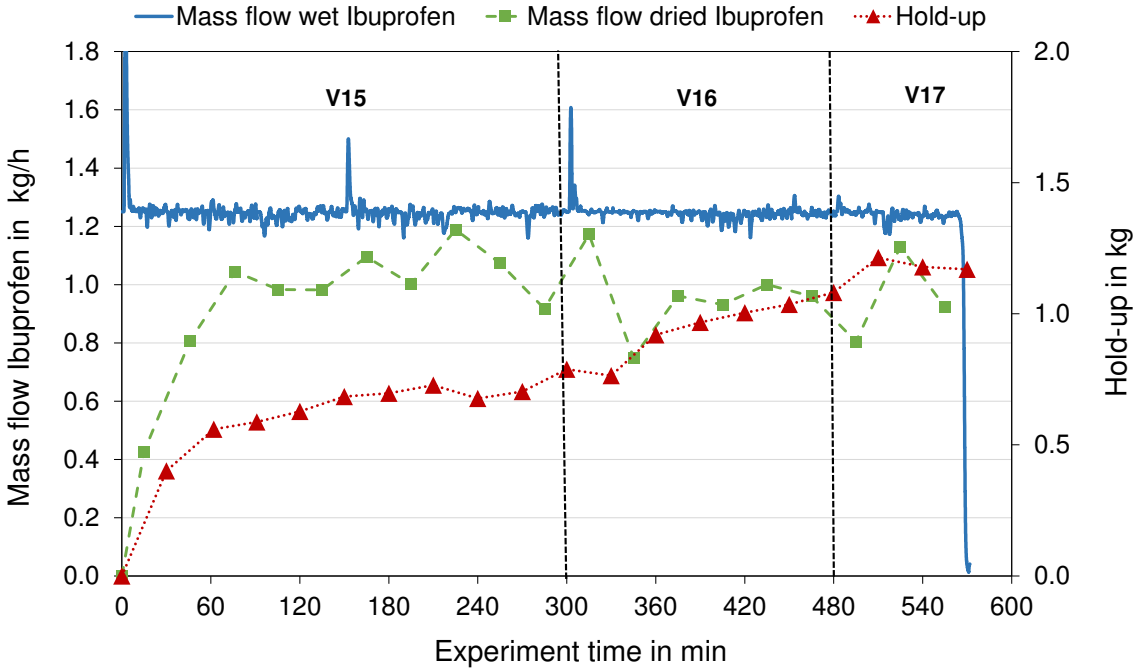

Figure 3.47.: Mass flow of wet and dried Ibuprofen as well as hold-up over experiment time of test runs V15 to V17.

Table 3.8.: Mass balance of test run V15 to V17

		Ibuprofen [kg]	Water [kg]	Drying air [kg]	Total [kg]
In	Feeder	9.06	2.780	0.0	11.84
	Air	0.0	0.0	45.04	45.04
Out	Product	7.83	1.242	0.0	9.07
	Condenser	0.0	0.736	0.0	0.74
	Air	0.0	0.511	35.06	35.57
	Lost air	0.0	0.356	9.98	10.33
	Hold-up	1.23	-0.065	0.0	1.17

No Ibuprofen was found in the condensate and condenser. A small amount of Ibuprofen was transported through the air holes of the half shell cover due to material accumulation on the outlet side of the dryer. The space between half shell cover and filter was mainly free and no Ibuprofen deposits were found in the filter.
Material accumulations occurred at the inlet and outlet of the dryer as shown in figure 3.48. The material accumulation on the inlet in figure 3.48 was already partly removed with a vacuum cleaner. The whole inlet connection of the lid was filled up with accumulated material, as shown in figure 3.50. In addition, material deposits were observed in the rotary valve as shown in figure 3.49.

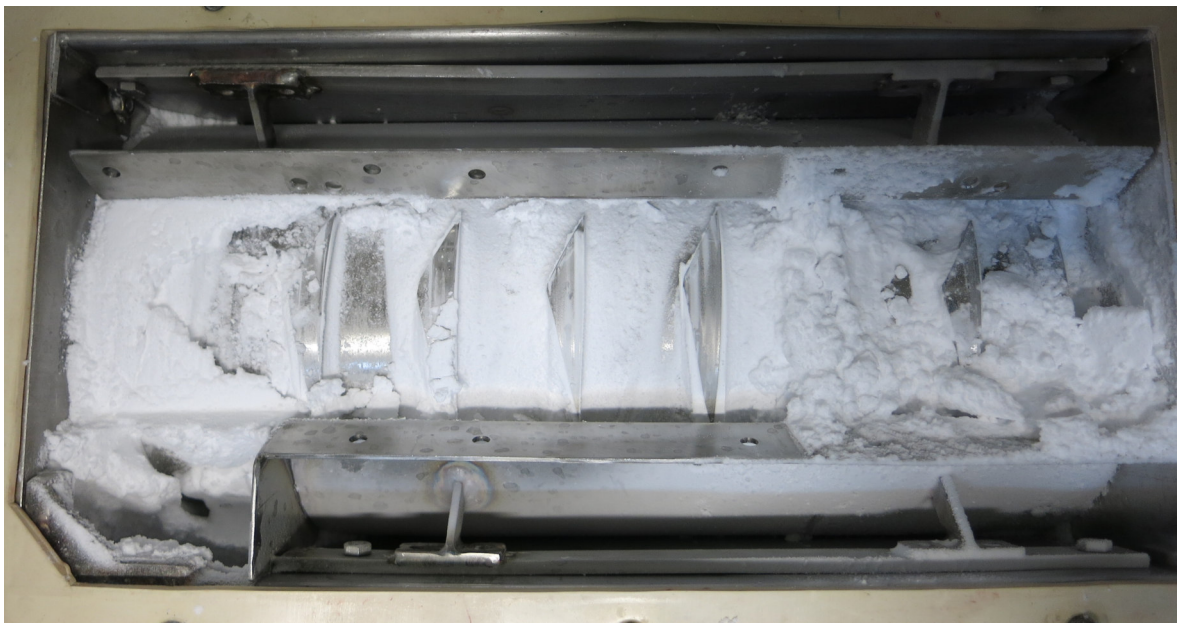

Figure 3.48.: Material inside the dryer at the end of refeed test runs V15 to V17 without top half shell covers. The material deposit on the inlet was already partly cleaned with a vacuum cleaner.

Figure 3.49.: Top view on the material deposits inside the rotary valve.

Figure 3.50.: Top view on the material deposits at the dryer inlet.

3.2.3.1. Summary of Refeed Test Runs V15 to V17

- Refeed of the product is possible.
- It was possible to dry Ibuprofen powder with a water content of 29.7 wt.% to 2.1 wt.% with three refeed cycles.
- Hold-up increased for all refeed test runs.
- Fluctuating mass flow of dried product

3.2.4. V18 - V19

In test run V18 1.22 kg/h of wet Ibuprofen with a measured water content of 8.9 wt.% was fed into the dryer for 300 minutes. A hold-up of 1.49 kg was reached at the end of the test run. The hold-up was constant after about 200 minutes with a small decrease around minute 260. With the mass balance of the dryer a hold-up water content of 6.79 wt% was calculated. The mass balance of test run V18 is shown in table 3.10. The hold-up and the mass flows of wet and dried Ibuprofen over time are shown in figure 3.51. The mass flow of dried product was fluctuating during the whole test run. The dried Ibuprofen had an average water content of 3.0 wt.%. The water content over time is shown in figure 3.52. A condensate mass flow of 26.6 g/h was measured. 17.8 g/h water left the dryer with the humid air. The calculated mass flow of evaporated water was 72.0 g/h compared to a measured mass flow of 44.4 g/h. 1.0 Nm^3/h of drying air with an average measured water load of 13.9 g/kg and a relative humidity of 92.9 % left the dryer at the air outlet. The humid air after the filter had a water load of 35.4 g/kg with an average relative humidity of 56.8 % and an average temperature of 46.5°C. 29% of the air flow was lost between inlet and outlet. The calculated mass flow of water in the lost air was 17.8 g/h. All results of test run V18 are given in table 3.9.

Table 3.9.: Results and set values of drying test runs V18 and V19.

			V18	V19
Setup	Water content (feed)	[wt.%]	8.9%	9.5%
	Mass flow (feed)	[kg/h]	1.22	1.27
	Shaft speed	[rpm]	60	60
	Air flow (inlet)	[Nm^3/h]	1.4	3.7
Results	Hold-up	[kg]	1.49	1.56
	Experiment time	[min]	300	302
	Steady state (dried Ibuprofen)	[min]	-	-
	Mass flow (dried)	[kg/h]	-	-
	Water content (dried)	[wt.%]	3.0%	0.4%
	Evaporated water (calc)	[g/h]	72.0	112.6
	Evaporated water (measured)	[g/h]	44.4	78.3
	Mass flow condensate	[g/h]	26.6	22.9
	Mass flow water in air	[g/h]	17.8	55.4
	Mass flow water in lost air	[g/h]	17.8	19.0
	Air flow (outlet)	[Nm^3/h]	1.0	2.9
	Lost air flow	[%]	29%	20%
	Water load of air	[g/kg]	13.9	15.2
	Relative humidity (outlet)	[%]	92.9%	81.7%
	Water load of lost air	[g/kg]	35.4	20.4
	Relative humidity (filter)	[%]	56.8%	38.8%

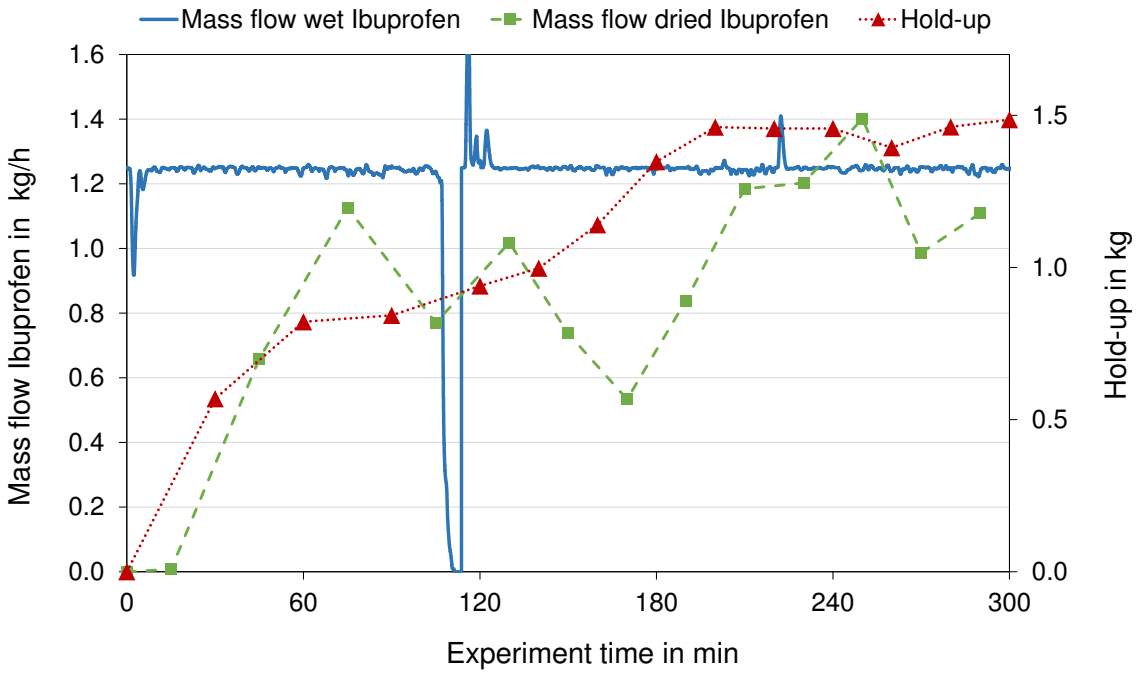

Figure 3.51.: Mass flow of wet and dried Ibuprofen as well as hold-up over experiment time of test run V18.

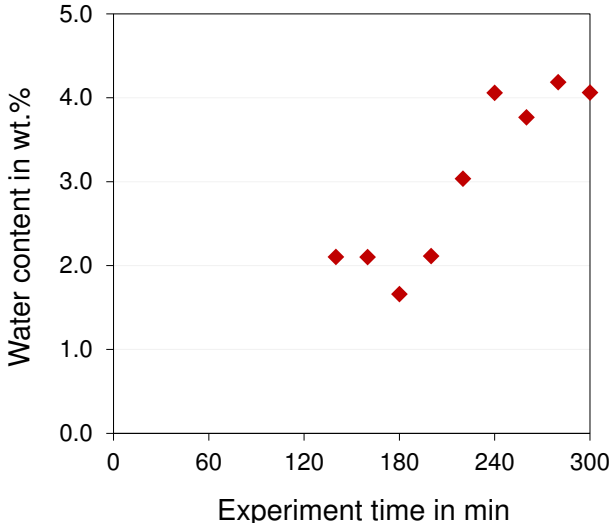

Figure 3.52.: Water content of test run V18 over experiment time.

Table 3.10.: Mass balance of test run V18

		Ibuprofen [kg]	Water [kg]	Drying air [kg]	Total [kg]
In	Feeder	5.54	0.539	0.0	6.08
	Air	0.0	0.0	8.77	8.77
Out	Product	4.16	0.127	0.0	4.29
	Condenser	0.0	0.133	0.0	0.13
	Air	0.0	0.089	6.27	6.36
	Lost air	0.0	0.089	2.51	2.60
	Hold-up	1.39	0.101	0.0	1.49

No Ibuprofen was found in the condensate and condenser. Ibuprofen was pressed through the air holes of the half shell cover due to material accumulation on the outlet side of the dryer (see figure 3.54). This material deposits had a vermiform shape as shown in figure 3.53. Material accumulations occurred also at the inlet of the dryer as shown in figure 3.53. Material deposits were found in the rotary valve.

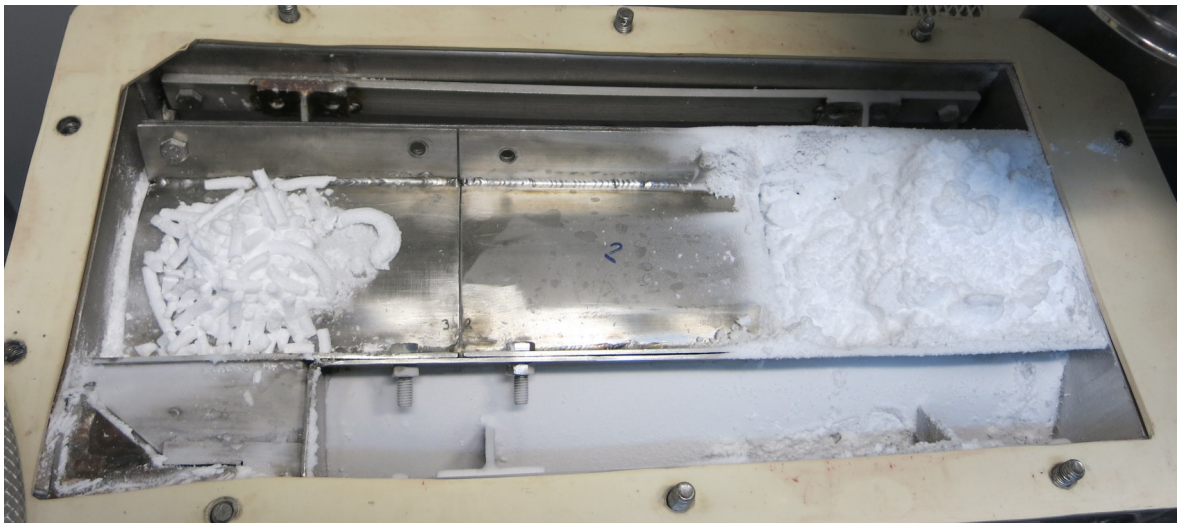

Figure 3.53.: Material inside the dryer at the end of test run V18.

Figure 3.54.: Material inside the dryer at the end of test run V18 without top half shell covers. The material deposit on the inlet was already removed with a vacuum cleaner.

Before test run V19 further modifications of the experimental setup were made. The air holes of the half shell cover were changed to one big hole (see figure 3.55). The paddles on the outlet side of the dryer were optimized for better ejection of the material into the outlet pipe as shown in figure 3.57. To further reduce the dead volume of the dryer, two plastic plates, covered with Teflon tape, were glued on the inner dryer wall at the inlet and outlet as shown in figure 3.57. A thermocouple was installed to measure the temperature of the material flow between the shaft and the half shell covers. The thermocouple was inserted into the dryer through the compressed air connection located in the middle of the lid and was then put through a small hole in the half shell cover as shown in figure 3.56. The variable area flow meter for the heating water were changed from a throughput range of 17 to 170 l/h to 2.5 to 25 l/h to reduce the heating water flow.

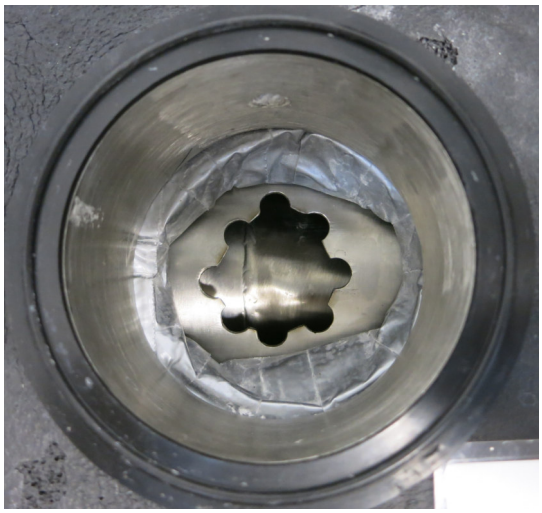

Figure 3.55.: Hole in the half shell cover for the air flow.

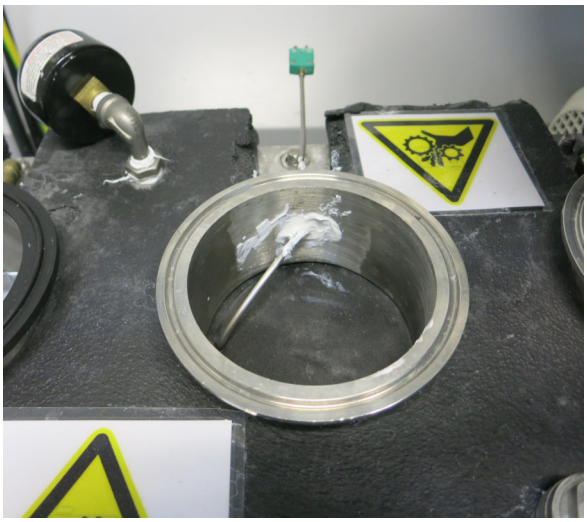

Figure 3.56.: Installation of the thermocouple to measure the temperature of the material flow through the dryer.

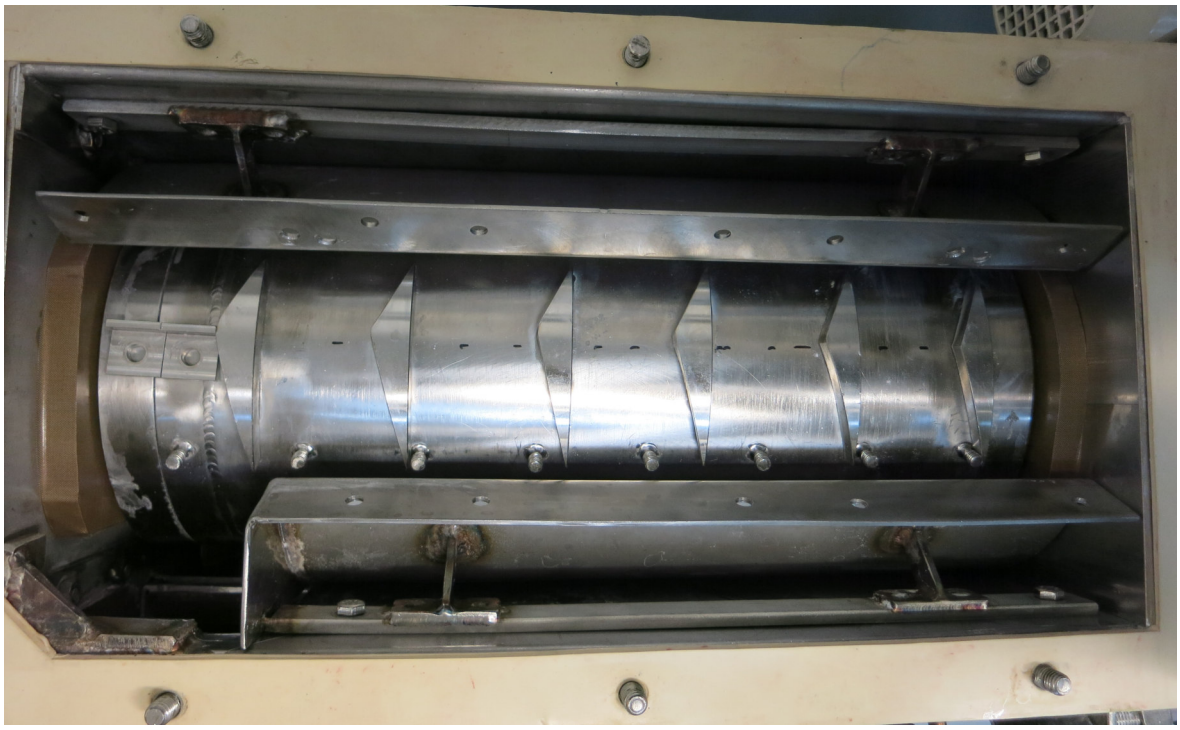

Figure 3.57.: Paddle configuration of test run V19. On the inlet and outlet side of the dryer Teflon-covered plastic plates were glued on the inner dryer wall.

In test run V19 an average feed flow of 1.27 kg/h wet Ibuprofen with a measured water content of 9.5 wt.% was fed into the dryer for 302 minutes. A hold-up of 1.56 kg was reached at the end of the test run. The hold-up increased during the whole test run. With the mass balance of the dryer a hold-up water content of 5.91 wt% was calculated. The mass balance of test run V19 is shown in table 3.11. The hold-up and the mass flows of wet and dried material over time are shown in figure 3.58. It was not possible to calculate the mass flow of dried product due to fluctuations (see figure 3.58. The dried Ibuprofen had an average water content of 0.4 wt.%. The water content over time is shown in figure 3.59. A condensate mass flow of 22.9 g/h was measured. 55.4 g/h water left the dryer with the humid air. The calculated mass flow of evaporated water was 112.6 g/h compared to a measured mass flow of 78.3 g/h. 2.9 Nm^3/h of drying air with an average measured water load of 15.2 g/kg and a relative humidity of 81.7 % left the dryer at the air outlet. The humid air after the filter had a water load of 20.4 g/kg with an average relative humidity of 38.8 % and an average temperature of 42.1°C. 20% of the air flow was lost between inlet and outlet. The calculated mass flow of water in the lost air was 19.0 g/h. All results of test run V19 are given in table 3.9.

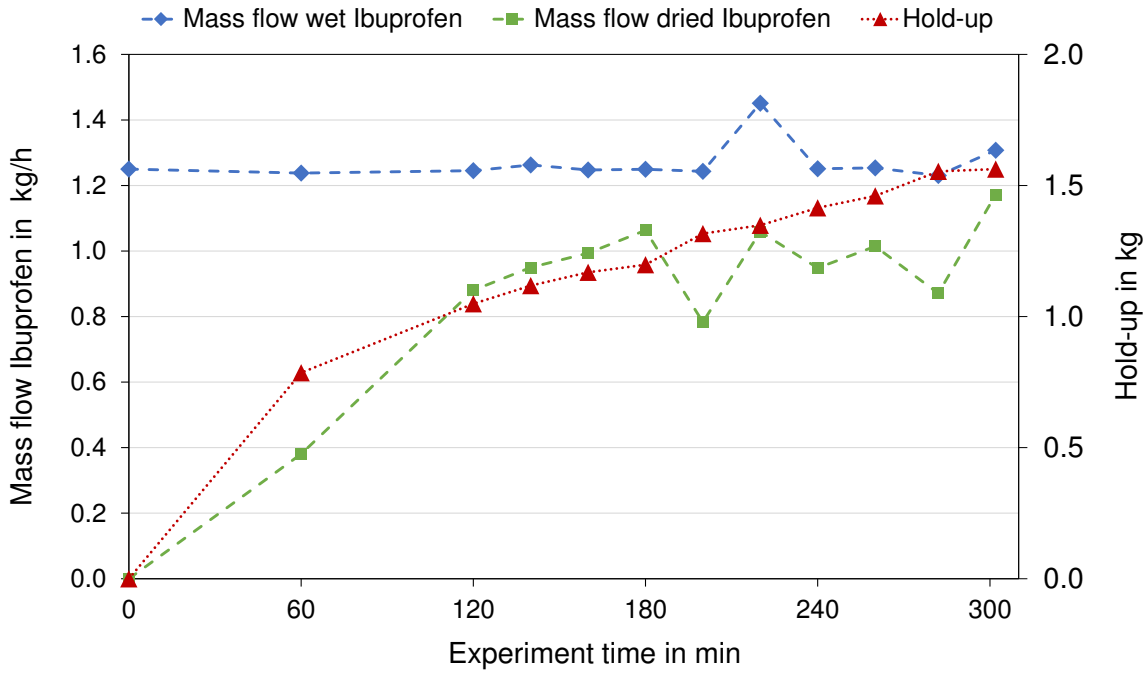

Figure 3.58.: Mass flow of wet and dried Ibuprofen as well as hold-up over experiment time of test run V19.

Table 3.11.: Mass balance of test run V19

		Ibuprofen [kg]	Water [kg]	Drying air [kg]	Total [kg]
In	Feeder	5.70	0.595	0.0	6.29
	Air	0.0	0.0	23.86	23.86
Out	Product	4.23	0.016	0.0	4.24
	Condenser	0.0	0.115	0.0	0.12
	Air	0.0	0.277	19.19	19.47
	Lost air	0.0	0.095	4.67	4.77
	Hold-up	1.47	0.092	0.0	1.56

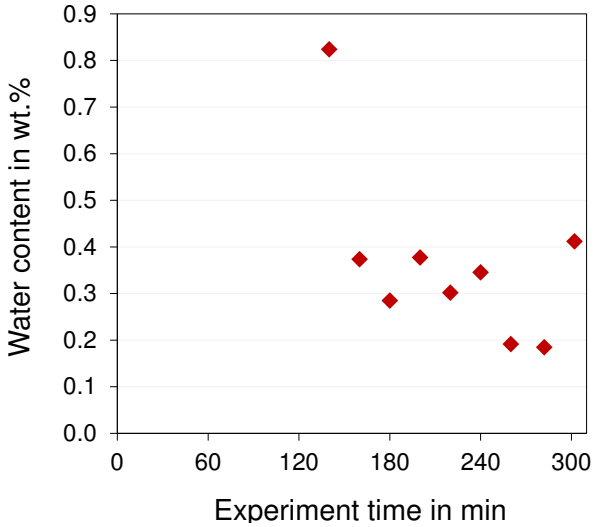

Figure 3.59.: Water content of test run V19 over experiment time.

No Ibuprofen was found in the condensate and condenser. Ibuprofen was pressed through the air hole of the half shell cover due to material accumulation on the outlet side of the dryer (see figure 3.61). A small hole was visible in the material deposits at the outlet, most likely due to the air flow from the dryer into the filter. The material accumulations occurred also at the inlet of the dryer as shown in figure 3.60. The material deposits inside the dryer are shown in figure 3.62. On this picture the material deposit at the inlet was already partly removed with a vacuum cleaner. The compacted material on the shaft after removing the half shell covers is shown in figure 3.63. The loose material was removed with a vacuum cleaner before the picture was taken.

Figure 3.60.: Top view on the material deposits at the inlet of the dryer after test run V19

Figure 3.61.: Top view on the material deposits at the outlet of the dryer after test run V19.

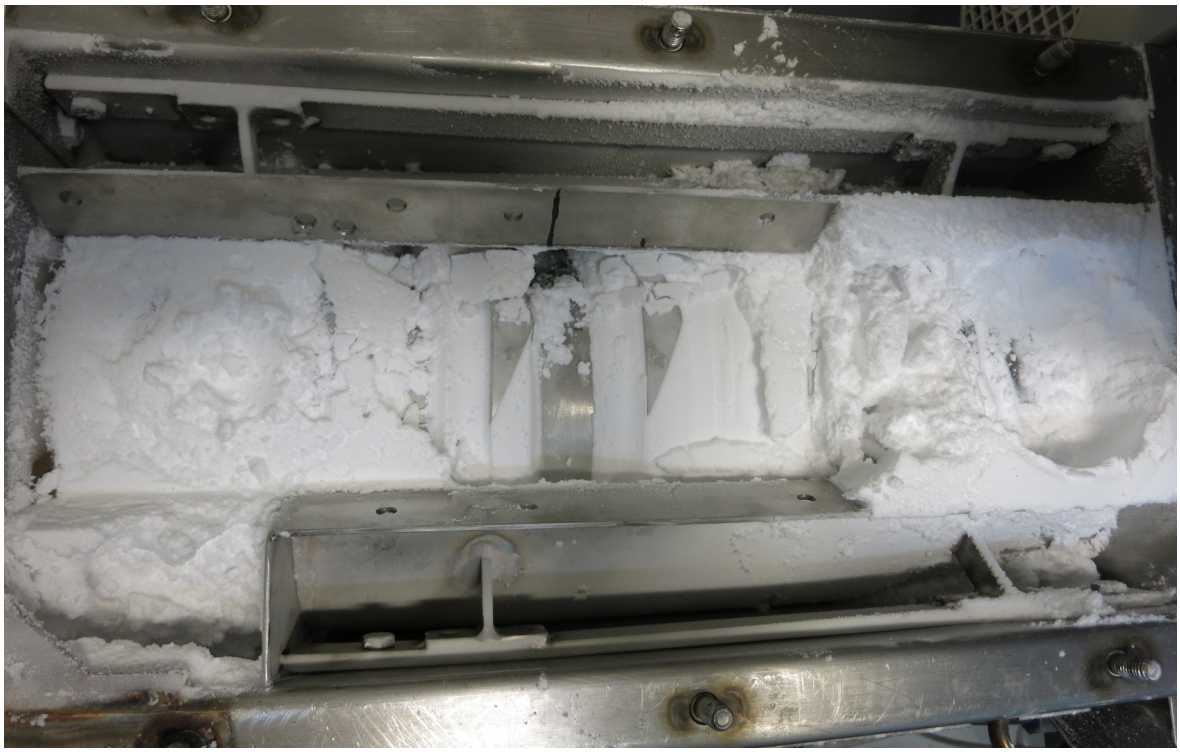

Figure 3.62.: Material at the end of test run V19 without the top half shell covers. The material deposit on the inlet was already partly removed with a vacuum cleaner.

Figure 3.63.: Compacted material deposits on the shaft after removing the half shell covers. Loose material was removed with a vacuum cleaner before the picture was taken. One paddle broke off during cleaning.

3.2.4.1. Summary of Test Runs V18 and V19

- Installation of paddles at the outlet as depicted in figure 3.57 did not improve the material ejection. The outlet of the dryer should be located at the bottom side for drying Ibuprofen powder
- The hold-up was not reduced by the plastic plates (see figure 3.57).
- Material was transported through the air hole in the half shell cover. The air hole needs to be closed till material transport at the outlet is fixed.

3.3. Particle Size Distribution

The particle size distribution of raw, wet and dried Ibuprofen was measured to investigate the influence of mixing (moisturizing of the raw Ibuprofen with water in a high shear mixer), drying (flow through the dryer) and the water content on the particle size of the powder.

The particle size distribution of raw, wet and dried Ibuprofen of test run V6 was measured only in wet dispersion mode. The particle size increased slightly after mixing with water and decreased almost to the initial size of raw Ibuprofen after drying. The volume density distribution q3 of test run V6 is shown in figure 3.64.

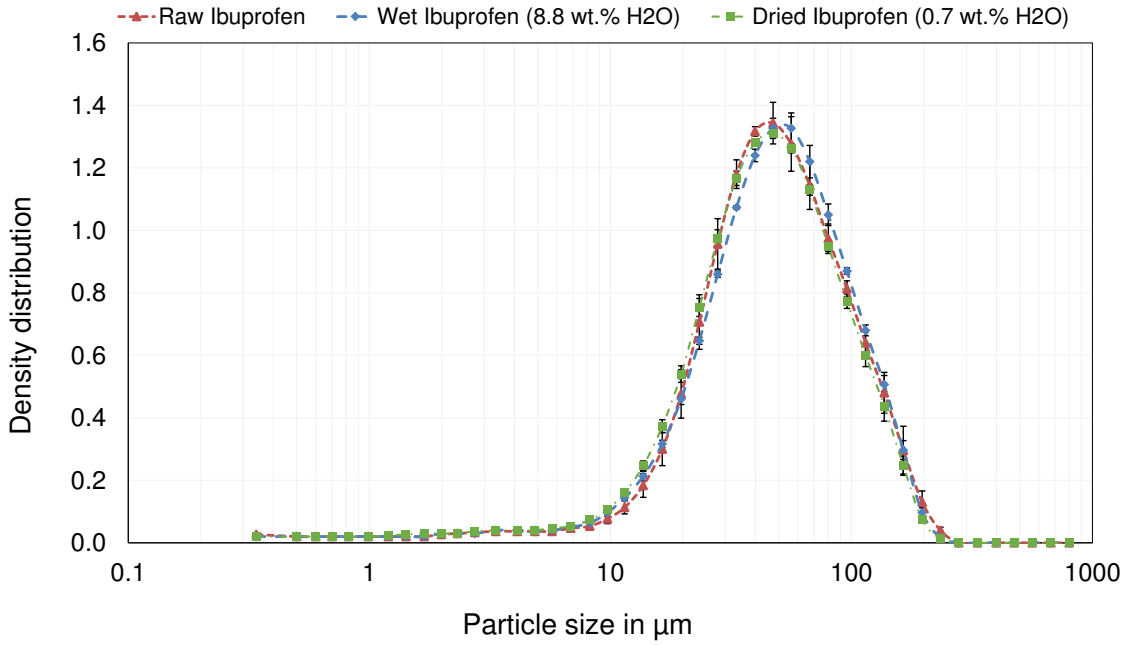

Figure 3.64.: Volume density distribution of raw wet (8.8 wt.% H_2O) and dried (0.7 wt.% H_2O) Ibuprofen of test run V6, measured in wet dispersion mode.

For test run V7 to V9 the particle size was measured in wet and dry dispersion mode. The volume density distribution q3 of raw, wet and dried Ibuprofen for wet dispersion mode of test runs V7 to V9 are shown in figure A.1, A.2 and A.3 in the appendix. Wet and dried Ibuprofen showed larger particles than raw Ibuprofen. The particle size increased due to the formation of particle agglomerates. This particle agglomerates were probably not broken up due to the dispersion in water.
Raw Ibuprofen of test run V7 to V9 had a mean particle diameter of 36.1 µm. The mean particle diameters, VMD and span for wet and dried Ibuprofen, of test run V7 to V9, for wet dispersion are shown in table 3.12.

In dry dispersion mode a pressure titration of raw, wet and dried Ibuprofen was performed at 0.5, 1.0 and 2.0 bar dispersion pressure. A pressure titration is a series of repeat measurements at different dispersion pressures to find the optimal dispersion pressure and to check if a particle size plateau is reached with increasing dispersion pressure [43]. The particle size measured in dry dispersion mode also increased for wet and dried Ibuprofen compared to raw Ibuprofen. The VMD, mean particle diameter

and the span of the particle size distribution are shown in table 3.13 for dry dispersion at 0.5 bar, table 3.14 for dry dispersion at 1.0 bar and table 3.16 for dry dispersion at 2.0 bar.

The VMD of raw, wet and dried Ibuprofen, measured in dry dispersion mode was compared to the VMD measured in wet dispersion mode as shown in figure 3.65 for test run V7. The VMD and mean particle diameter measured in wet dispersion mode showed bigger particles than in dry dispersion mode. This was another indication for unbroken particle agglomerates in wet dispersion mode.

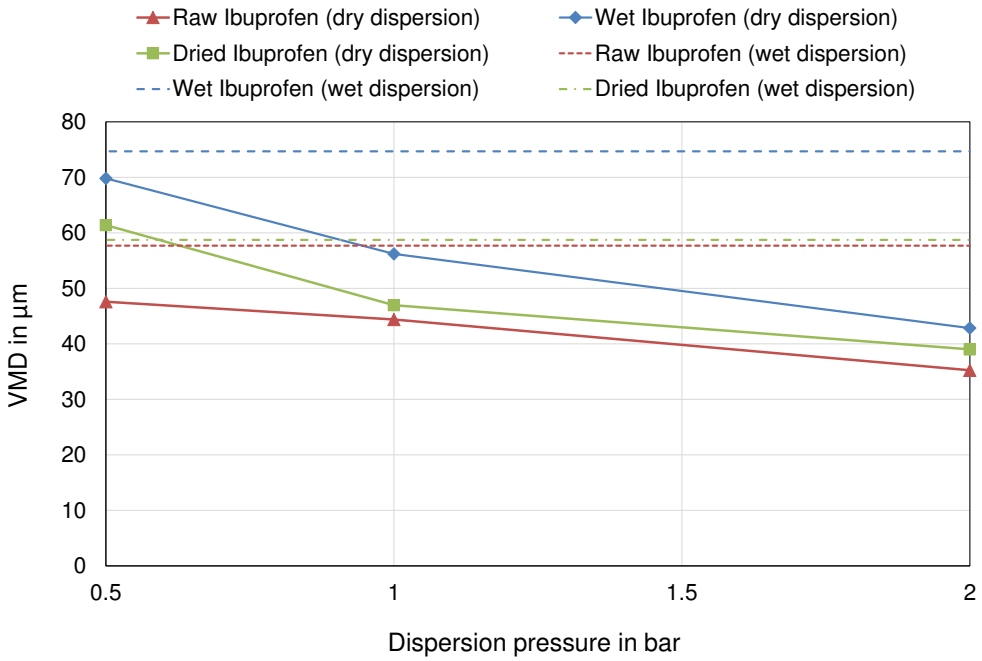

Figure 3.65.: VMD of raw, wet (16.0 wt.% H_2O) and dried (9.6 wt.% H_2O) Ibuprofen of test run V7 over dispersion pressure compared to the VDM of raw, wet and dried Ibuprofen measured with wet dispersion mode.

The volume density distributions q3 over dispersion pressure of raw, wet and dried Ibuprofen for wet and dry dispersion are shown in figure 3.66, 3.67 and 3.68.
It was found that the overall particle size decreased with increasing dispersion pressure. This was due to the breakage of the particle agglomerates or the particles itself. It was not possible to inspect the particles after the dry dispersion measurement, therefore it was not possible to find out if only the agglomerates were broken or not.
The volume density distributions over dispersion pressure for wet and dried Ibuprofen measured with wet and dry dispersion are shown in figure A.4 to A.7 for test run V8 and V9 in the appendix. In test run V9 the particle size distribution of wet and dried Ibuprofen, measured at 0.5 bar dispersion pressure, showed more bigger particles. This was maybe due to stronger interparticular forces between the particles due to the high water content and the low dispersion pressure of 0.5 bar.
A clear decrease of the VMD with increasing dispersion pressure was found. This effect can be explained by breakage of particle agglomerates [37] or also breakage of the primary particle. No particle size plateau was reached. For all further particle size measurement in dry dispersion mode, 1.5 bar dispersion pressure was also measured to

increase the pressure titration accuracy.

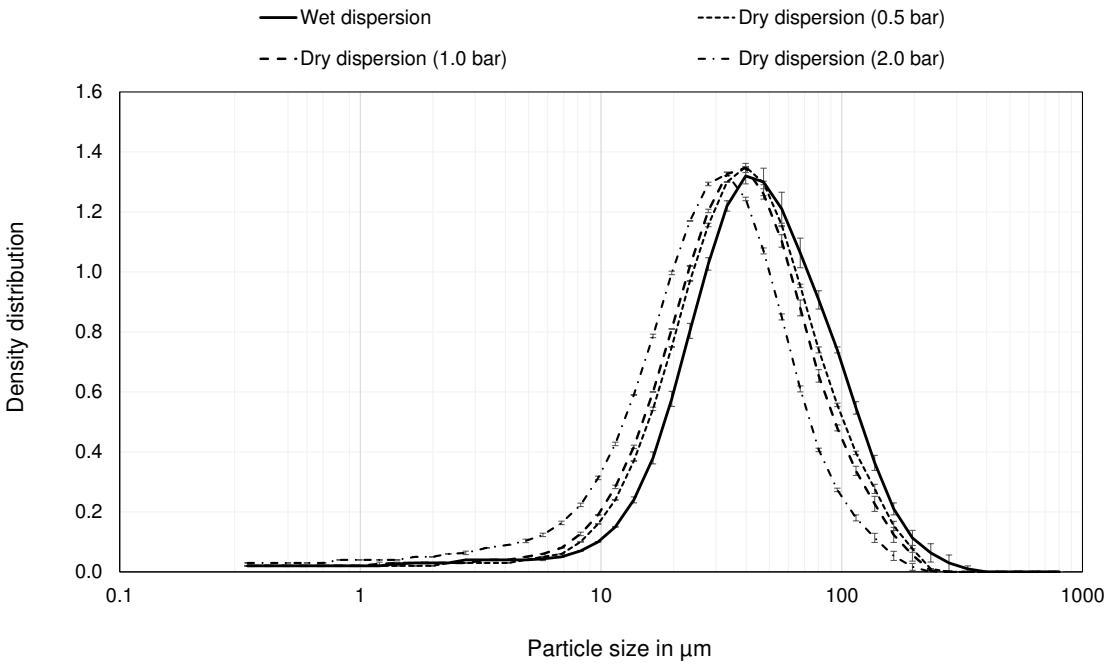

Figure 3.66.: Volume density distribution of raw Ibuprofen of test run V7 to V9 over dispersion pressure compared to the volume density distribution of raw Ibuprofen measured in wet dispersion mode.

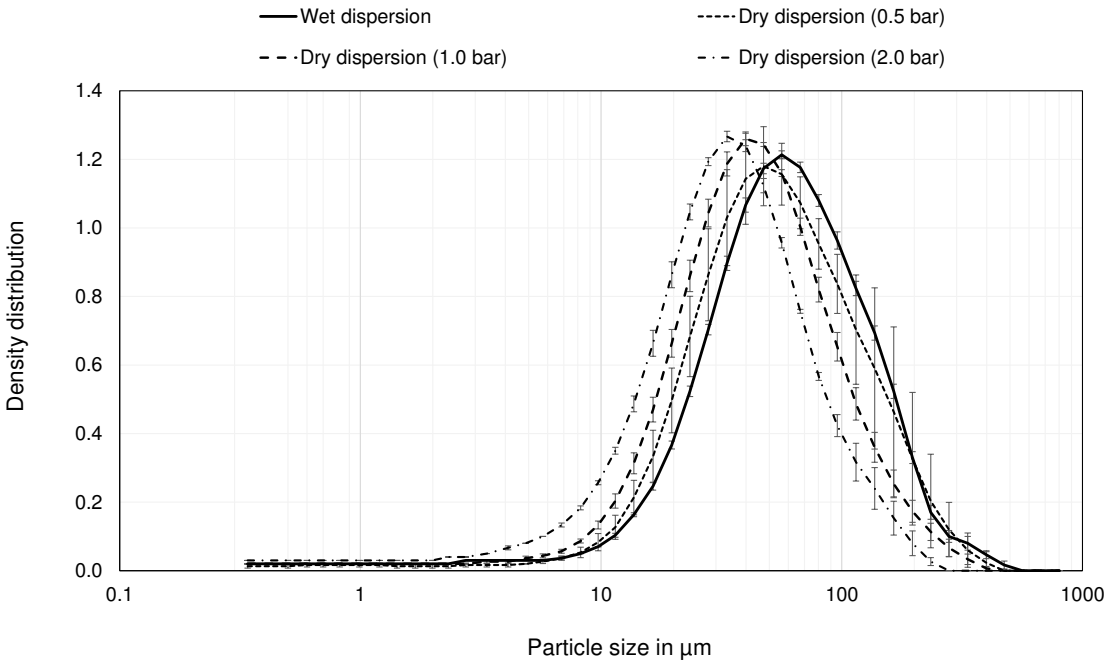

Figure 3.67.: Volume density distribution of wet (16.0 wt.% H_2O) Ibuprofen of test run V7 over dispersion pressure compared to the volume density distribution of wet Ibuprofen measured in wet dispersion mode.

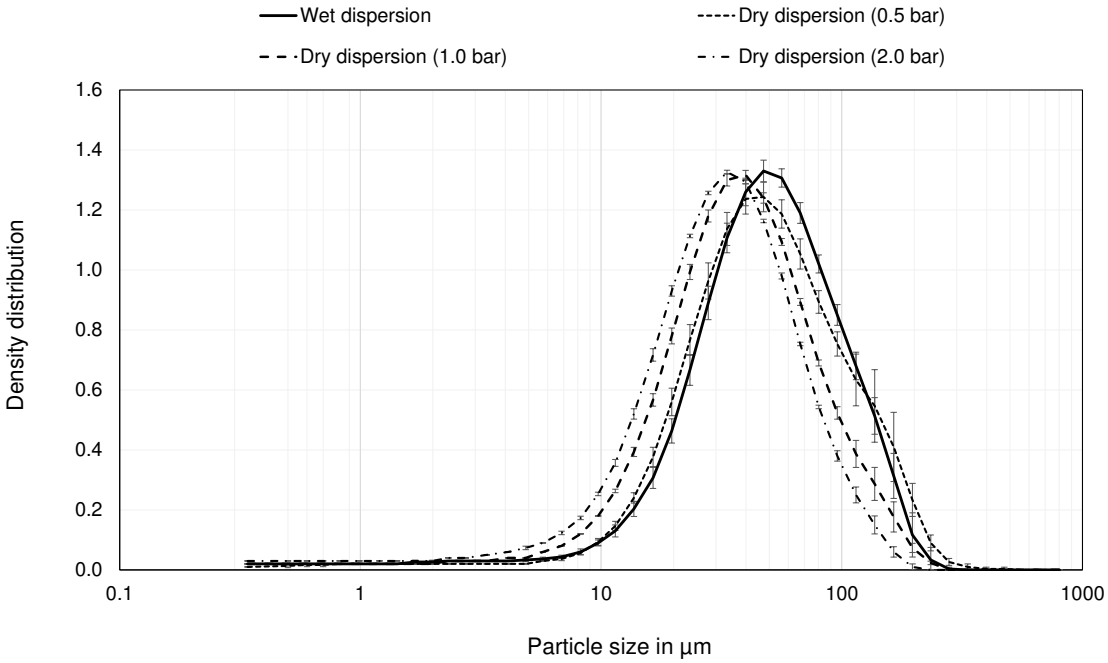

Figure 3.68.: Volume density distribution of dried (9.6 wt.% H_2O) Ibuprofen of test run V7 over dispersion pressure compared to the volume density distribution of dried Ibuprofen measured in wet dispersion mode.

In figure 3.69 the VMD measured with wet and dried dispersion mode is shown over the water content for test run V7 to V9. In wet dispersion mode the measured particle size was not influenced by the water content. For dry dispersion mode, the VMD increased with increasing water content. The effect of the water content on the VMD decreased with increasing dispersion pressure.

For test run V10 to V13 the particle size was only measured in dry dispersion mode. The same observations as for the previous test runs were made. The particle size increased slightly after mixing and drying due to particle agglomeration. The volume density distributions of raw, wet and dried Ibuprofen, for test run V10 to 13, for all dispersion pressures, are shown in figure A.9 to A.32 in the appendix. Test run V11 and V12 were done with a shaft speed of 120 instead of 60 rpm. The shaft speed had no influence on the particle size.
The VMD of raw, wet and dried Ibuprofen over the dispersion pressure is shown exemplary in figure 3.70 for test run V10. The slope of the VMD line decreased with increasing dispersion pressure, but a particle size plateau was not reached. The dispersion pressure has to be increased to see if a particle size plateau can be reached. The VMD, mean particle diameter and the span of the particle size distribution of test run V10 to V13 are shown in table 3.13 to 3.16 for dry dispersion from 0.5 to 2.0 bar.

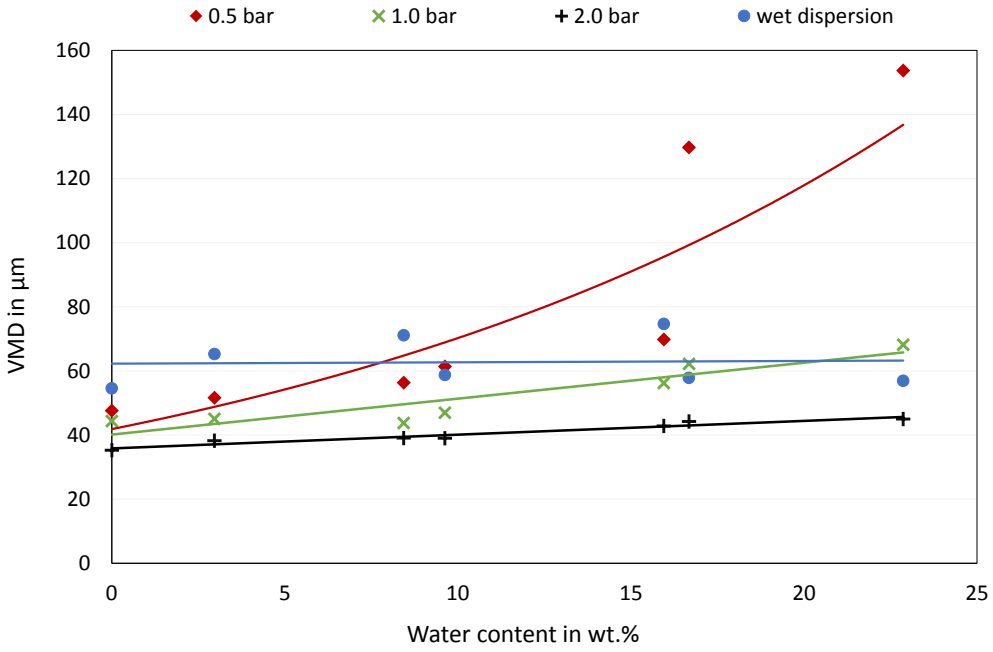

Figure 3.69.: VMD of raw, wet and dried Ibuprofen of test run V7 to V9, measured with wet and dried dispersion over water content.

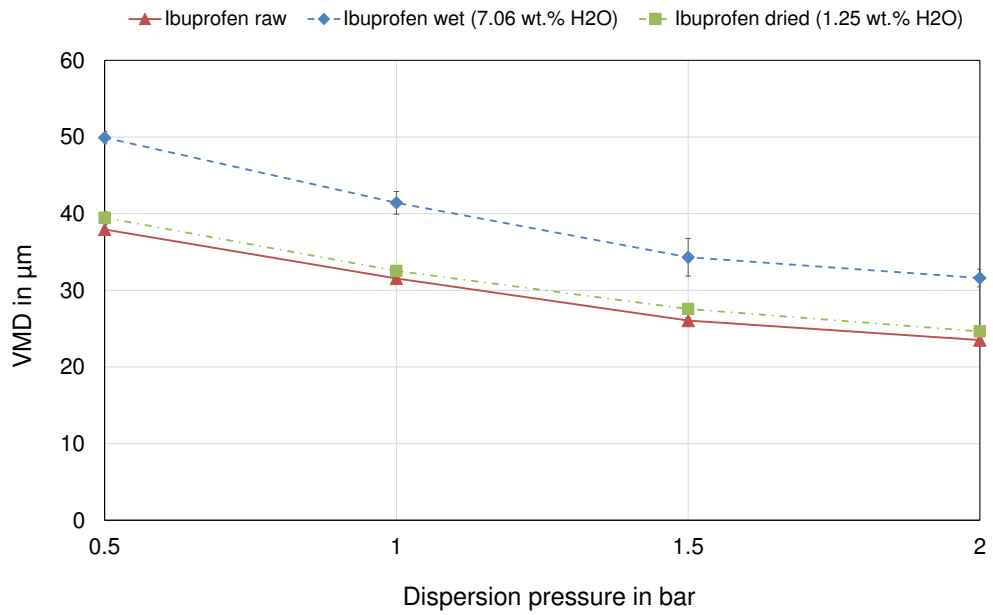

Figure 3.70.: VMD of raw, wet (7.1 wt.% H_2O) and dried (1.3 wt.% H_2O) Ibuprofen of test run V10 over dispersion pressure.

Table 3.12.: VMD, mean particle diameter and span for test run V7 to V9 measured with wet dispersion.

Test run	Material	Water content w [wt.%]	Volume mean diameter VMD [µm]	Mean particle diameter d_{50} [µm]	Span s [-]
V7	Raw Ibuprofen	0.0	54.6	43.7	2.07
	Wet Ibuprofen	16.0	74.7	57.7	2.25
	Dried Ibuprofen	9.6	58.7	48.7	2.01
V8	Wet Ibuprofen	8.4	71.1	61.9	1.80
	Dried Ibuprofen	3.0	65.2	56.3	1.75
V9	Wet Ibuprofen	22.9	56.9	45.8	2.17
	Dried Ibuprofen	16.7	57.8	47.6	2.07

Table 3.13.: VMD, mean particle diameter and span for test run V7 to V13 for a dispersion pressure of 0.5 bar.

Test run	Material	Water content w [wt.%]	Volume mean diameter VMD [µm]	Mean particle diameter d_{50} [µm]	Span s [-]
V7	Raw Ibuprofen	0.0	47.6	38.7	2.04
	Wet Ibuprofen	16.0	69.8	52.8	2.32
	Dried Ibuprofen	9.6	61.4	47.4	2.30
V8	Wet Ibuprofen	8.4	56.3	45.8	2.04
	Dried Ibuprofen	3.0	51.7	42.2	2.01
V9	Wet Ibuprofen	22.9	153.7	101.2	3.33
	Dried Ibuprofen	16.7	129.8	78.9	3.74
V10	Raw Ibuprofen	0.0	37.9	31.3	2.10
	Wet Ibuprofen	7.1	49.9	39.5	2.26
	Dried Ibuprofen	1.3	39.5	32.4	2.13
V11	Wet Ibuprofen	7.7	54.6	41.5	2.44
	Dried Ibuprofen	3.7	45.7	36.7	2.18
V12	Wet Ibuprofen	9.4	54.8	42.4	2.39
	Dried Ibuprofen	0.3	47.2	37.1	2.38
V13	Wet Ibuprofen	9.5	45.0	36.7	2.03
	Dried Ibuprofen	2.8	47.0	36.9	2.29

Table 3.14.: VMD, mean particle diameter and span for test run V7 to V13 for a dispersion pressure of 1.0 bar.

Test run	Material	Water content w [wt.%]	Volume mean diameter VMD [µm]	Mean particle diameter d_{50} [µm]	Span s [-]
V7	Raw Ibuprofen	0.0	44.4	36.1	2.03
	Wet Ibuprofen	16.0	56.2	42.6	2.27
	Dried Ibuprofen	9.6	47.0	37.3	2.14
V8	Wet Ibuprofen	8.4	43.8	35.4	2.07
	Dried Ibuprofen	3.0	45.0	36.0	2.13
V9	Wet Ibuprofen	22.9	68.2	47.8	2.77
	Dried Ibuprofen	16.7	62.2	45.0	2.62
V10	Raw Ibuprofen	0.0	31.5	25.2	2.35
	Wet Ibuprofen	7.1	41.4	32.7	2.33
	Dried Ibuprofen	1.3	32.5	26.0	2.31
V11	Wet Ibuprofen	7.7	43.4	33.5	2.42
	Dried Ibuprofen	3.7	36.1	28.9	2.33
V12	Wet Ibuprofen	9.4	42.3	33.6	2.24
	Dried Ibuprofen	0.3	36.4	29.1	2.24
V13	Wet Ibuprofen	9.5	42.2	33.5	2.25
	Dried Ibuprofen	2.8	36.8	29.2	2.33

Table 3.15.: VMD, mean particle diameter and span for test run V10 to V13 for a dispersion pressure of 1.5 bar.

Test run	Material	Water content w [wt.%]	Volume mean diameter VMD [µm]	Mean particle diameter d_{50} [µm]	Span s [-]
V10	Raw Ibuprofen	0.0	26.0	21.1	2.42
	Wet Ibuprofen	7.1	34.3	27.5	2.30
	Dried Ibuprofen	1.3	27.6	21.9	2.47
V11	Wet Ibuprofen	7.7	35.9	28.7	2.24
	Dried Ibuprofen	3.7	32.0	24.2	2.63
V12	Wet Ibuprofen	9.4	32.7	27.2	2.11
	Dried Ibuprofen	0.3	30.9	24.1	2.45
V13	Wet Ibuprofen	9.5	38.1	29.3	2.42
	Dried Ibuprofen	2.8	32.1	25.0	2.47

Table 3.16.: VMD, mean particle diameter and span for test run V7 to V13 for a dispersion pressure of 2.0 bar.

Test run	Material	Water content w [wt.%]	Volume mean diameter VMD [µm]	Mean particle diameter d_{50} [µm]	Span s [-]
V7	Raw Ibuprofen	0.0	35.2	29.0	2.06
	Wet Ibuprofen	16.0	42.8	33.4	2.30
	Dried Ibuprofen	9.6	39.0	32.2	2.02
V8	Wet Ibuprofen	8.4	39.1	31.7	2.10
	Dried Ibuprofen	3.0	38.2	31.2	2.04
V9	Wet Ibuprofen	22.9	45.0	35.8	2.21
	Dried Ibuprofen	16.7	44.3	34.3	2.29
V10	Raw Ibuprofen	0.0	23.5	18.2	2.62
	Wet Ibuprofen	7.1	31.6	25.0	2.35
	Dried Ibuprofen	1.3	24.6	19.5	2.52
V11	Wet Ibuprofen	7.7	32.4	25.6	2.35
	Dried Ibuprofen	3.7	25.5	20.2	2.54
V12	Wet Ibuprofen	9.4	32.7	25.9	2.32
	Dried Ibuprofen	0.3	26.8	20.9	2.50
V13	Wet Ibuprofen	9.5	32.6	25.9	2.31
	Dried Ibuprofen	2.8	25.6	20.7	2.44

3.3.1. Summary of Particle Size Distribution Measurements

- The particle size of wet and dried Ibuprofen increased slightly after mixing and drying due to particle agglomeration.
- Particle size measured in wet dispersion mode showed bigger particles than in dry dispersion mode with the lowest dispersion pressure of 0.5 bar. The dispersed particles of wet dispersion have to be observed under a microscope, to verify if the particle agglomerates are broken up.
- A higher water content of the powder increased the measured particle size in dry dispersion mode.
- No particle size plateau was reached with dispersion pressures between 0.5 and 2.0 bar. The dispersion pressure has to be increased.
- A shaft speed of 120 rpm had no influence on the particle size.
- Microscopy observations are necessary to verify if mixing and drying has an influence on the particles. The particles could be destroyed by mixing or drying, but due to agglomeration of the particles, the measured particle size increased.

3.4. Particle Shape (optical)

Particle size measurements with laser diffraction are not able to provide any information on the shape of the particles. Particle breakage or abrasion through mixing or drying would change the shape of the particle.

The sphericity and aspect ratio of raw, wet and dried Ibuprofen of test run V10 was measured with the Qicpic high speed image analysis sensor. Due to a defect of the device, the particle shape was only measured at 0.5 and 2.0 bar dispersion pressure. The cumulative distribution Q3 of raw, wet and dried Ibuprofen is shown over sphericity and aspect ratio in figure 3.72 and 3.73 for a dispersion pressure of 2.0 bar. Both, sphericity and aspect ration were not changed by mixing or drying. A dispersion pressure of 0.5 bar led to the same results.

In general, the particle size of the measured powders were too small for image analysis. The image resolution of the Qicpic was too low. Small particles had a size of only one or two pixels as shown in figure 3.71. Therefore, the accuracy of the measurement method is not sensitive enough to detect particle breakage or abrasion.

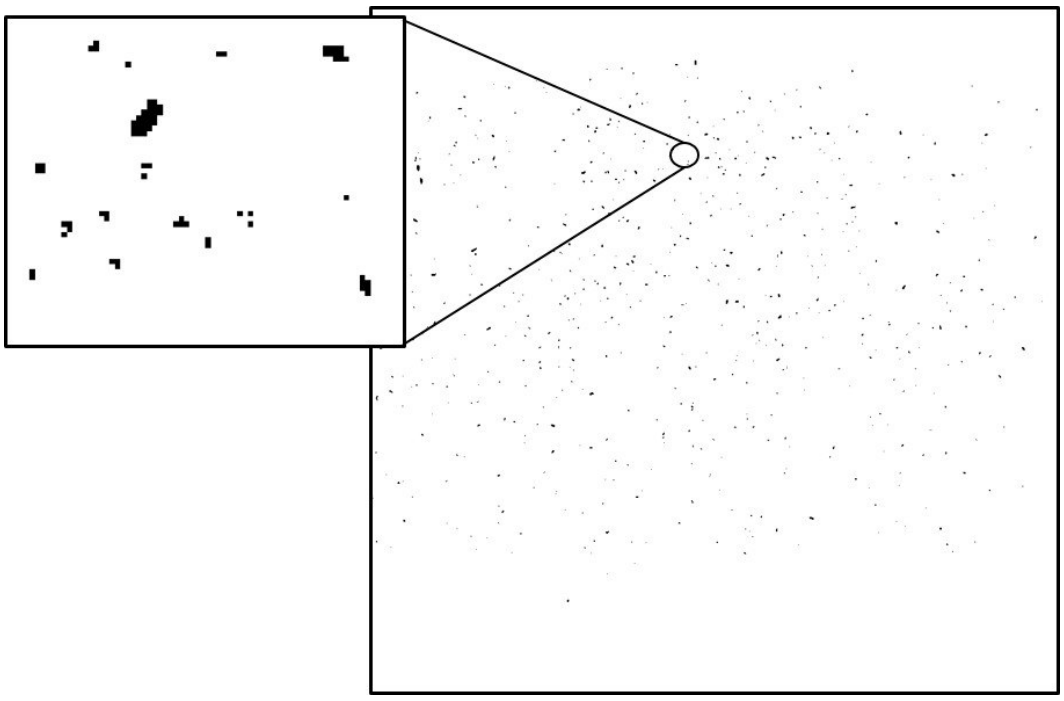

Figure 3.71.: Picture of raw Ibuprofen particles taken with the Qicpic high speed image analysis sensor.

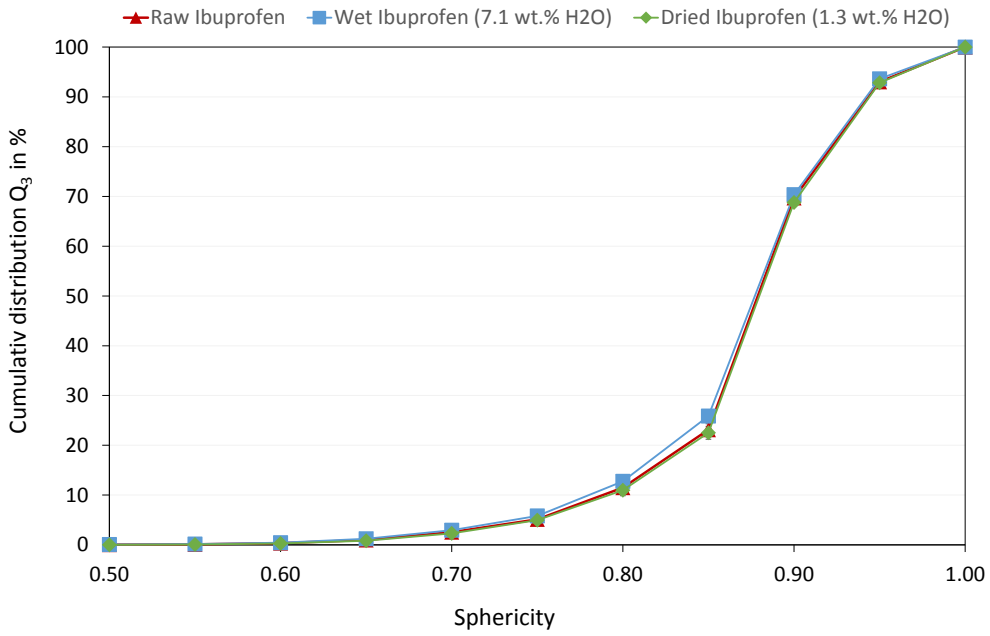

Figure 3.72.: Cumulative distribution of raw, wet and dried Ibuprofen of test run V10 over the sphericity at 2 bar dispersion pressure.

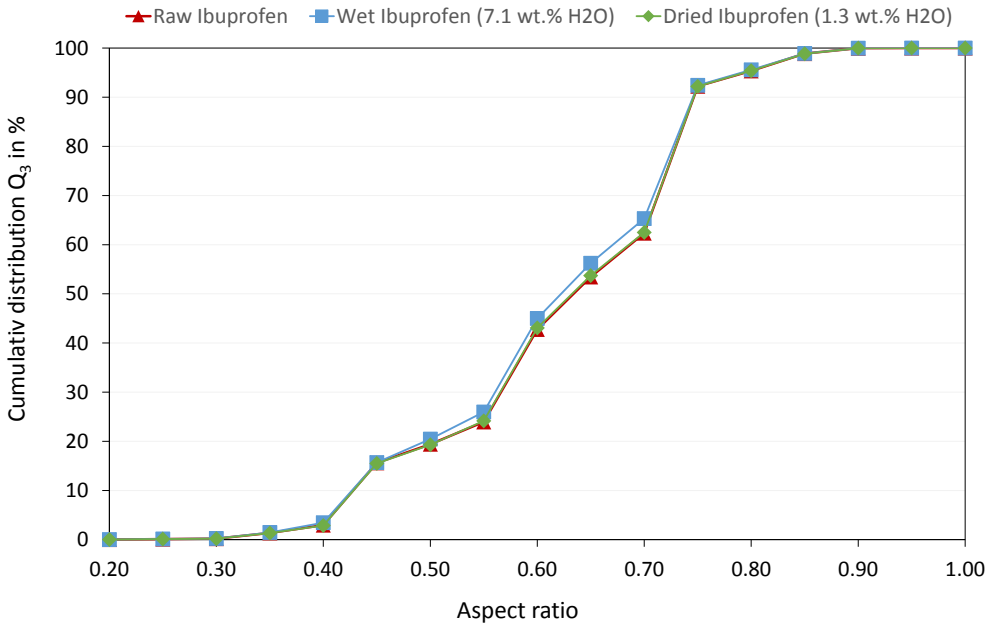

Figure 3.73.: Cumulative distribution of raw, wet and dried Ibuprofen of test run V10 over the aspect ratio at 2 bar dispersion pressure.

3.5. Microscopy

Particle size and shape as well as the surface texture of the particles for raw, wet and dried Ibuprofen of test run V10 were inspected with a microscope. No change in particle size, shape or surface texture was observed as shown in figure 3.74. Therefore, mixing and drying did not destroy the particles. No abrasion of particles was visible.

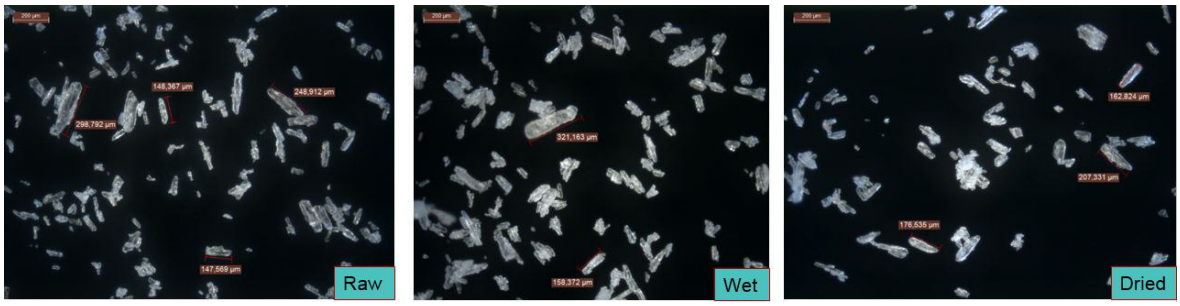

Figure 3.74.: Comparison of raw, wet (7.1 wt.% H_2O) and dried Ibuprofen (1.3 wt.% H_2O) recorded with 5x magnification.

Raw Ibuprofen showed more small particles than wet (7.1 wt.% H_2O) and dried (1.3 wt.% H_2O) Ibuprofen (compare figure 3.75 with figure 3.77 and 3.79. This correlated with the particle size distribution measurement (see chapter 3.3), where a higher fines content for raw Ibuprofen was found.
For wet and dried Ibuprofen, smaller particles adhered on bigger particles and formed small particle agglomerates as shown in figure 3.78 and 3.80. For raw Ibuprofen, mostly single particles were observed (see figure 3.76).

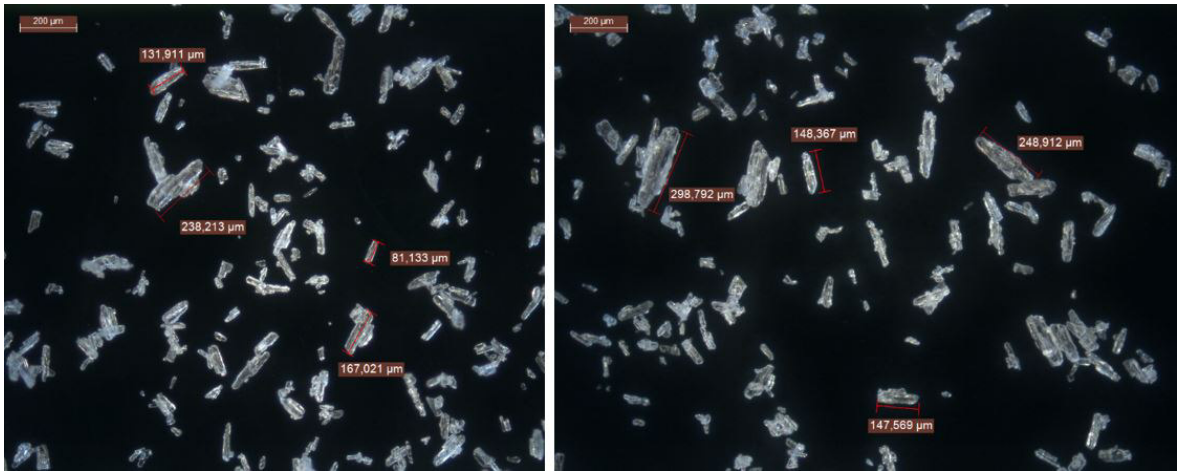

Figure 3.75.: Microscopy pictures of raw Ibuprofen from test run V10 at 5x magnification.

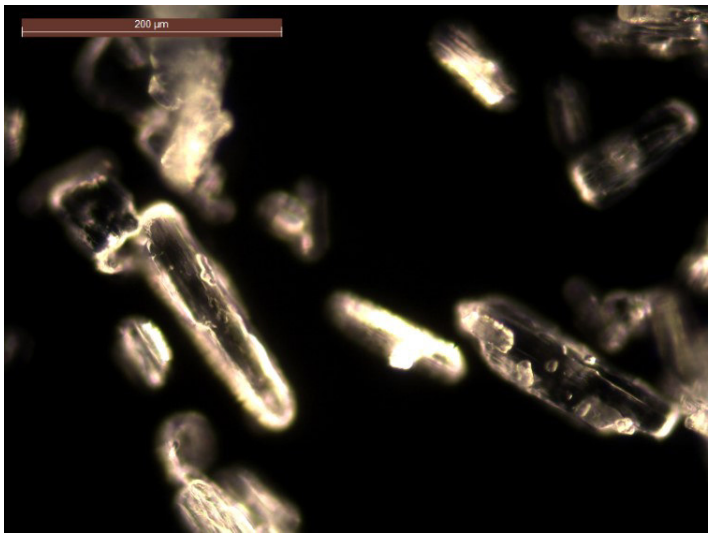

Figure 3.76.: Microscopy pictures of raw Ibuprofen from test run V10 at 20x magnification.

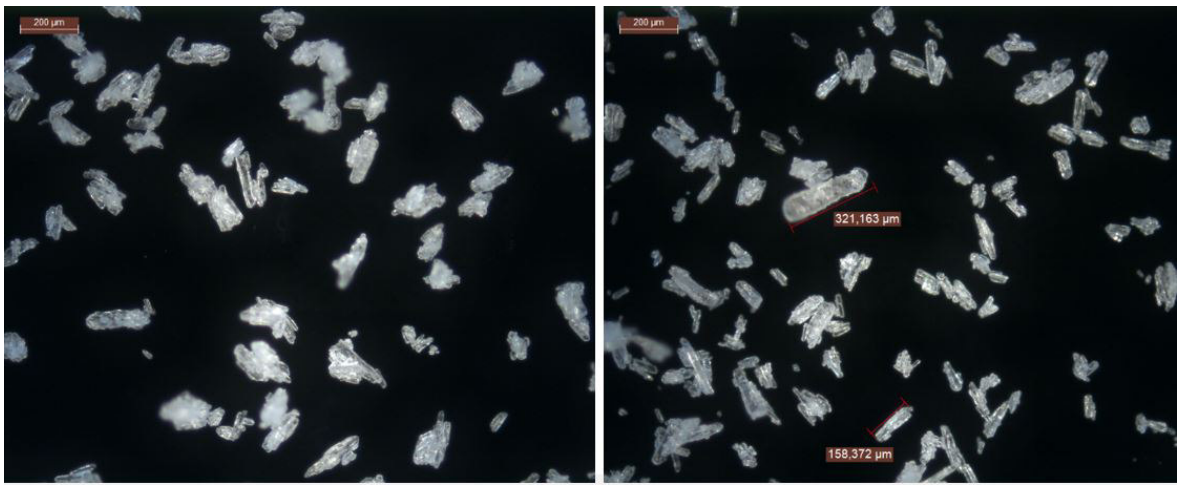

Figure 3.77.: Microscopy pictures of wet Ibuprofen (7.1 wt.% H_2O) from test run V10 at 5x magnification.

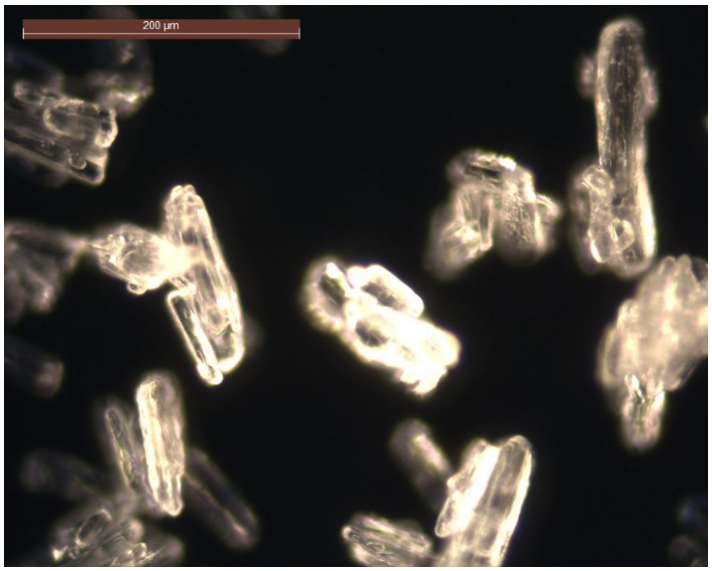

Figure 3.78.: Microscopy pictures of wet Ibuprofen (7.1 wt.% H_2O) from test run V10 at 20x magnification.

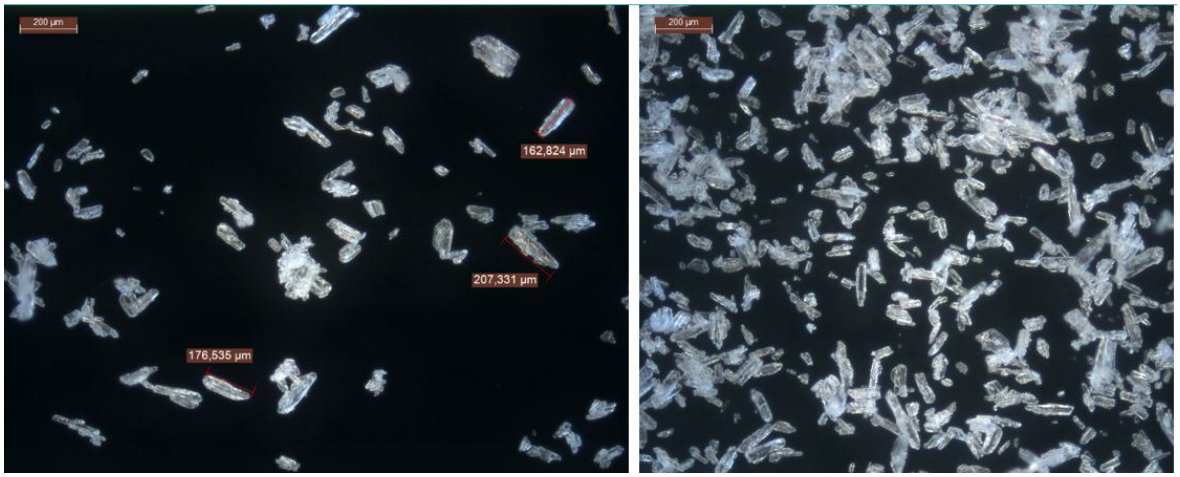

Figure 3.79.: Microscopy pictures of dried Ibuprofen (1.3 wt.% H_2O) from test run V10 at 5x magnification.

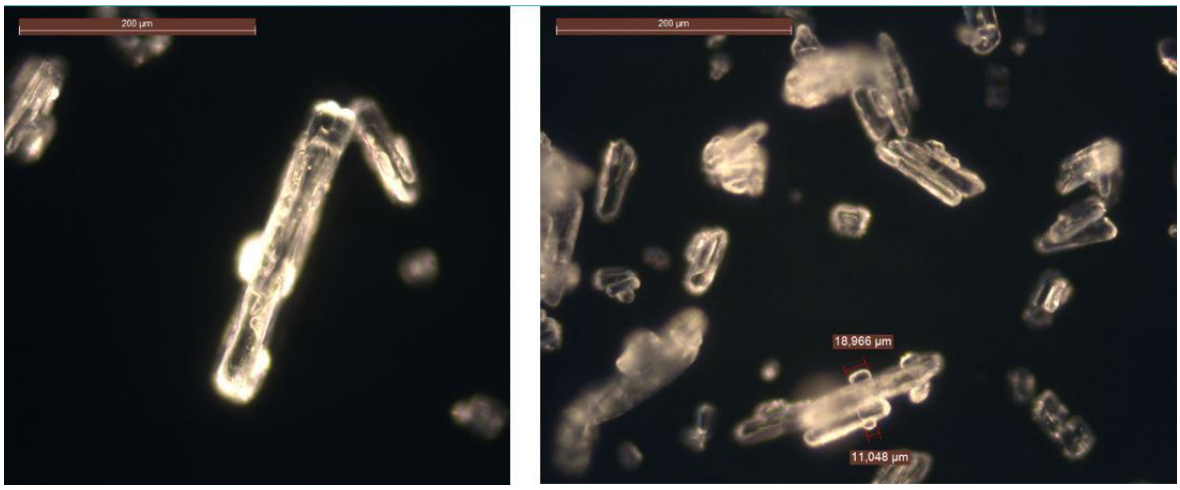

Figure 3.80.: Microscopy pictures of dried Ibuprofen (1.3 wt.% H_2O) from test run V10 at 20x magnification.

To observe the mixing behavior of water and Ibuprofen, water was added in excess to a raw Ibuprofen sample with a Pasteur pipette. After adding the water to the powder a water film enclosed the Ibuprofen particles as shown in figure 3.81 on the left side. After 30 seconds a second photo was taken. All the visible water was already evaporated as shown in figure 3.81 on the right side. This is an indication that the water of wet Ibuprofen forms a thin film on the surface of the particles and therefore evaporates fast due to the high surface area.

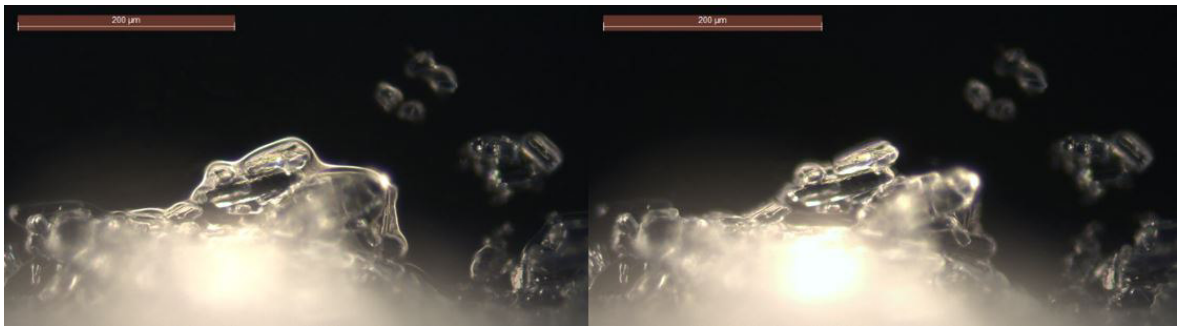

Figure 3.81.: Left: raw Ibuprofen with water in excess. Right: same picture of raw Ibuprofen after 30 seconds. All of the visible water evaporated within 30 seconds.

3.6. Powder rheology

3.6.1. Basic Flowability Energy, Specific Energy, Stability and Flow Rate Index

The Basic Flowability Energy (BFE) is a key flowability parameter, reflecting the powders resistance to forced flow [20]. It is also highly sensitive and differentiating in relation to small differences in flow properties [31].

The BFE of raw, wet and dried Ibuprofen was measured for test run V5 to V19 to examine the influence of mixing and drying on the flowability of the powder. Raw Ibuprofen was measured for test run V5 to V9 and for test run V10 to V19 separately because the raw material was taken from different barrels of the manufacturer. Raw Ibuprofen of test run V5 to V9 had a BFE of 906.2 mJ compared to 1005.5 mJ for Test run V10 to V19.

In general, the BFE decreased slightly after mixing with water if the water content of the powder was less than 10 wt.%. The BFE of wet Ibuprofen from test run V11 (1005.9 mJ) did not change after mixing with water. For higher water contents the BFE increased compared to the BFE of raw Ibuprofen. In most cases a low BFE represents good flow properties of a powder, but also the opposite behavior can occur [32]. The highest BFE (2320.6 mJ) was reached in test run V15 for wet Ibuprofen with a water content of 29.7 wt.%. For most powders the BFE increased with increasing water content of the powder, [32] due to the higher density of wet powder compared to dry powder.
For dried Ibuprofen no clear trend was found. Depending on the test run the BFE of dried Ibuprofen either increased, decreased or stayed constant compared to wet Ibuprofen.

To compensate the varying bulk densities the flow energy was also expressed as Specific Energy (SE). The SE is a measure of how easily a powder will flow in an unconfined or low stress environment and provides an indication of the cohesion of a powder under low stress conditions [20, 31]. The Specific Energy is most dependant on the shear forces that act between particles. Due to the low stress environment, cohesion and other physical properties like particle size, shape and texture are often the most influential property [44]. As described in chapter 3.3, 3.4 and 3.5 the particle size, shape and surface texture of single particles was not changed by mixing or drying, but the addition of water led to particle agglomeration and therefore to an increased particle size.
The SE was between 8.8 mJ/g for dried Ibuprofen of V8 and 12.7 mJ/g for wet Ibuprofen of V15. A cohesive flow behavior is represented by an SE $\leq$ 10.0 mJ/g and very cohesive flow behavior by an SE $\geq$ 10.0 mJ/g. No clear correlation between the SE and the water content, mixing or drying were found.

The Stability Index (SI) ranged from 0.69 for dried Ibuprofen of test run V5 to 1.00 for dried Ibuprofen of test run V9. Ibuprofen with higher water contents had a slight tendency to have a higher SI and therefore a more stable rheology. Possible causes for an SI $\leq$ 1 are attrition and de-agglomeration of the particles during testing.

The sensitivity of a powder to flow rate changes is an important parameter when describing it's flow properties [33]. This can be described by the Flow Rate Index (FRI). The FRI ranged from 0.94 for wet Ibuprofen of test run V5 and 1.12 for dried Ibuprofen of test run V8, therefore the powders were not sensitive to changes in flow rate. The FRI of 1.29 measured for wet Ibuprofen of test run V6 was the only outlier. The mean BFE, SI, FRI and SE for raw, wet and dried Ibuprofen for different test runs are shown in table 3.17.

Table 3.17.: Mean BFE, SE, SI and FRI of raw, wet and dried Ibuprofen for different test runs.

		Water content	Mean BFE	Mean SI	Mean FRI	Mean SE
Test run	Material	w [wt.%]	BFE [mJ]	SI [-]	FRI [-]	SE [mJ/g]
V5	Raw Ibuprofen	0.0%	906.2	0.80	1.07	10.4
	Wet Ibuprofen	9.0%	865.5	0.85	0.94	10.0
	Dried Ibuprofen	0.03%	1449.4	0.69	1.01	12.2
V6	Wet Ibuprofen	8.8%	832.5	0.97	1.29	9.0
	Dried Ibuprofen	0.7%	910.5	0.84	0.95	10.0
V7	Wet Ibuprofen	16.0%	1176.8	0.94	0.98	9.3
	Dried Ibuprofen	9.6%	896.7	0.99	1.05	9.1
V8	Wet Ibuprofen	8.4%	885.4	0.94	1.04	9.0
	Dried Ibuprofen	3.0%	750.7	0.85	1.12	8.8
V9	Wet Ibuprofen	22.9%	1632.8	0.97	0.97	10.4
	Dried Ibuprofen	16.7%	1266.1	1.00	0.99	9.5
V10	Raw Ibuprofen	0.0%	1005.5	0.81	0.98	9.6
	Wet Ibuprofen	7.1%	935.5	0.97	1.04	10.2
	Dried Ibuprofen	1.3%	828.3	0.94	1.10	10.3
V11	Wet Ibuprofen	7.7%	1005.9	0.94	1.04	9.9
	Dried Ibuprofen	3.7%	955.7	0.84	1.01	10.0
V15 - V17	Wet Ibuprofen	29.7%	2320.6	0.91	1.05	12.7
	Dried Ibuprofen	2.1%	877.1	0.77	1.11	9.8
V18	Wet Ibuprofen	8.9%	990.3	0.83	1.04	10.0
	Dried Ibuprofen	3.0%	1214.4	0.79	1.01	11.2
V19	Wet Ibuprofen	9.5%	897.4	0.87	0.98	8.8

3.6.2. Compressibility

The Compressibility is not a direct measure of the flowability of a powder, but it is a useful indicator whether a powder has a cohesive flow behavior or is free flowing [31]. A high compressibility of a powder is often associated with high cohesion [45]. Particle size, shape and surface texture have considerable impact on a powders compressibility [34].
The compressibility ranged from 29.4% to 39.4%. For test runs with water contents lower than 10.0 wt.% the compressibility decreased with increasing water content, except for test run V10 were the compressibility of wet Ibuprofen was slightly higher than for raw Ibuprofen. The compressibility over the applied normal stress for raw, wet and dried Ibuprofen is shown exemplary in figure 3.82 for test run V18. For higher water contents no clear correlation between compressibility and mixing, drying or the water content of the powder was found due to the poor repeatability of the compressibility measurement.
The compressibility for raw, wet and dried Ibuprofen of all test runs are shown in table 3.18.

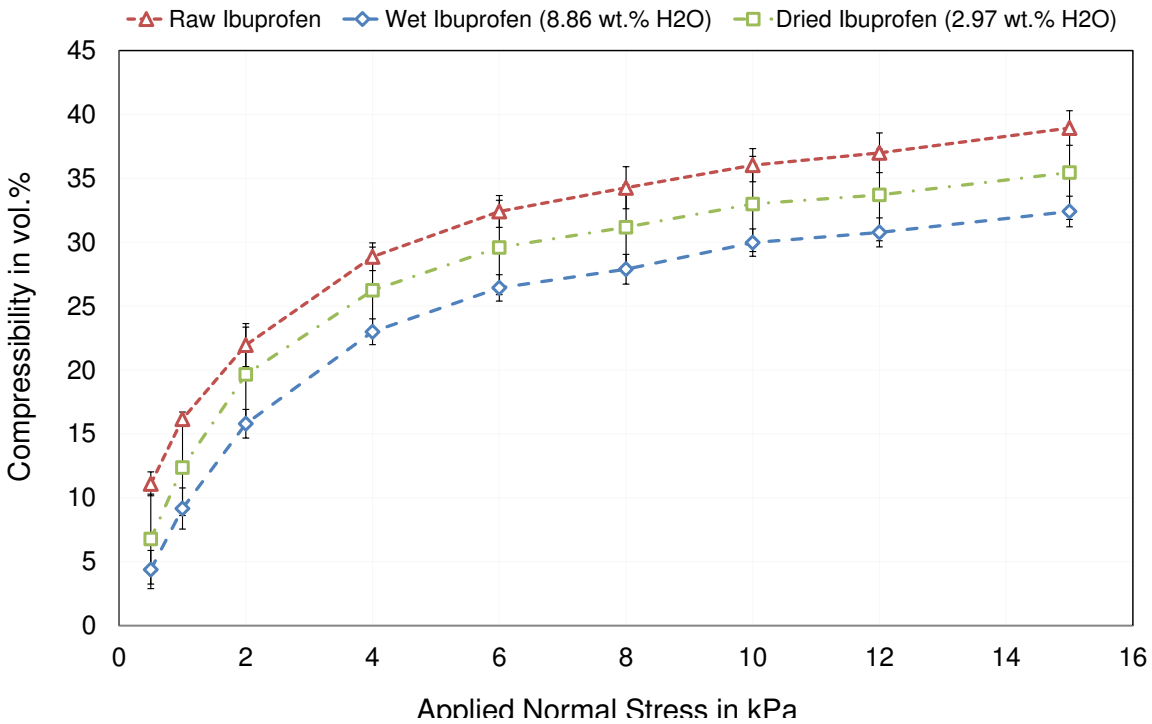

Figure 3.82.: Compressibility of raw, wet (8.9 wt.% H_2O) and dried (3.0 wt.% H_2O) Ibuprofen of test run V18.

Table 3.18.: Compressibility of raw, wet and dried Ibuprofen for different test runs.

			Compressibility (without water)									
		Water content	0.50 kPa	1.00 kPa	2.00 kPa	4.00 kPa	6.00 kPa	8.00 kPa	10.0 kPa	12.0 kPa	15.0 kPa
Test run	Material	w [wt.%]	C [%]	C [%]	C [%]	C [%]	C [%]	C [%]	C [%]	C [%]	C [%]
V7	Raw Ibuprofen	0.0%	11.1	16.2	22.0	28.9	32.4	34.3	36.0	37.0	38.9
	Wet Ibuprofen	16.0%	5.0	10.4	16.2	22.2	25.3	27.0	28.3	29.3	31.0
	Dried Ibuprofen	9.6%	6.1	12.7	20.3	26.5	29.6	31.2	32.6	33.3	34.9
V8	Wet Ibuprofen	8.4%	4.1	9.1	15.5	21.4	24.4	25.9	27.4	28.2	29.6
	Dried Ibuprofen	3.0%	9.2	15.9	23.3	29.1	32.0	33.9	34.9	36.1	37.2
V9	Wet Ibuprofen	22.9%	4.6	10.7	17.8	24.0	27.8	30.1	31.6	33.4	35.1
	Dried Ibuprofen	16.7%	7.2	13.2	19.9	26.0	29.0	31.1	32.6	33.8	35.3
V10	Raw Ibuprofen	0.0%	11.1	16.2	22.0	28.9	32.4	34.3	36.0	37.0	38.9
	Wet Ibuprofen	7.1%	9.1	13.2	20.8	28.4	32.4	34.8	36.5	37.6	39.4
	Dried Ibuprofen	1.3%	4.4	10.4	18.2	25.3	28.8	30.5	32.1	33.1	34.7
V11	Wet Ibuprofen	7.7%	2.8	7.0	14.1	21.5	25.7	27.7	29.7	30.6	32.5
	Dried Ibuprofen	3.7%	3.2	8.5	15.7	22.1	25.5	27.1	28.5	29.4	30.8
V15 - V17	Wet Ibuprofen	29.7%	1.5	7.0	15.1	24.0	29.3	32.2	34.1	36.4	38.1
	Dried Ibuprofen	2.1%	9.0	15.8	22.9	28.9	31.8	33.7	34.8	36.0	37.0
V18	Wet Ibuprofen	8.9%	4.4	9.2	15.8	23.0	26.4	27.9	30.0	30.8	32.4
	Dried Ibuprofen	3.0%	6.8	12.4	19.6	26.2	29.6	31.2	33.0	33.7	35.5
V19	Wet Ibuprofen	9.5%	3.3	7.5	14.1	20.2	23.7	25.4	26.9	28.1	29.4

3.6.3. Shear Cell Test

The flow behavior of the Ibuprofen powders was characterised by the flow function ffc and the cohesion τ_0. The values for the flow function ffc, cohesion τ_0, unconfined yield stress σ_c, major principal stress σ_1 and the angle of internal friction Φ_i are shown in table 3.19. In figure 3.83 the flow function of test runs V9 to V19 are shown. The majority of the powder samples showed cohesive behavior. A flow function of 2.82 and 2.86 and a cohesion of 1.54 and 1.61 kPa was obtained for raw Ibuprofen as shown in table 3.19. Li Qu et al. measured a flow function of 4.02 and a cohesion of 1.24 kPa for raw Ibuprofen 25 from BASF [46]. Wet Ibuprofen of test runs V10 and V11 showed very cohesive flow behavior with flow functions of 1.96 and 1.98. In general, the flow function seemed to decrease slightly with increasing water content, but the data was fluctuating as shown in figure 3.84 (a). Cohesion seemed to increased slightly with increasing water content as shown in figure 3.84 (b). Due to the divergence of the measured data, the interpretation was difficult.
During the test runs, the opposite flow behavior was observed. With increasing water contend the powder seemed to flow better through the dryer and had lesser tendency to accumulate at the dryer outlet and inlet. Also the hold-up was lower for test runs with a higher feed water content. This difference was may be due to the formation of particle agglomerates in the wet powder which increased the particle size and therefore changed the flow behavior of the powder. Also the different stress state in the shear cell test (the powder was compressed and then sheared in a precise shear plane) and the dryer (loose/fluidised particle transport) was a possible reason for the contradictory observations of the flowability of the powder.

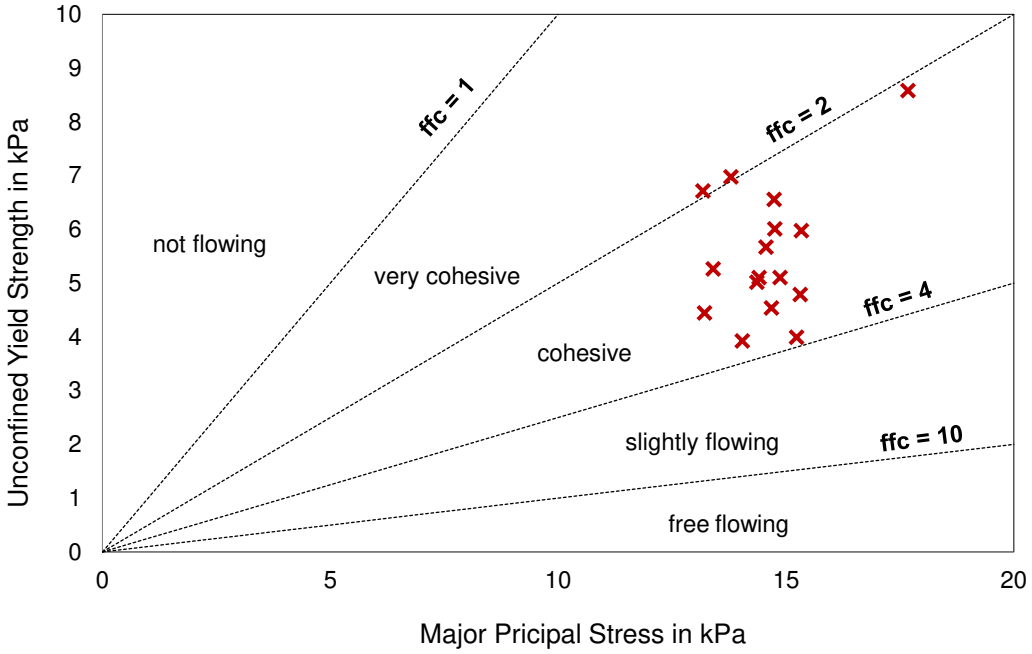

Figure 3.83.: Flow Function (ffc) for all samples of all test runs.

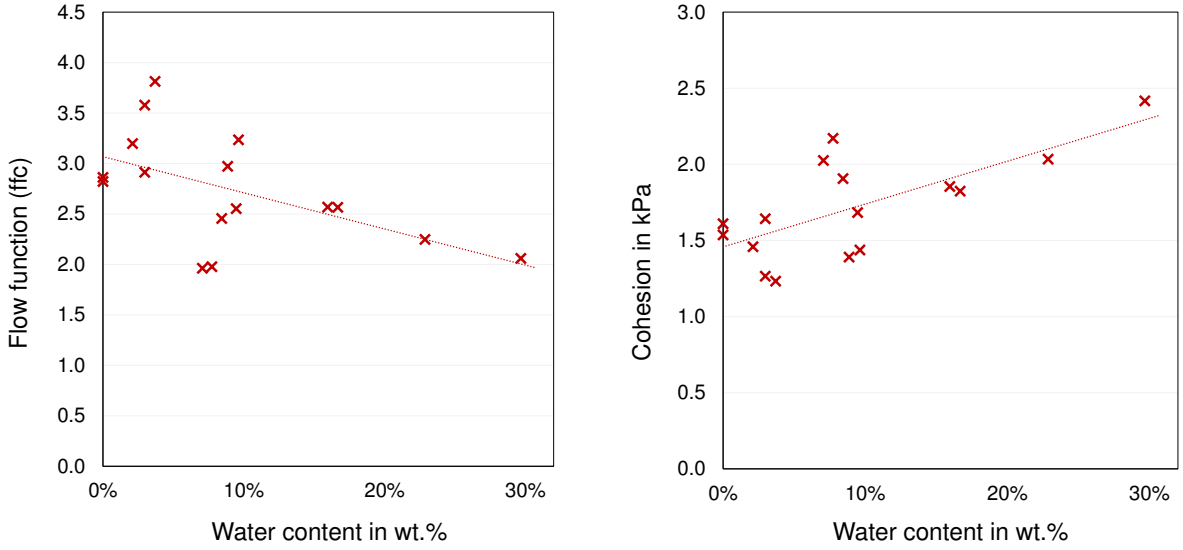

(a) (b)

Figure 3.84.: (a): ffc over water content of test runs V9 to V19. (b): Cohesion over water content of test runs V9 to V19.

Table 3.19.: Cohesion, Unconfined Yield Stress, Major Principal Stres, Flow function and Angle of Internal Friction for different test runs.

Test run	Material	Water content w [wt.%]	Cohesion τ_0 [kPa]	Unconfined Yield Stress σ_c [kPa]	Major Principal Stres σ_1 [kPa]	Flow function ffc [-]	Angle of Internal Friction Φ_i [°]
V7	Raw Ibuprofen	0.00%	1.54	5.02	14.36	2.86	27.02
	Wet Ibuprofen	15.95%	1.85	5.67	14.56	2.57	23.62
	Dried Ibuprofen	9.62%	1.44	4.54	14.68	3.23	25.30
V8	Wet Ibuprofen	8.43%	1.91	6.01	14.75	2.46	25.20
	Dried Ibuprofen	2.97%	1.27	3.92	14.04	3.58	24.35
V9	Wet Ibuprofen	22.87%	2.03	6.56	14.74	2.25	26.35
	Dried Ibuprofen	16.68%	1.82	5.98	15.34	2.57	27.21
V10	Raw Ibuprofen	0.00%	1.61	5.10	14.41	2.82	25.49
	Wet Ibuprofen	7.06%	2.03	6.72	13.18	1.96	27.81
V11	Wet Ibuprofen	7.73%	2.17	6.98	13.79	1.98	26.20
	Dried Ibuprofen	3.70%	1.23	3.99	15.23	3.81	26.64
V15 - V17	Wet Ibuprofen	29.67%	2.42	8.58	17.67	2.06	31.21
	Dried Ibuprofen	2.10%	1.46	4.79	15.31	3.20	27.28
V18	Wet Ibuprofen	8.86%	1.39	4.44	13.21	2.97	25.92
	Dried Ibuprofen	2.97%	1.64	5.10	14.87	2.91	24.47
V19	Wet Ibuprofen	9.46%	1.68	5.26	13.40	2.55	24.80

3.6.4. Carr Index and Hausner Ratio

Raw Ibuprofen showed very poor flowability. Wet Ibuprofen showed poor flowability for 15.95 wt.% H_2O and very poor flowability for 8.43 and 22.87 wt.% H_2O. Values of Hausner Ratio and Carr Index are shown in table 3.20. The Water content had little influence on compressibility and therefore also on Hausner Ratio and Carr Index as shown in figure 3.85 and 3.86. No correlation between the flowability of the powder and the water content, mixing or drying was found.

Table 3.20.: Hausner Ratio, Carr Index and Compressibility (tapped and FT4) of raw and wet Ibuprofen

	Hausner Ration	Carr Index	Compressibility (tapped)	Compressibility (FT4)
	H [-]	CI [%]	C_t [%]	C_{FT4} [%]
Raw Ibuprofen	1.52	34.1	34.1	38.9
Wet Ibuprofen (8,43 wt.% H_2O)	1.49	32.7	32.7	28.7
Wet Ibuprofen (15,95 wt.% H_2O)	1.40	28.3	28.3	29.1
Wet Ibuprofen (22.87 wt.% H_2O)	1.51	33.8	33.8	31.9

Compressibility measurements by tapping and with the FT4 delivered similar results(see table 3.20). No correlation between the compressibility and the water content was found.

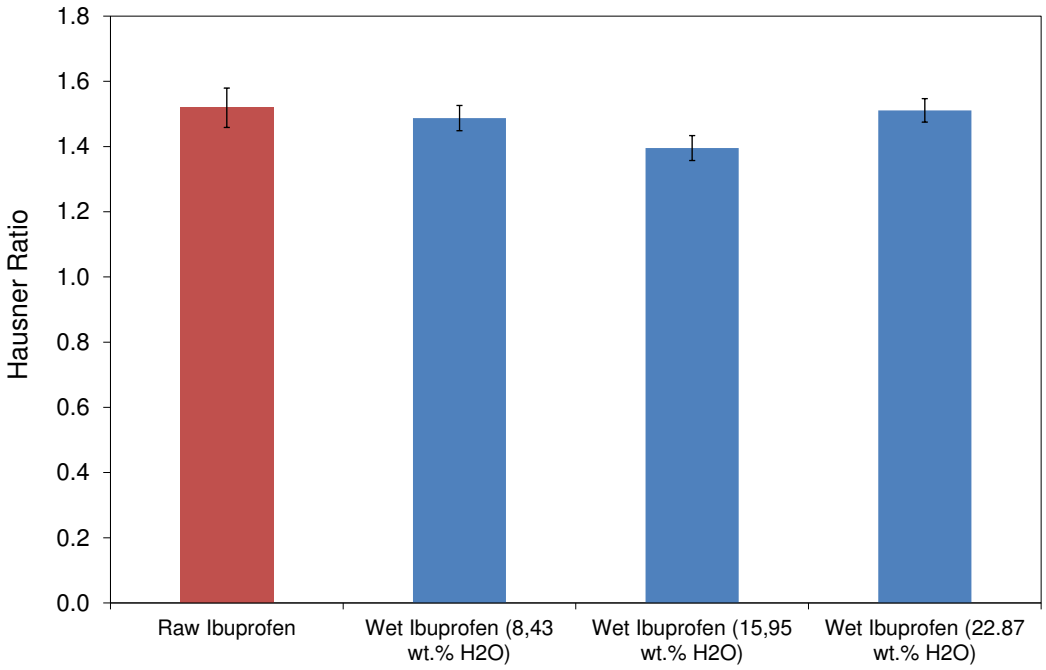

Figure 3.85.: Hausner Ratio of raw and wet Ibuprofen (8.43, 15.95 and 22.87 wt.% H_2O).

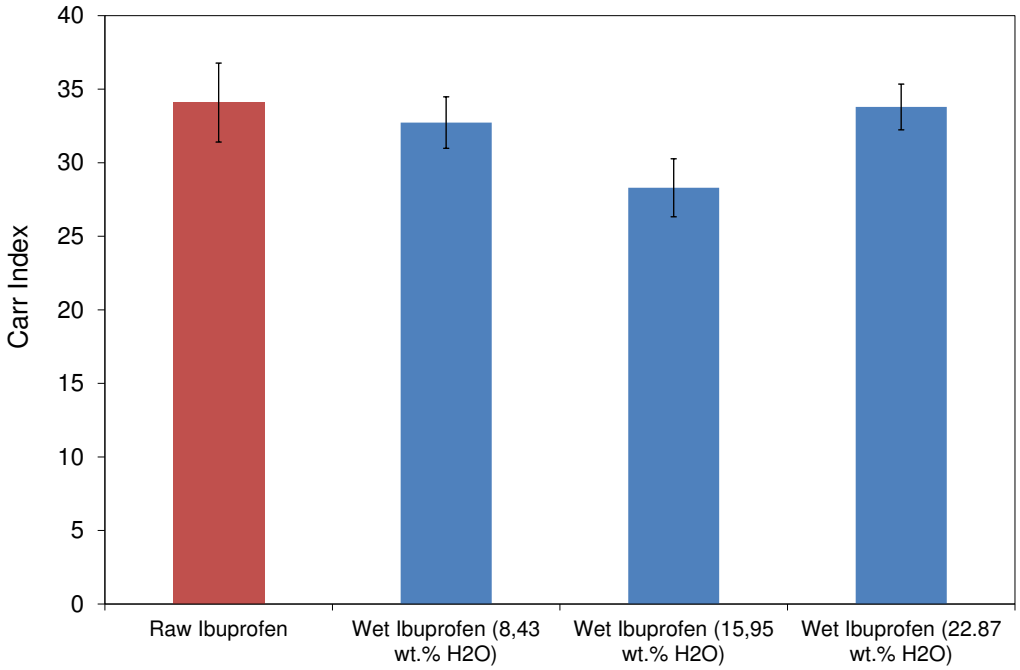

Figure 3.86.: Carr Index of raw and wet Ibuprofen (8.43, 15.95 and 22.87 wt.% H_2O).

3.6.5. Summary of Powder Rheology Measurements

- In general, Ibuprofen showed cohesive to very cohesive flow behavior.
- Poor reproducibility of all measured rheology results especially for the compressibility and shear cell test.
- No clear correlation between the measured flow behavior and mixing, drying or the water content of the powder was found
- Inconsistent results between the different powder characterization techniques were found. This inconsistency between different powder characterization techniques has been a long term source of confusion in powder industries [24, 47]. Different properties under different stress states were measured and it is not appropriate to compare the results of static characterization techniques to a dynamic process. It is important that the stress state of the powder characterization matches the stress state of the powder in the process as good as possible [24].
- The rheology measurements showed a decreased flowability for powders with high water content, whereby during the test runs a better flowability with less material deposits and a lower hold-up was observed.

4. Conclusions and Outlook

A continuously operating, indirect heated, contact paddle dryer prototype from Hosokawa was tested and optimized for drying wet pharmaceutical powders, while not changing the particle size. Due to its cohesive flow behavior, Ibuprofen ($x_{50} = 25\mu m$) was used as test substance.

The feed flow, water content, air flow rate and shaft speed were varied to investigate their influence on the drying performance. It was possible to feed 2.5 kg/h of wet Ibuprofen into the dryer for up to 3 hours without blockages of the outlet. A feed mass flow of 1.25 kg/h was successfully fed into the dryer up to 9.5 h. Steady state was only reached for two test runs. A lower air flow rate resulted in a slightly higher water content of the dried product, and a higher water load of the air due to longer residence time of the air in the dryer. A higher shaft speed increased slightly the amount of evaporated water from the wet powder due to better mixing, but also led to blockages at the outlet of the dryer. Slower shaft speeds may reduce the chance of a blockage of the outlet, but it was not possible to test shaft speeds slower than 60 rpm due to the given gear.
The optimal settings for drying wet Ibuprofen were a feed flow of 1.25 kg/h, a high water content of 30 wt.% and a shaft speed of 60 rpm. The air flow rate had only little influence on the drying performance. Longer test runs are necessary to determine whether steady state will be reached or not. The dryer is also suitable to dry wet Ibuprofen powder in several steps by re-feeding the dried material.

For precise temperature control of the electrical heated parts of the dryer, the thermostats have to be replaced and the sensor positions have to be optimized to minimize temperature fluctuations. Although the paddle configuration at the outlet was optimized several times, it was not possible to improve the material ejection of the dried material into the outlet pipe. All measures taken to reduce material accumulations and the dead volume of the dryer had no impact on the measured hold-up.
Based on the performed experiments and the obtained results, the prototype dryer will be improved and modified. The water content measurements delivered sometimes physically not reasonable results, because more water was evaoprated than fed into the dryer with wet material. The sealing of the dryer must be improved to avoid lost air through voids of the housing. Thus, improved sealing of the dryer enables also drying under vacuum. The free space in the dryer has to be reduced further to decrease the hold up. Also the paddle configuration and the outlet design has to be adapted for different materials to be dried. The outlet of the dryer should be located at the bottom side for drying wet Ibuprofen powder and most likely for cohesive powders in general.

The drying process is designed to enable drying without changes of the particle size. Therefore, the particle size and the shape of the Ibuprofen powder was measured before and after drying. No particle attrition or breakage was found. After drying, a slight

decrease in particle size due to breakage of the particle agglomerates was observed. These particle agglomerates were formed during mixing of raw Ibuprofen with water and were not caused by the drying process. For this reason, the drying technology is suitable to dry wet Ibuprofen powders without changing the particle size distribution. It has to be investigated if agglomeration of the particles during mixing can be avoided.

In general, a higher water content of the powder led to a better flowability and therefore fewer material accumulations and a lower hold-up. Contradictory results of the flow behavior between different flowability measurements and test run observations were obtained. Therefore, it was difficult to interpret the measured flowability data. However, all Ibuprofen powders showed cohesive to very cohesive flow behavior.

Bibliography

[1] Ibrahim Dincer, Calin Zamfirescu, and Alper Ozalp. *Drying Phenomena*. John Wiley & Sons Inc, 2016.

[2] Dilip Parikh. Solids drying: Basics and applications. *Chemical Engineering -New York- Mcgraw Hill Incorporated then Chemical Week Publishing Llc-*, 121, 04 2014.

[3] A. Bodhmage. Correlation between physical properties and flowability indicators for fine powders. Master's thesis, Department of Chemical Engineering University of Saskatchewan, Saskatoon, Canada, 2006.

[4] Arun S. Mujumdar. *Handbook of Industrial Drying*. CRC Press, fourth edition edition, 2014.

[5] R.B. Keey. *Drying principles and practice*. International series of monographs in chemical engineering. Pergamon Press, 1972.

[6] Tim O. Althaus. *Flow and Extrudability of Highly Unsaturated Wet Powders*. PhD thesis, Swiss Federal Institute of Technology Zurich, 2009.

[7] M.C. Coelho and N. Harnby. The effect of humidity on the form of water retention in a powder. *Powder Technology*, 20(2):197 – 200, 1978.

[8] J.J Fitzpatrick, S.A Barringer, and T Iqbal. Flow property measurement of food powders and sensitivity of jenike's hopper design methodology to the measured values. *Journal of Food Engineering*, 61(3):399 – 405, 2004.

[9] Lauren Briens Allison Crouter. The effect of moisture on the flowability of pharmaceutical excipients. *AAPS PharmSciTech*, 15:65–74, 2014.

[10] Clive Washington. *Particle Size Analysis In Pharmaceutics And Other Industries: Theory And Practice*. CRC Press, 2005.

[11] Matthias Stieß. *Mechanische Verfahrenstechnik - Partikeltechnologie 1*. Springer-Verlag Berlin Heidelberg, 3 edition, 2009.

[12] Alena Mudroch and Paul Mudroch. *Manual of Physicochemical Analysis and Bioassessment of Aquatic Sediments*. TAYLOR & FRANCIS, 1997.

[13] Jerzy Leszczynski and Tomasz Puzyn, editors. *Towards Efficient Designing of Safe Nanomaterials*. RSC Nanoscience & Nanotechnology. The Royal Society of Chemistry, 2013.

[14] I. N. McCave, R. J. Bryant, H. F. Cook, and C. A. Coughanowr. Evaluation of a laser-diffraction-size analyzer for use with natural sediments. *Journal of Sedimentary Research*, 56(4):561, 1986.

[15] Wolfgang Witt Ulrich Köhler, Thomas Stübinger. Laser - diffraction results from dynamic image analysis data. *WCPT*, 2010.

[16] Ulrich Köhler, Thomas Stübinger, Joachim List, and Wolfgang Witt. Investigations on non-spherical reference material using laser diffraction and dynamic image analysis. *Particulate Systems Analysis*, 2008.

[17] Paul Kippax and Graham Calvert. Investigating the dispersion of dry powders. *diffraction theory*, 2011.

[18] Henk G. Merkus. *Particle Size Measurements*. Springer Netherlands, 2009.

[19] Dietmar Schulze. *Powders and Bulk Solids*. Springer, 2010.

[20] Reg Freeman. Measuring the flow properties of consolidated, conditioned and aerated powders — a comparative study using a powder rheometer and a rotational shear cell. *Powder Technology*, 174(1):25 – 33, 2007. Special Edition from the PSA2005 Conference.

[21] Paul D Jager, Tommasina Bramante, and Paul Luner. Assessment of pharmaceutical powder flowability using shear cell based methods and application of jenike's methodology. *J Pharm Sci*, 104, 07 2015.

[22] T.A. Bell. Industrial needs in solids flow for the 21st century. *Powder Handling & Processing*, 11:9–12, 01 1999.

[23] Jörg Schwedes. Review on testers for measuring flow properties of bulk solids. *Granular Matter*, 5(1):1–43, May 2003.

[24] Matthew Krantz, Hui Zhang, and Jesse Zhu. Characterization of powder flow: Static and dynamic testing. *Powder Technology*, 194(3):239 – 245, 2009.

[25] Rakhi B Shah, Mobin A Tawakkul, and Mansoor Khan. Comparative evaluation of flow for pharmaceutical powders and granules. *AAPS PharmSciTech*, 9:250–8, 02 2008.

[26] BASF SE. Technical information: Ibuprofen, April 2010.

[27] Tao Lu Lowe, Heikki Tenhu, and Henrik Tylli. Effect of hydrophobicity of a drug on its release from hydrogels with different topological structures. *Journal of Applied Polymer Science*, 73(6):1031–1039, 1999.

[28] Alice P. Gast Arthur W. Adamson. *Physical Chemistry of Surfaces*. Wiley, 1997.

[29] Sigma-Aldrich. Product specification: sodium pyrophosphate tetrabasic, 2017.

[30] D. Geldart, E.C. Abdullah, and A. Verlinden. Characterisation of dry powders. *Powder Technology*, 190(1):70 – 74, 2009. Selection of Papers from the Symposium Powder Science and Technology - Powders and Sintered Material STP-PMF 2007.

[31] R. Freeman and Xiaowei Fu. Characterisation of powder bulk, dynamic flow and shear properties in relation to die filling. *Powder Metallurgy*, 51(3):196–201, 2008.

[32] Freeman Technology. *The Basic Flowability Energy*, April 2013.

[33] Freeman Technology. *Variable Flow Rate Method*, June 2007.

[34] Freeman Technology. *Compressibility*, April 2013.

[35] Dietmar Schulze. Flow properties of powders and bulk solids, 2017.

[36] Andrew W Jenike, Utah Engineering Experiment Station, and University of Utah. *Storage and flow of solids*. Salt Lake City, Utah : University of Utah, 1964. Bibliography: p. 194-198.

[37] F. Boschini, V. Delaval, K. Traina, N. Vandewalle, and G. Lumay. Linking flowability and granulometry of lactose powders. *International Journal of Pharmaceutics*, 494(1):312 – 320, 2015.

[38] G. Lumay, F. Boschini, K. Traina, S. Bontempi, J.-C. Remy, R. Cloots, and N. Vandewalle. Measuring the flowing properties of powders and grains. *Powder Technology*, 224:19 – 27, 2012.

[39] J. Cain. An alternative technique for determining ansi/cema standard 550 flowability ratings for granular materials. *Powder Handling & Processing*, 14(3):218–220, 2002.

[40] Joseph L. Kanig Leon Lachman, Herbert A. Lieberman. *The theory and practice of industrial pharmacy*. Philadelphia: Lea & Faber, 3rd ed. edition, 1986.

[41] A. Levy and H. Kalman. *Handbook of Conveying and Handling of Particulate Solids*. ELSEVIER SCIENCE & TECHNOLOGY, 2001.

[42] European Pharmacopoeia Commission. Council Of Europe. *European pharmacopoeia*. Council Of Europe, 7.0 edition, 2010.

[43] Rod Jones. Successful particle size analysis of dry powders. *G.I.T Laboratory Jornal*, 2:46 – 48, 2002.

[44] Freeman Technology. *Specific Energy*, January 2008.

[45] Xiaowei Fu, Deborah Huck, Lisa Makein, Brian Armstrong, Ulf Willen, and Tim Freeman. Effect of particle shape and size on flow properties of lactose powders. *Particuology*, 10(2):203 – 208, 2012. Advances in Characterization and Modeling of Particulate Processes.

[46] Li Qu, Qi (Tony) Zhou, John A. Denman, Peter J. Stewart, Karen P. Hapgood, and David A.V. Morton. Influence of coating material on the flowability and dissolution of dry-coated fine ibuprofen powders. *European Journal of Pharmaceutical Sciences*, 78:264 – 272, 2015.

[47] DA Ploof and JW Carson. Quality control tester to measure relative flowability of powders. *Bulk Solids Handling*, 14:127–127, 1994.

A. Appendix

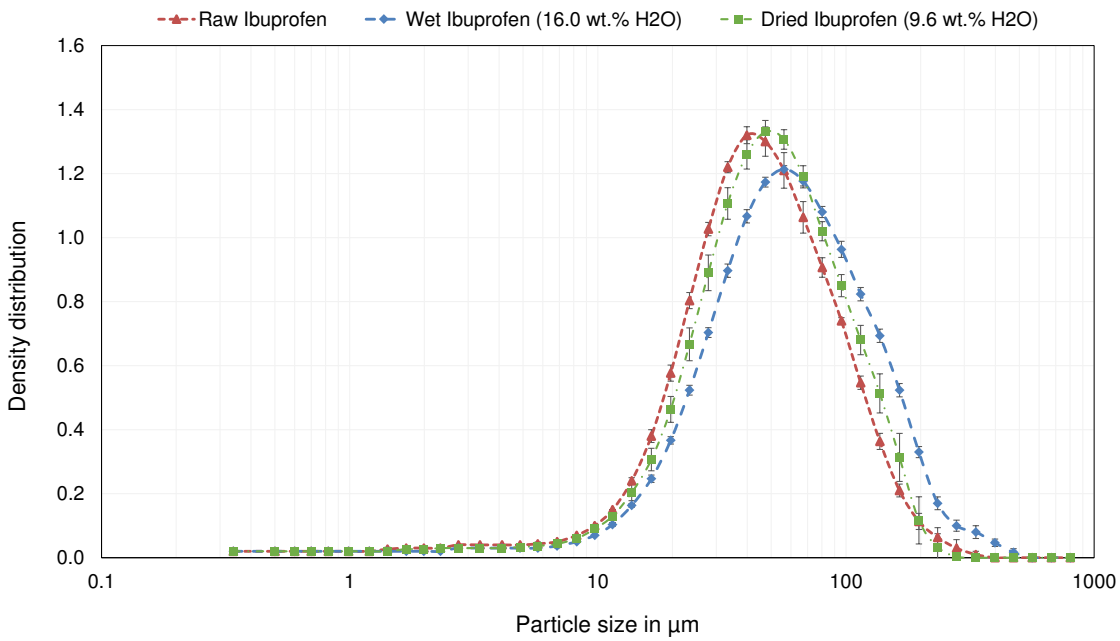

Figure A.1.: Volume density distribution of raw wet (16.0 wt.% H_2O) and dried (9.6 wt.% H_2O) Ibuprofen of test run V7, measured in wet dispersion mode.

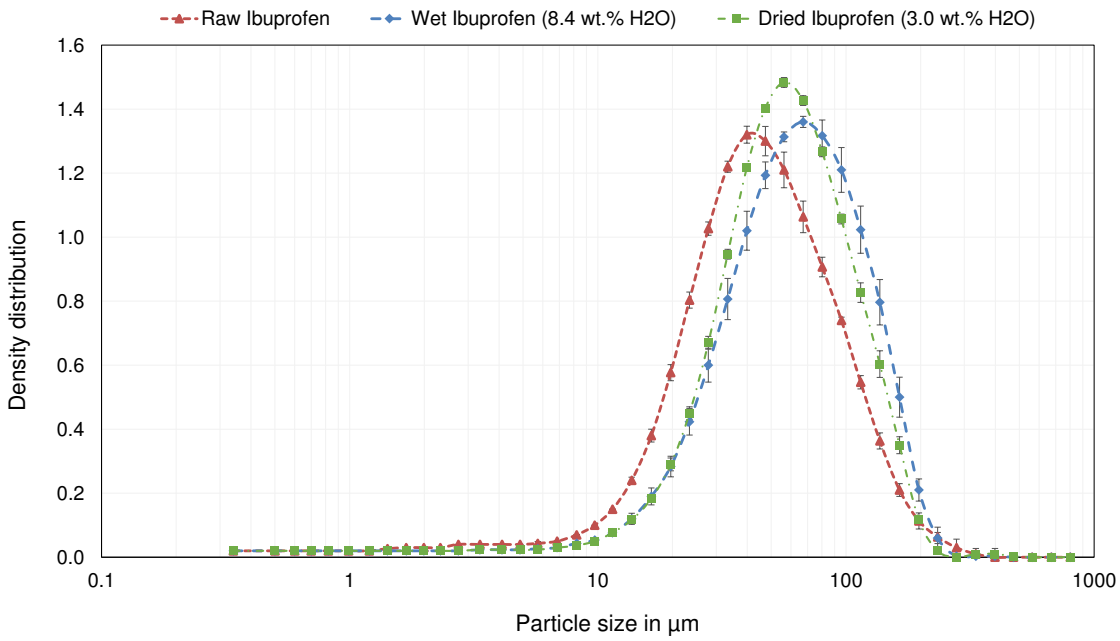

Figure A.2.: Volume density distribution of raw wet (8.4 wt.% H_2O) and dried (3.0 wt.% H_2O) Ibuprofen of test run V8, measured in wet dispersion mode.

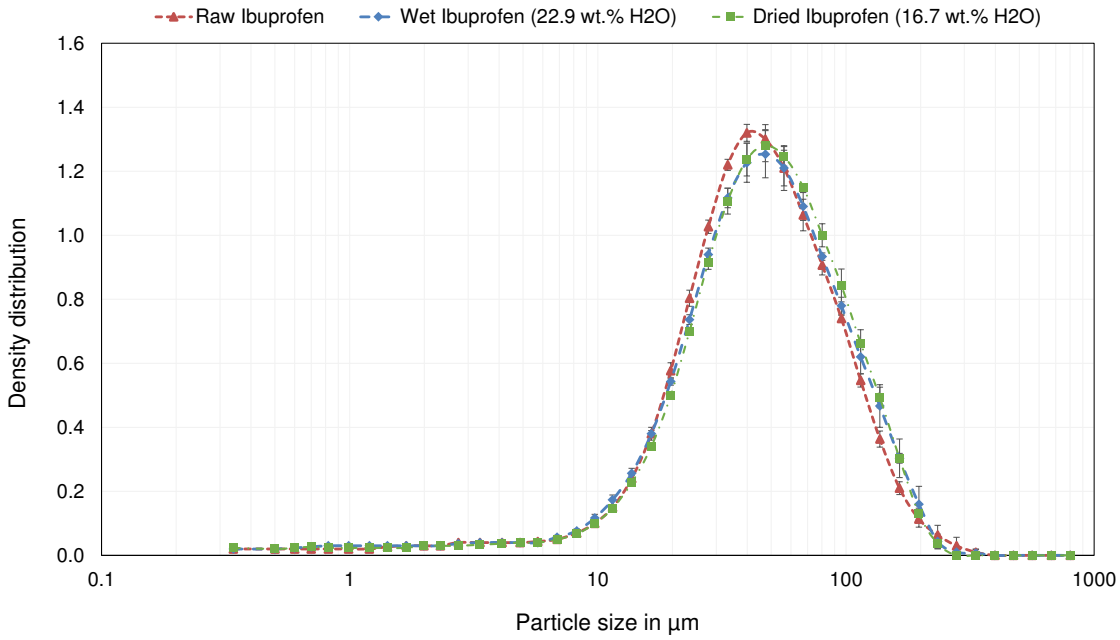

Figure A.3.: Volume density distribution of raw wet (22.9 wt.% H_2O) and dried (16.7 wt.% H_2O) Ibuprofen of test run V9, measured in wet dispersion mode.

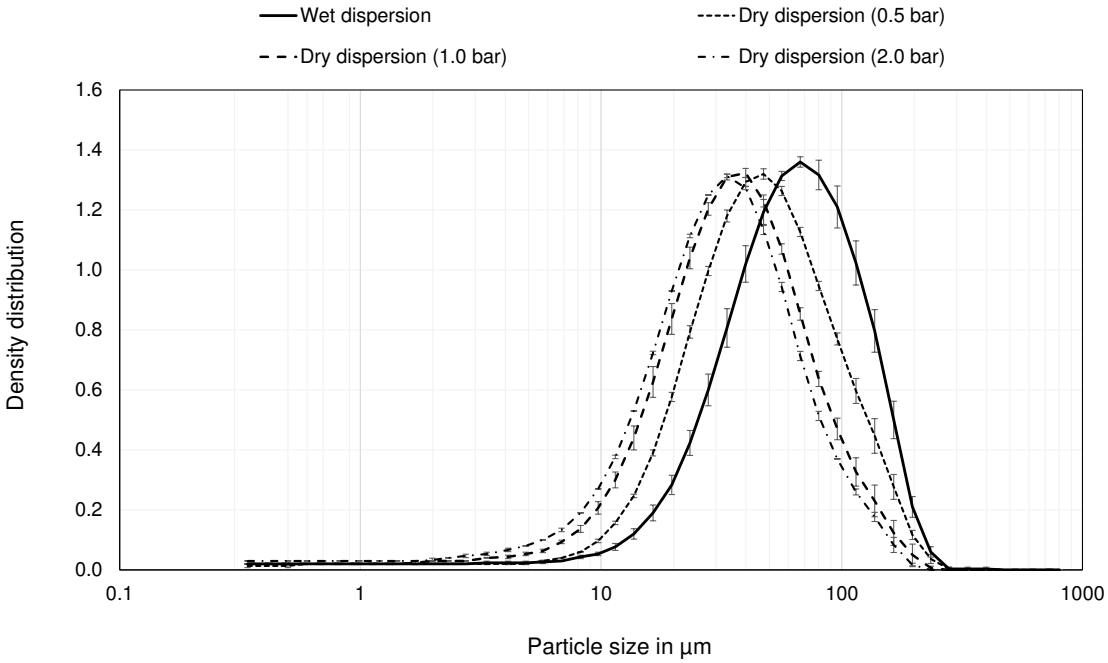

Figure A.4.: Volume density distribution of wet (8.4 wt.% H_2O) Ibuprofen of test run V8 over dispersion pressure compared to the volume density distribution of wet Ibuprofen measured in wet dispersion mode.

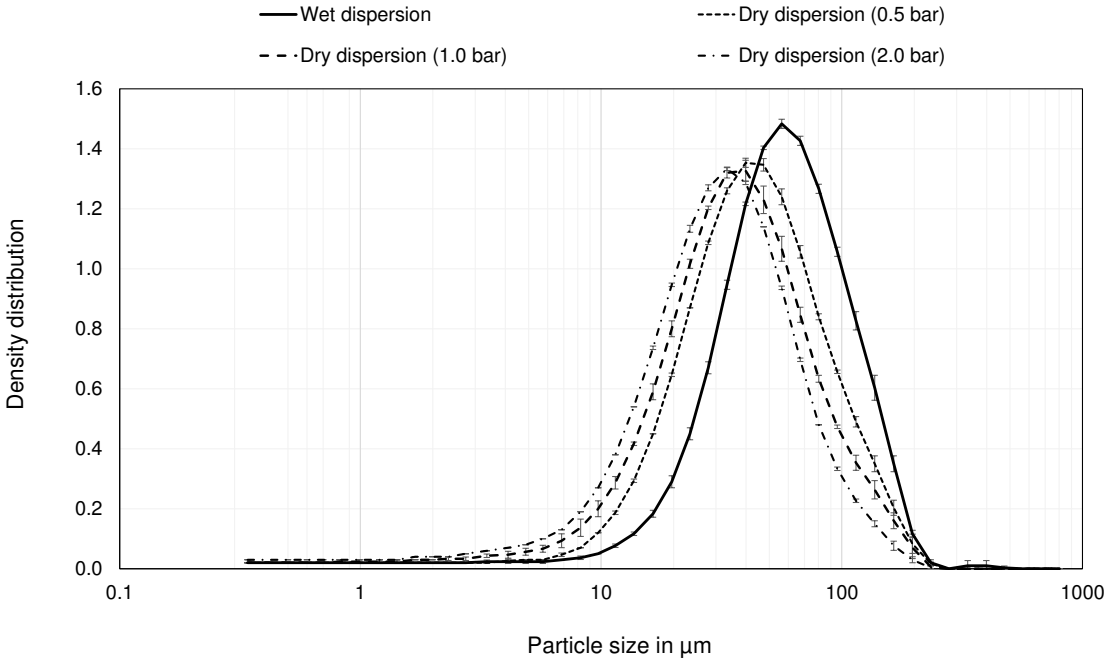

Figure A.5.: Volume density distribution of dried (3.0 wt.% H_2O) Ibuprofen of test run V8 over dispersion pressure compared to the volume density distribution of dried Ibuprofen measured in wet dispersion mode.

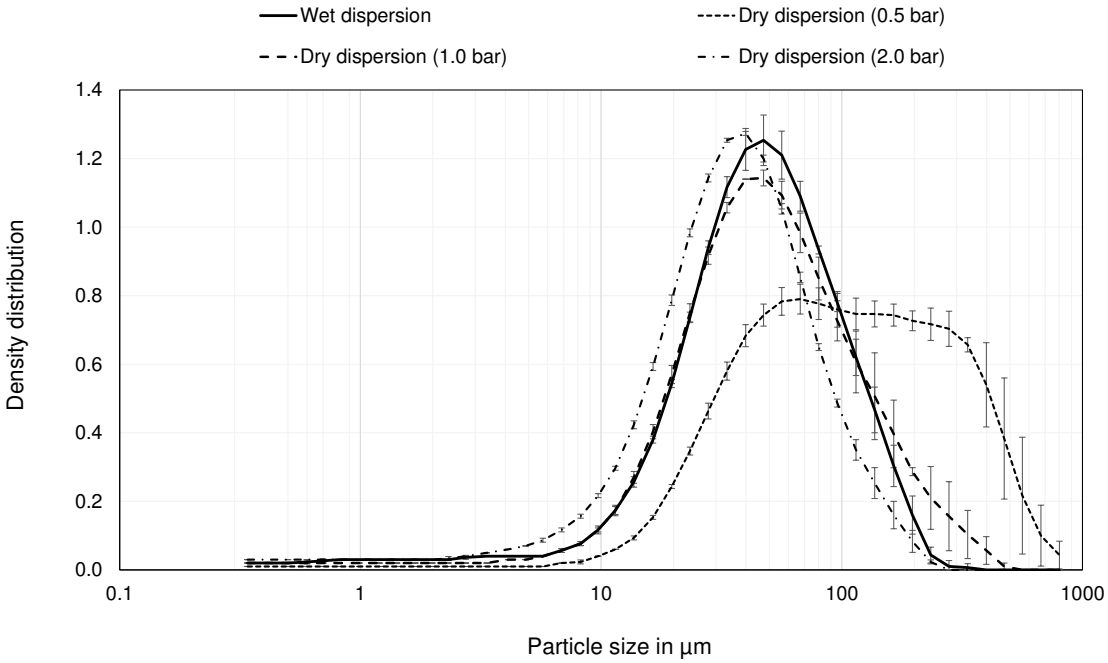

Figure A.6.: Volume density distribution of wet (22.9 wt.% H_2O) Ibuprofen of test run V9 over dispersion pressure compared to the volume density distribution of wet Ibuprofen measured in wet dispersion mode.

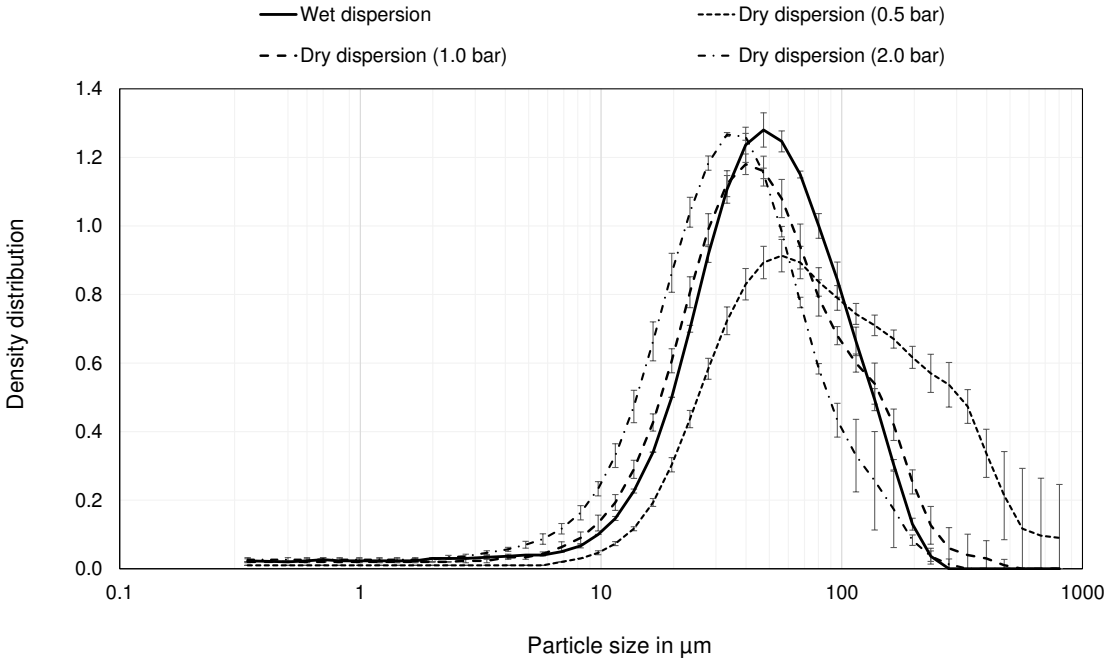

Figure A.7.: Volume density distribution of dried (16.7 wt.% H_2O) Ibuprofen of test run V9 over dispersion pressure compared to the volume density distribution of dried Ibuprofen measured in wet dispersion mode.

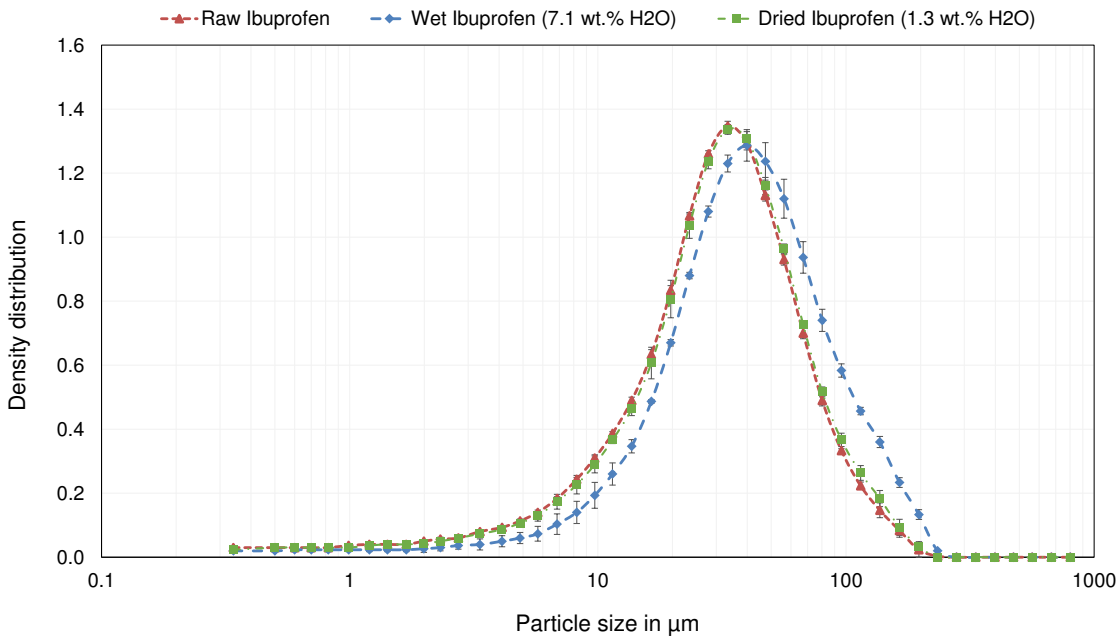

Figure A.8.: Volume density distribution of raw, wet (7.1 wt.% H_2O) and dried (1.3 wt.% H_2O) Ibuprofen of test run V10, measured in dry dispersion mode with 0.5 bar dispersion pressure.

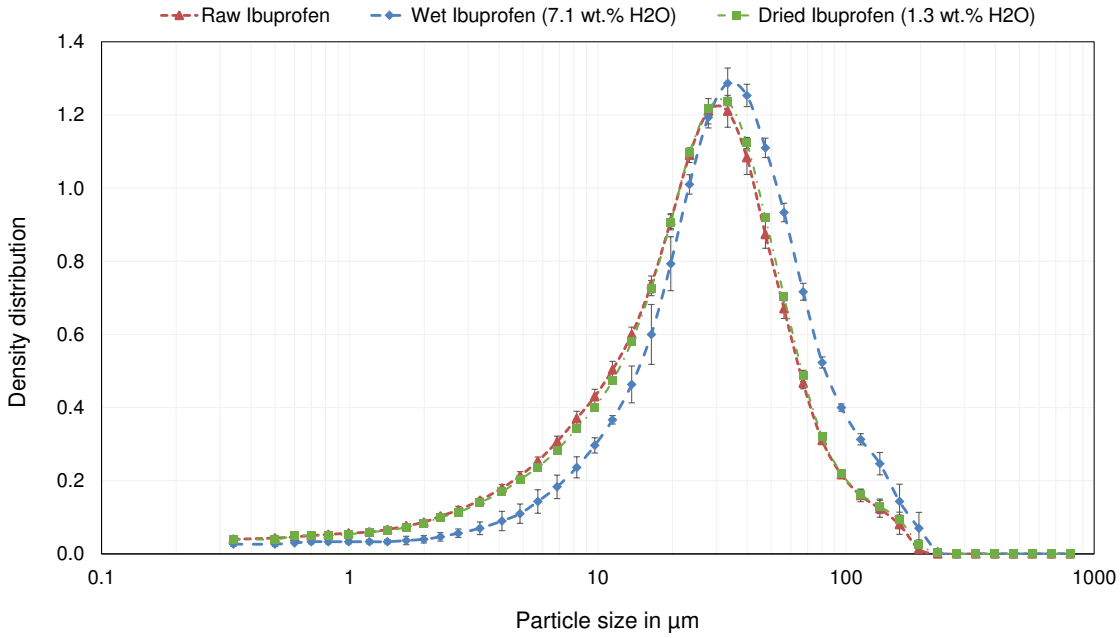

Figure A.9.: Volume density distribution of raw, wet (7.1 wt.% H_2O) and dried (1.3 wt.% H_2O) Ibuprofen of test run V10, measured in dry dispersion mode with 1.0 bar dispersion pressure.

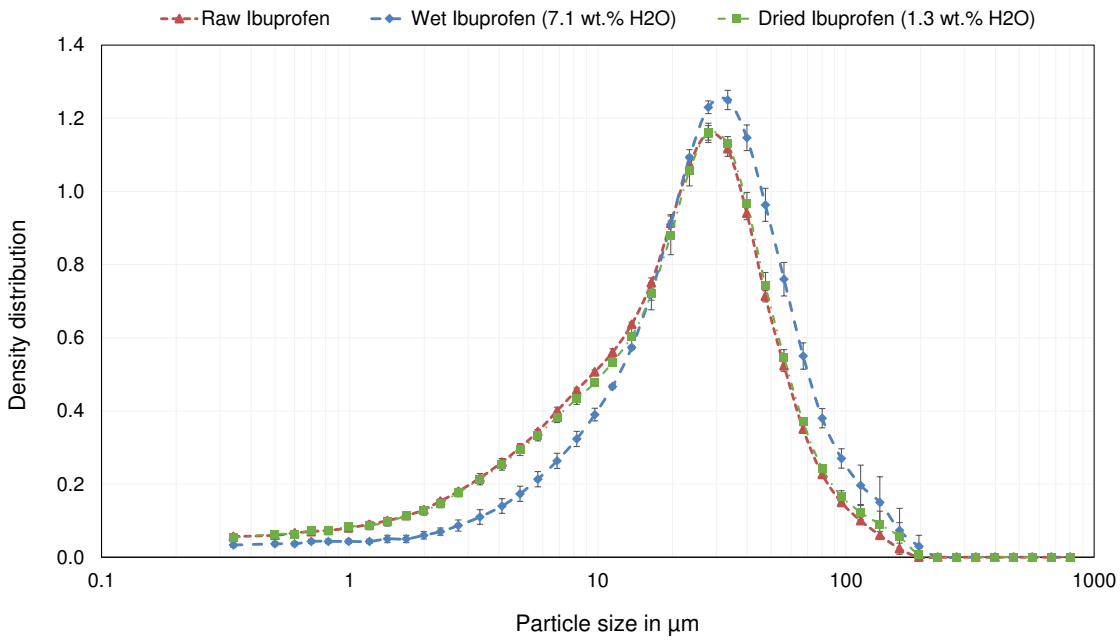

Figure A.10.: Volume density distribution of raw, wet (7.1 wt.% H_2O) and dried (1.3 wt.% H_2O) Ibuprofen of test run V10, measured in dry dispersion mode with 1.5 bar dispersion pressure.

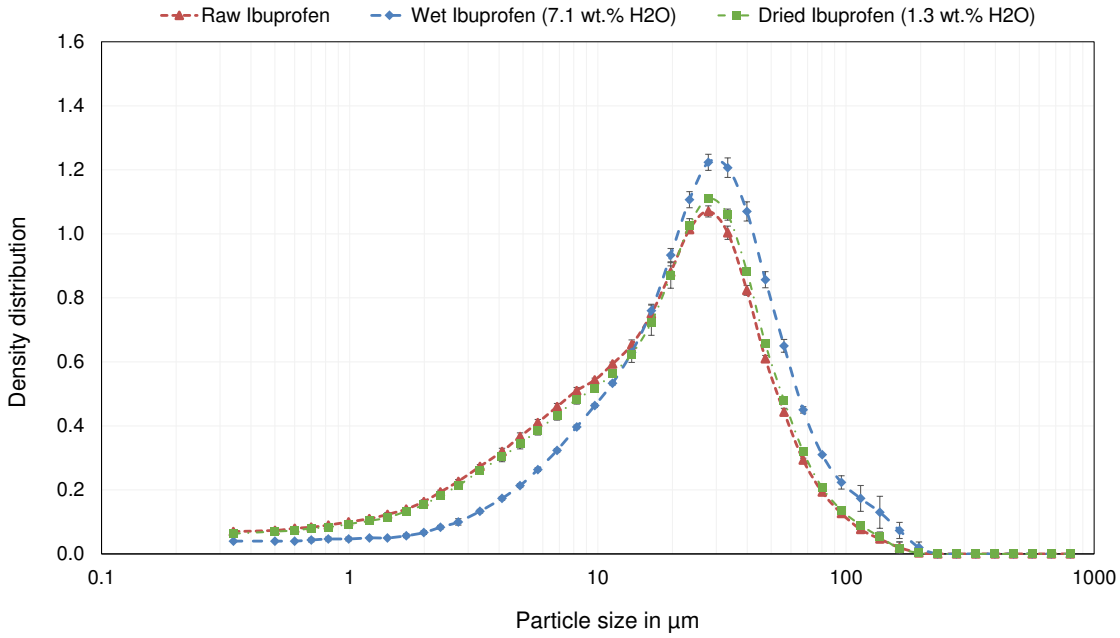

Figure A.11.: Volume density distribution of raw, wet (7.1 wt.% H_2O) and dried (1.3 wt.% H_2O) Ibuprofen of test run V10, measured in dry dispersion mode with 2.0 bar dispersion pressure.

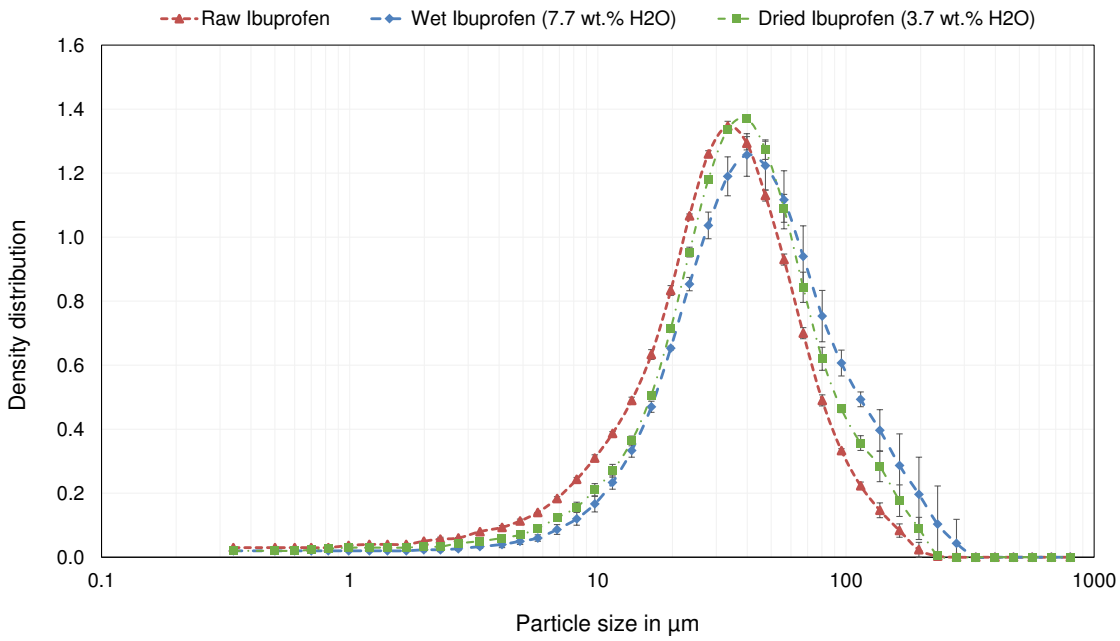

Figure A.12.: Volume density distribution of raw, wet (7.7 wt.% H_2O) and dried (3.7 wt.% H_2O) Ibuprofen of test run V11, measured in dry dispersion mode with 0.5 bar dispersion pressure.

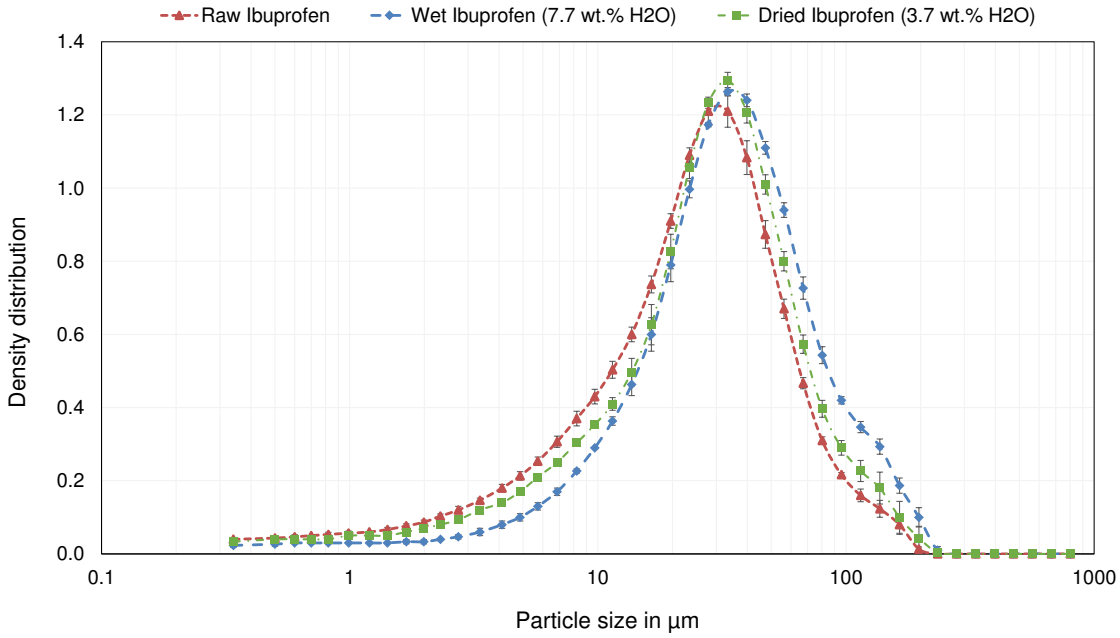

Figure A.13.: Volume density distribution of raw, wet (7.7 wt.% H_2O) and dried (3.7 wt.% H_2O) Ibuprofen of test run V11, measured in dry dispersion mode with 1.0 bar dispersion pressure.

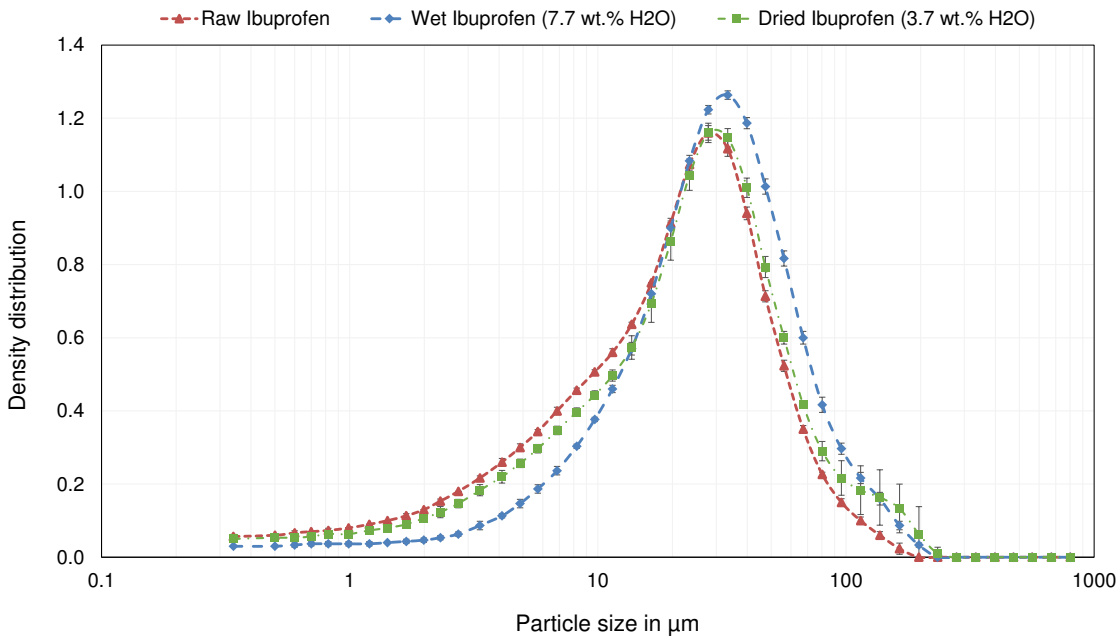

Figure A.14.: Volume density distribution of raw, wet (7.7 wt.% H_2O) and dried (3.7 wt.% H_2O) Ibuprofen of test run V11, measured in dry dispersion mode with 1.5 bar dispersion pressure.

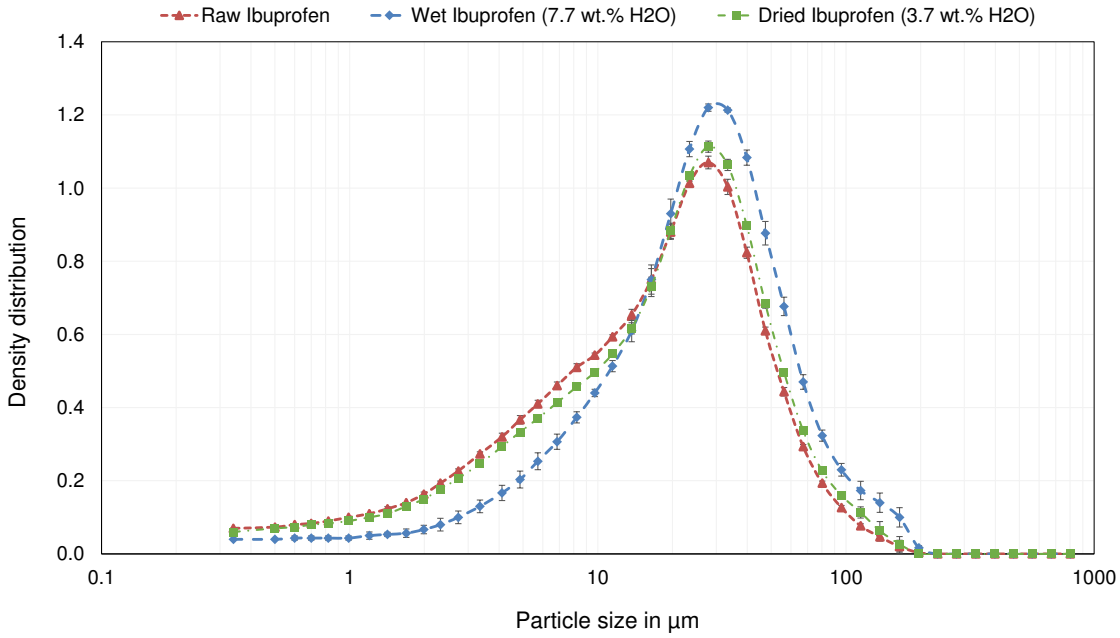

Figure A.15.: Volume density distribution of raw, wet (7.7 wt.% H_2O) and dried (3.7 wt.% H_2O) Ibuprofen of test run V11, measured in dry dispersion mode with 2.0 bar dispersion pressure.

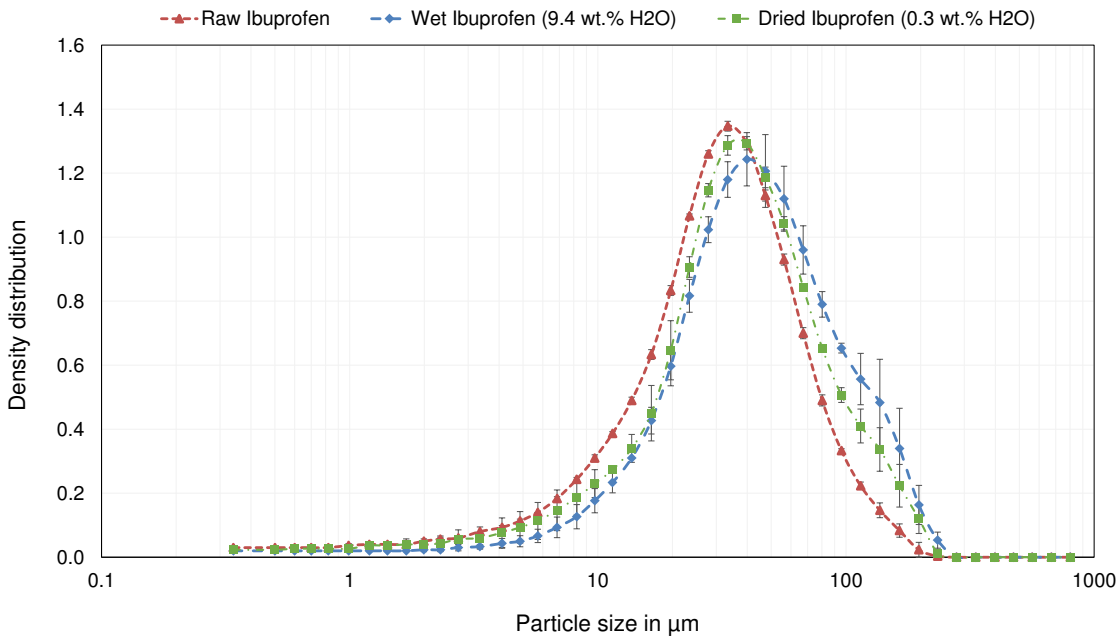

Figure A.16.: Volume density distribution of raw, wet (9.4 wt.% H_2O) and dried (0.3 wt.% H_2O) Ibuprofen of test run V12, measured in dry dispersion mode with 0.5 bar dispersion pressure.

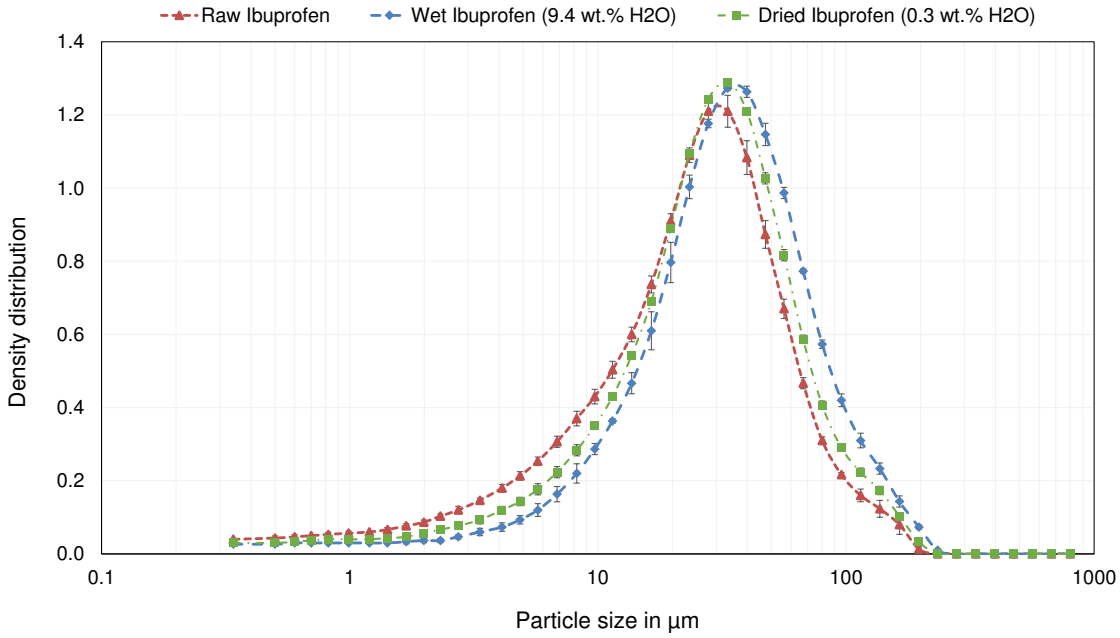

Figure A.17.: Volume density distribution of raw, wet (9.4 wt.% H_2O) and dried (0.3 wt.% H_2O) Ibuprofen of test run V12, measured in dry dispersion mode with 1.0 bar dispersion pressure.

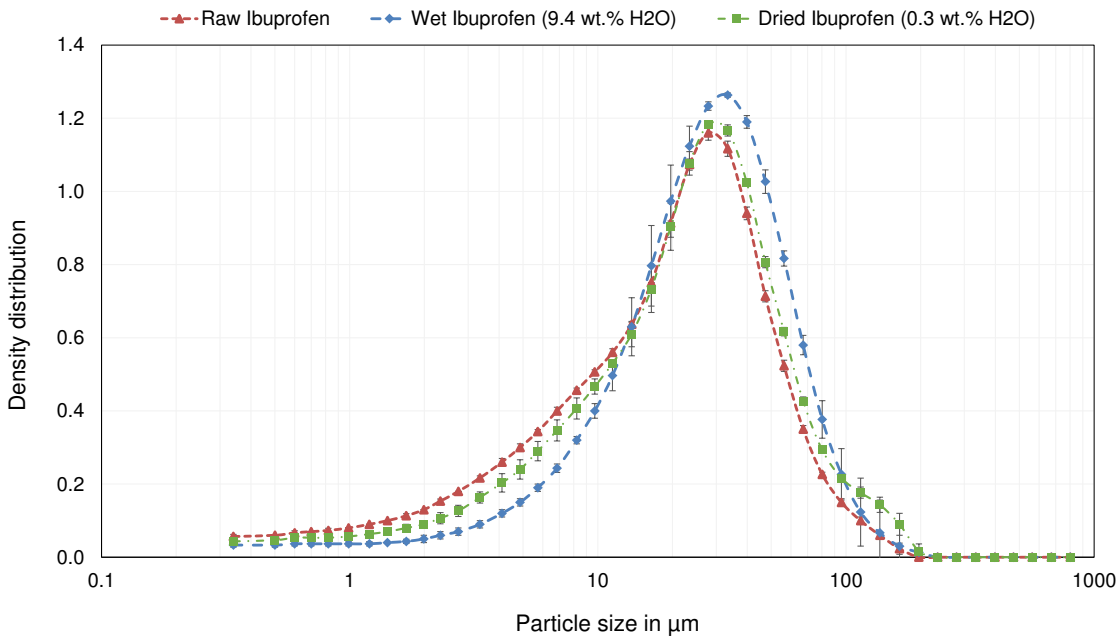

Figure A.18.: Volume density distribution of raw, wet (9.4 wt.% H_2O) and dried (0.3 wt.% H_2O) Ibuprofen of test run V12, measured in dry dispersion mode with 1.5 bar dispersion pressure.

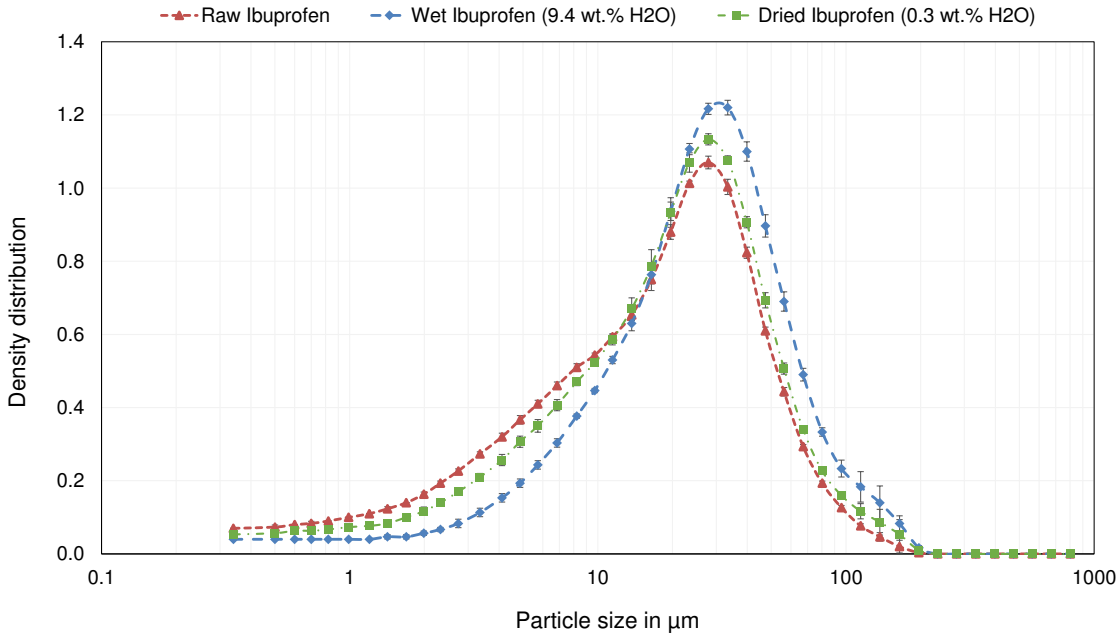

Figure A.19.: Volume density distribution of raw, wet (9.4 wt.% H_2O) and dried (0.3 wt.% H_2O) Ibuprofen of test run V12, measured in dry dispersion mode with 2.0 bar dispersion pressure.

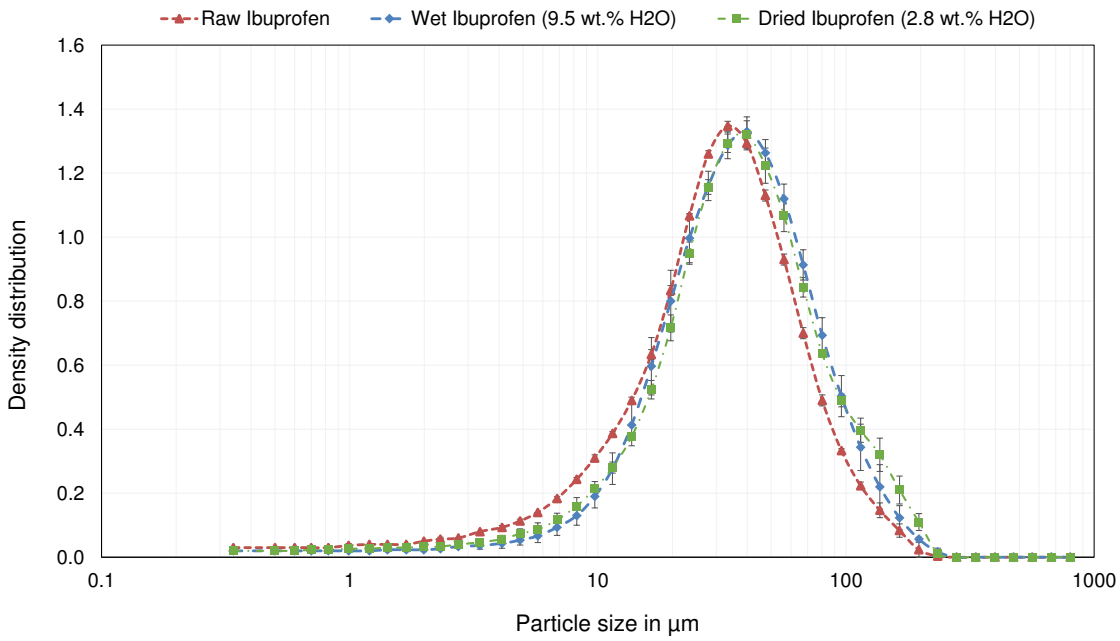

Figure A.20.: Volume density distribution of raw, wet (9.5 wt.% H_2O) and dried (2.8 wt.% H_2O) Ibuprofen of test run V13, measured in dry dispersion mode with 0.5 bar dispersion pressure.

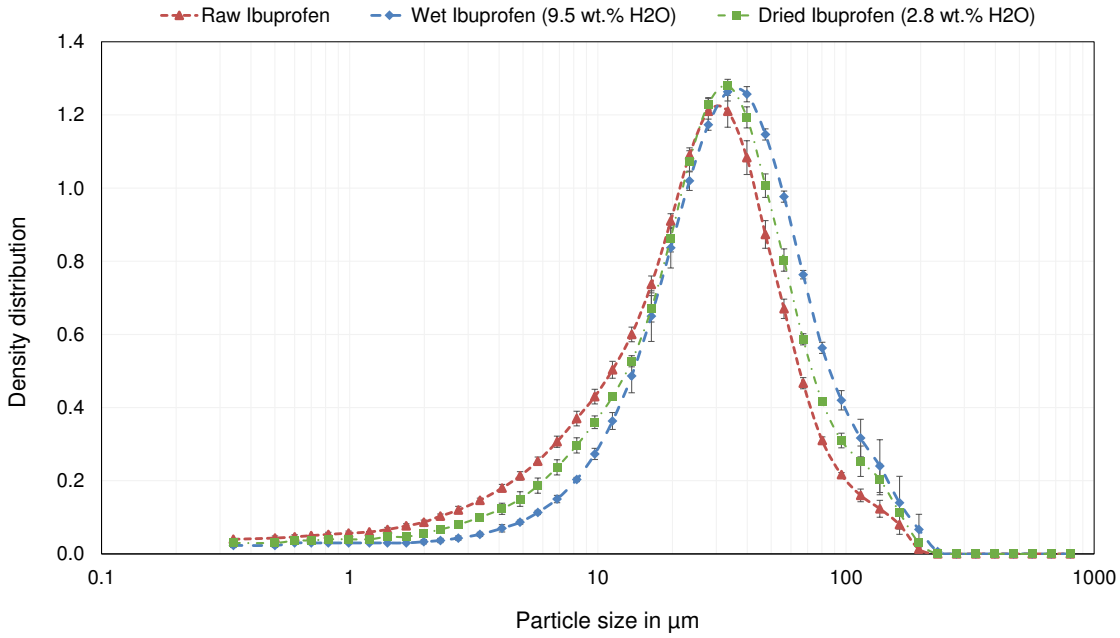

Figure A.21.: Volume density distribution of raw, wet (9.5 wt.% H_2O) and dried (2.8 wt.% H_2O) Ibuprofen of test run V13, measured in dry dispersion mode with 1.0 bar dispersion pressure.

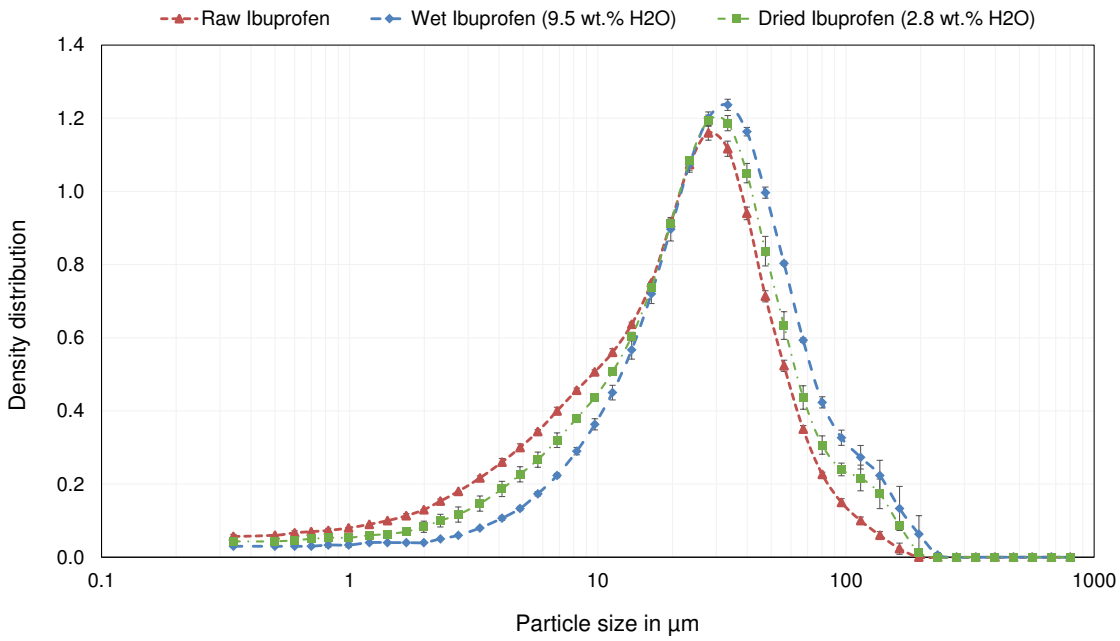

Figure A.22.: Volume density distribution of raw, wet (9.5 wt.% H_2O) and dried (2.8 wt.% H_2O) Ibuprofen of test run V13, measured in dry dispersion mode with 1.5 bar dispersion pressure.

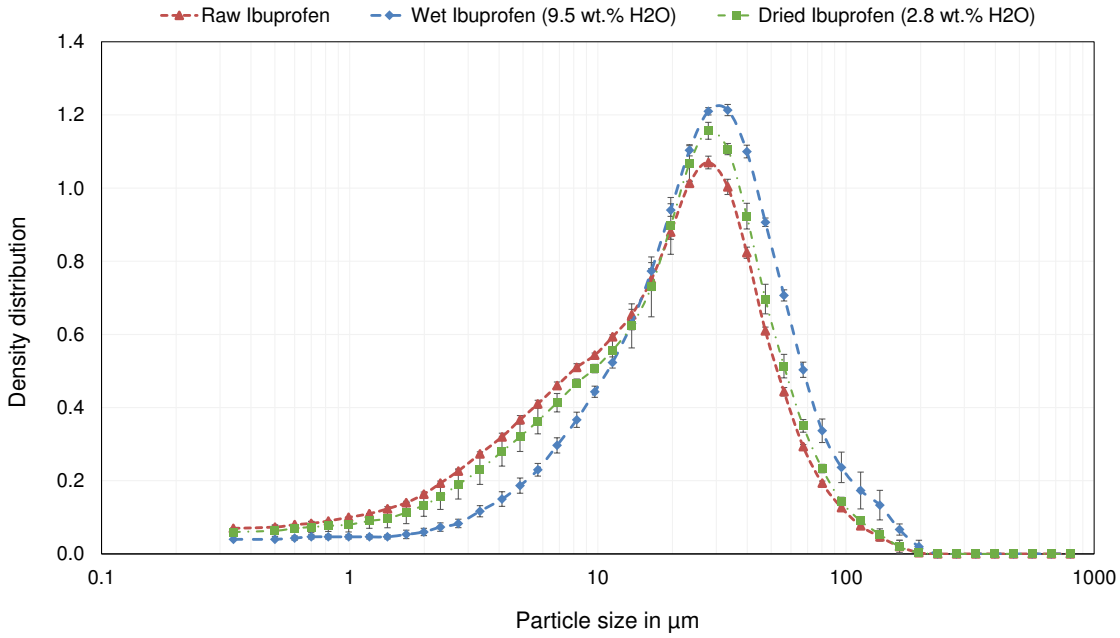

Figure A.23.: Volume density distribution of raw, wet (9.5 wt.% H_2O) and dried (2.8 wt.% H_2O) Ibuprofen of test run V13, measured in dry dispersion mode with 2.0 bar dispersion pressure.

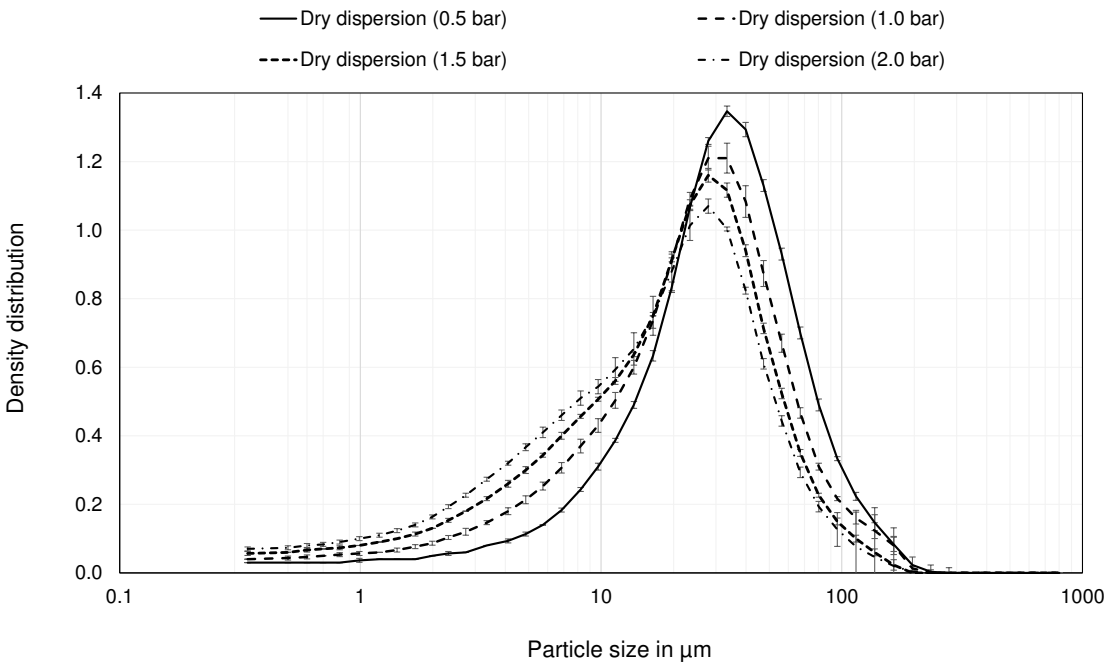

Figure A.24.: Volume density distribution of raw Ibuprofen of test run V10 to V13 over dispersion pressure.

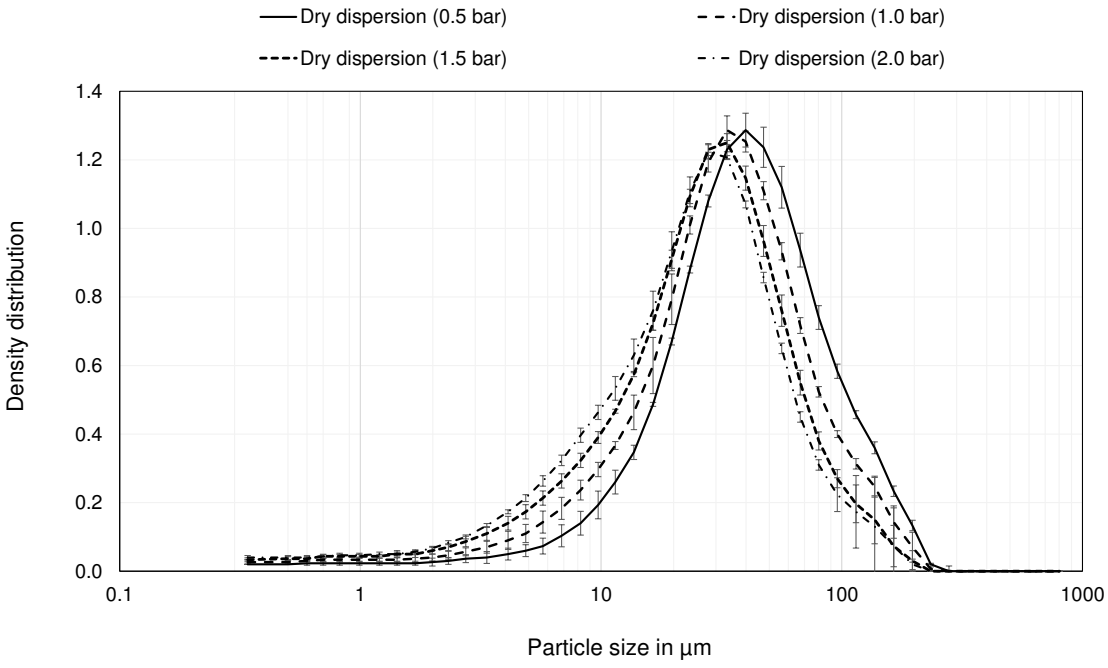

Figure A.25.: Volume density distribution of wet (7.1 wt.% H_2O) Ibuprofen of test run V10 over dispersion pressure.

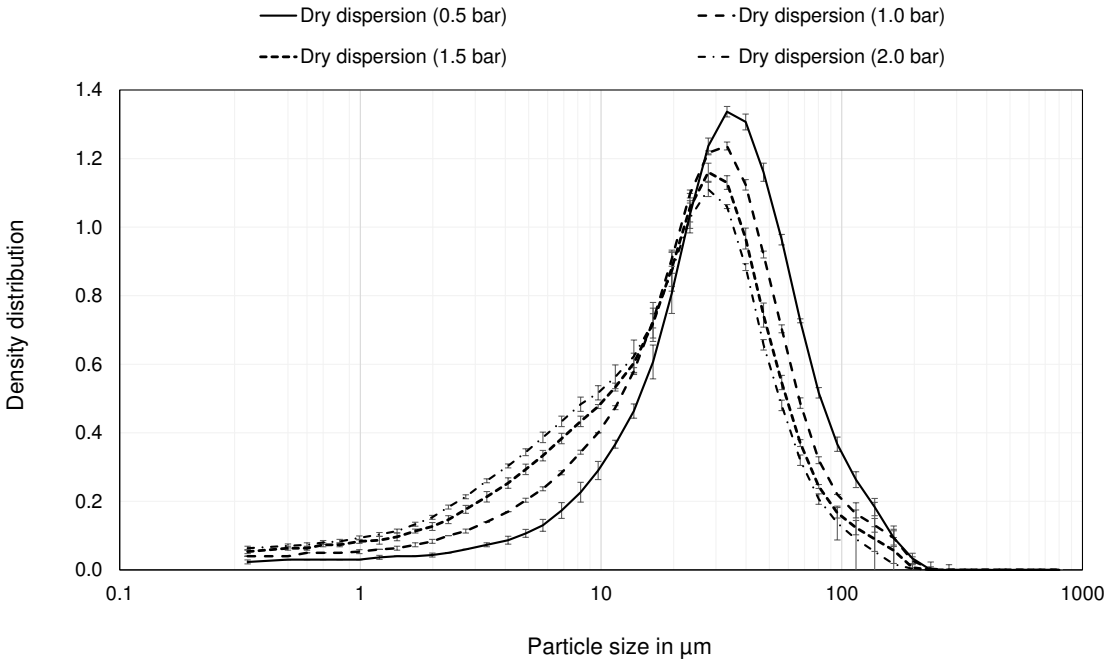

Figure A.26.: Volume density distribution of dried (1.3 wt.% H_2O) Ibuprofen of test run V10 over dispersion pressure.

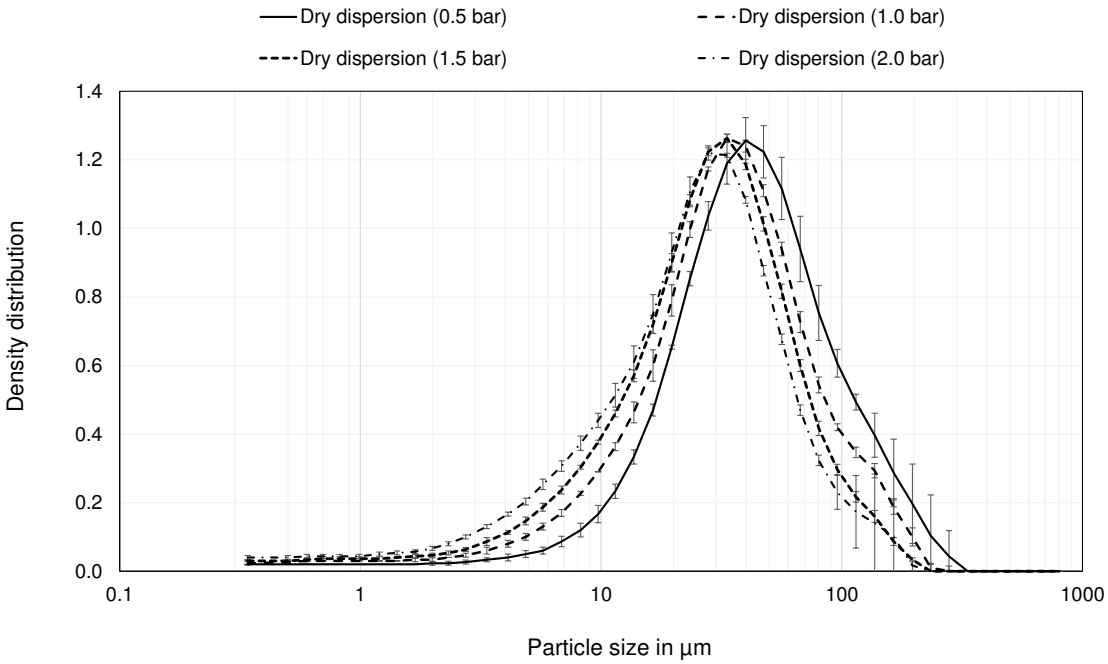

Figure A.27.: Volume density distribution of wet (7.7 wt.% H_2O) Ibuprofen of test run V11 over dispersion pressure.

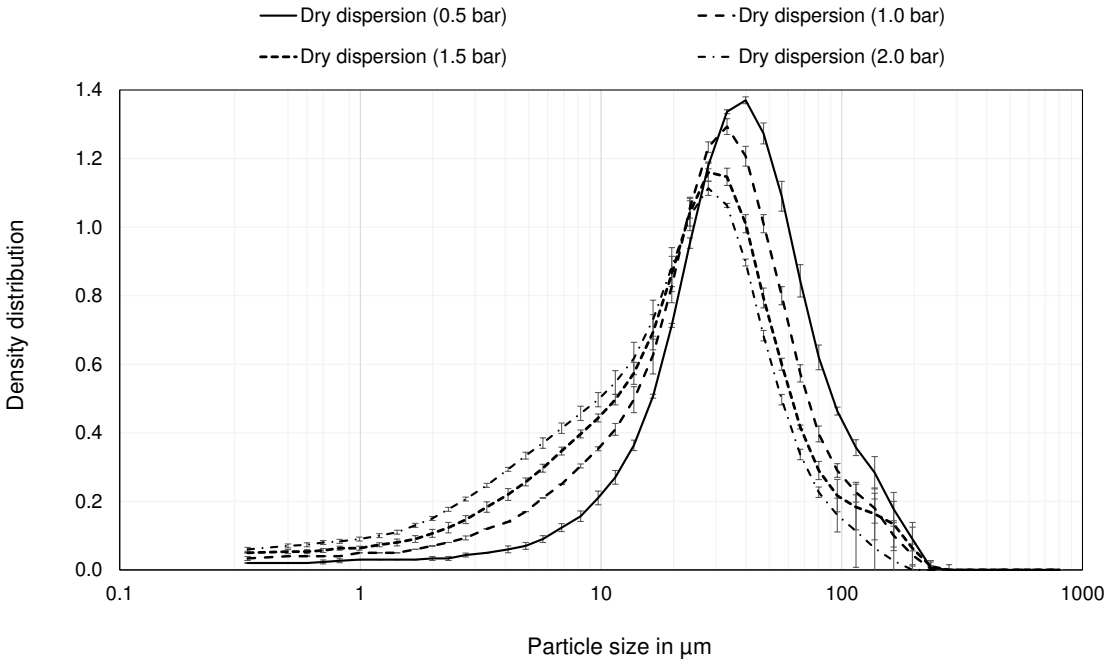

Figure A.28.: Volume density distribution of dried (3.7 wt.% H_2O) Ibuprofen of test run V11 over dispersion pressure.

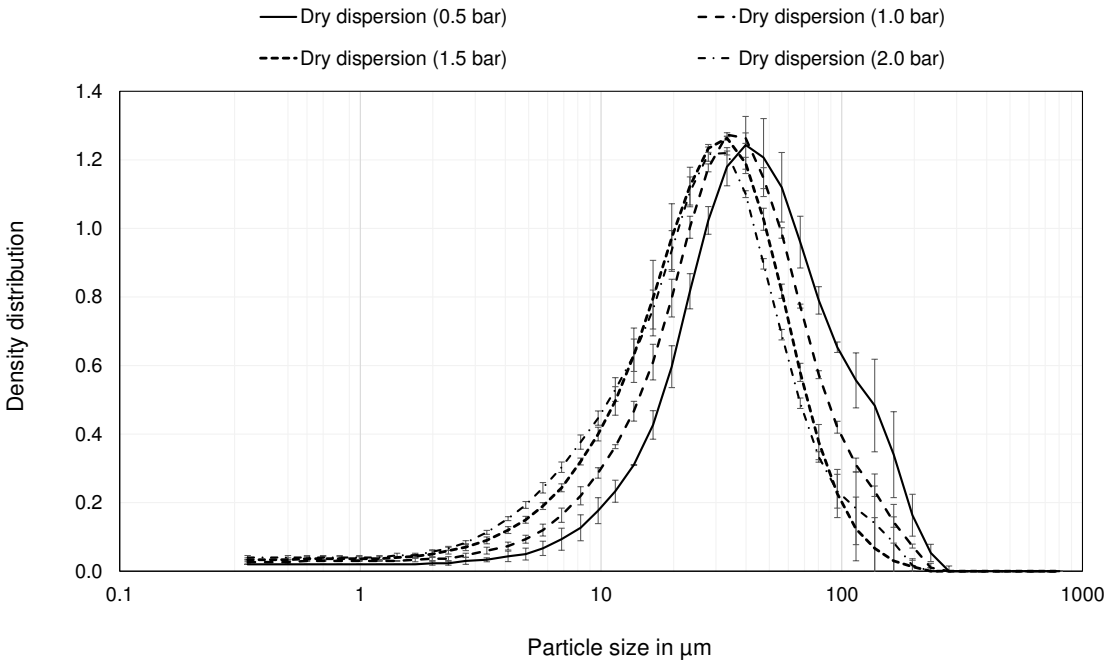

Figure A.29.: Volume density distribution of wet (9.4 wt.% H_2O) Ibuprofen of test run V12 over dispersion pressure.

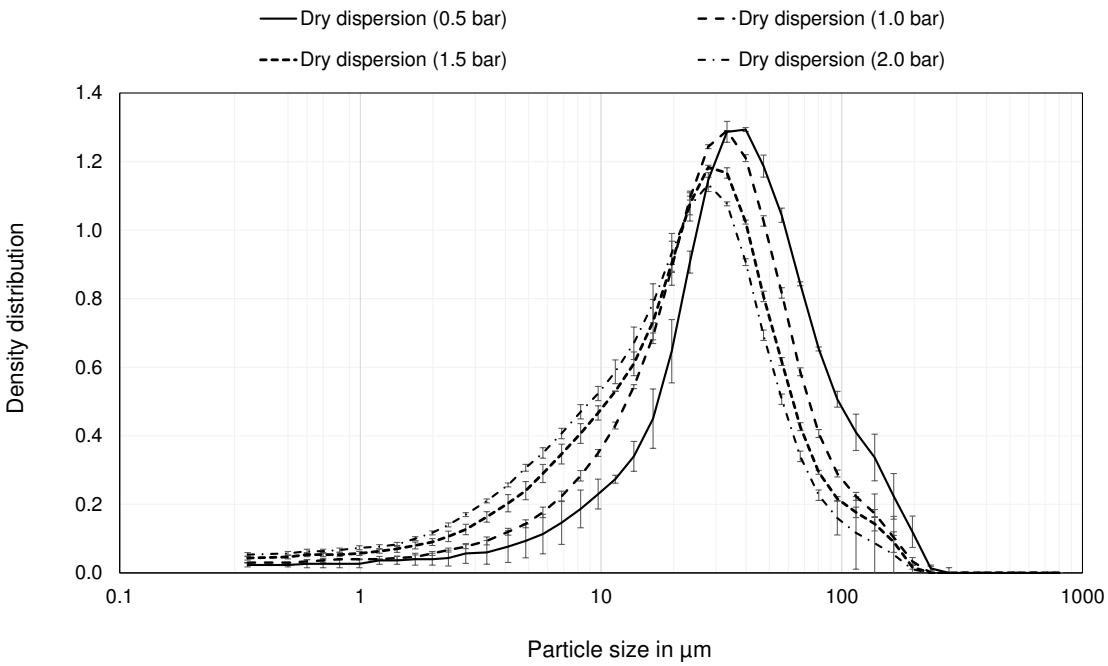

Figure A.30.: Volume density distribution of dried (0.3 wt.% H_2O) Ibuprofen of test run V12 over dispersion pressure.

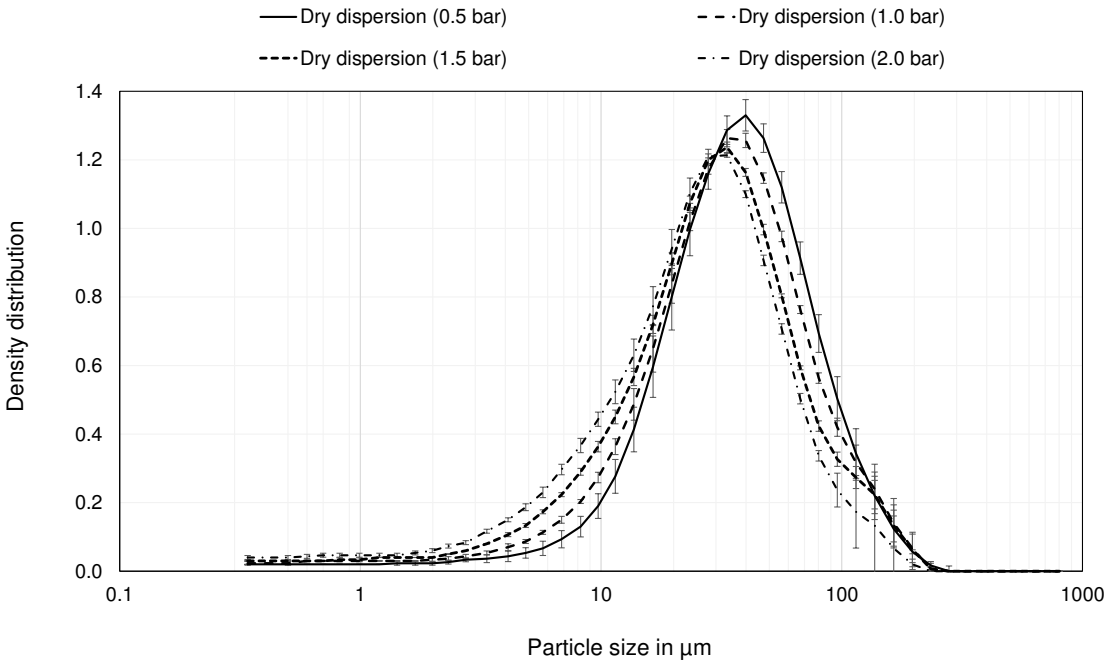

Figure A.31.: Volume density distribution of wet (9.5 wt.% H_2O) Ibuprofen of test run V13 over dispersion pressure.

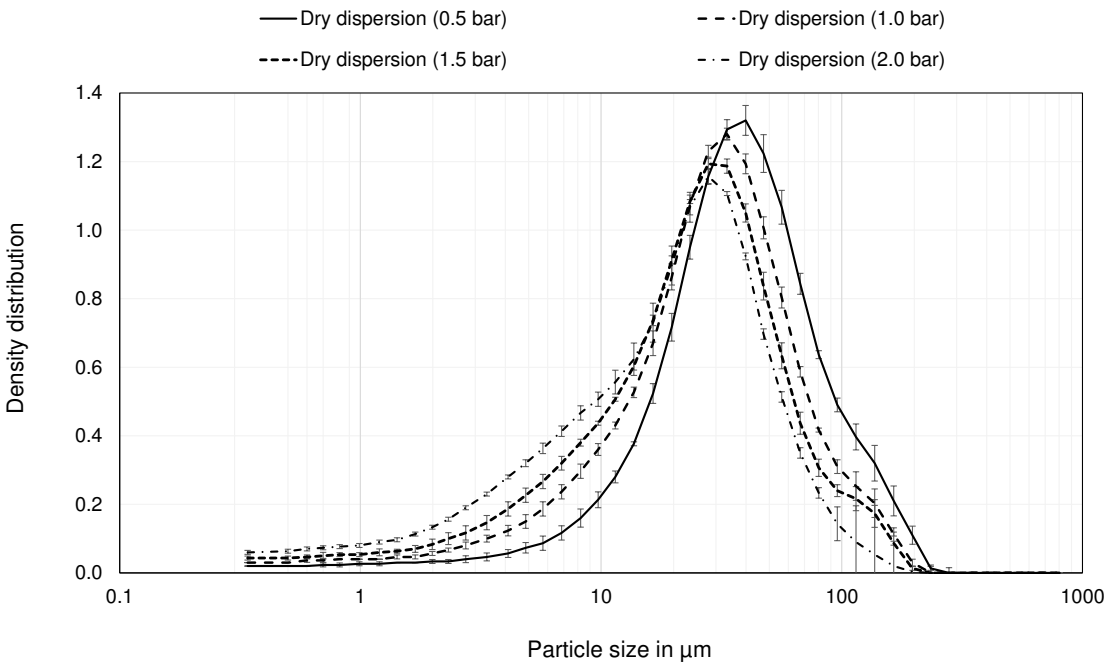

Figure A.32.: Volume density distribution of dried (2.8 wt.% H_2O) Ibuprofen of test run V13 over dispersion pressure.